

Electronic Thesis and Dissertation Repository

9-6-2016 12:00 AM

Constraining the Formation and Alteration of Sudbury Breccia, Ontario, Canada: Implications for Footwall Cu-Ni-PGE Exploration

Jonathan W. O'Callaghan
The University of Western Ontario

Supervisor

Dr. G.R. Osinski
The University of Western Ontario Joint Supervisor

Dr. R.L. Linnen
The University of Western Ontario

Graduate Program in Geology

A thesis submitted in partial fulfillment of the requirements for the degree in Master of Science

© Jonathan W. O'Callaghan 2016

Follow this and additional works at: <https://ir.lib.uwo.ca/etd>



Part of the [Geology Commons](#)

Recommended Citation

O'Callaghan, Jonathan W., "Constraining the Formation and Alteration of Sudbury Breccia, Ontario, Canada: Implications for Footwall Cu-Ni-PGE Exploration" (2016). *Electronic Thesis and Dissertation Repository*. 4075.

<https://ir.lib.uwo.ca/etd/4075>

This Dissertation/Thesis is brought to you for free and open access by Scholarship@Western. It has been accepted for inclusion in Electronic Thesis and Dissertation Repository by an authorized administrator of Scholarship@Western. For more information, please contact wlsadmin@uwo.ca.

Abstract

Sudbury breccia is an impactite situated in the footwall of the 1.85 Ga Sudbury impact structure, situated in Ontario. Developing exploration vectors towards Sudbury breccia-hosted Cu-Ni-PGE mineralization is inhibited by an insufficient understanding of the relative contributions of footwall lithologies versus impact melt. By combining whole-rock geochemistry, field observations, statistical modelling and petrography, this study has determined that Sudbury breccia is a parautochthonous shock melt, which does not require a melt sheet contribution. Furthermore, the trace metal content of the breccia is largely controlled by the assimilation of mafic footwall lithologies, the exception being breccia proximal to mineralization, where a hydrothermally remobilized component is identified. Mineral chemistries demonstrate that some metal remobilization in breccia from both the North and South Range is associated with shear zones and hydrothermal-metamorphic activity. Biotites, amphiboles, chlorites and titanites have geochemical signatures consistent with increased pressure and/or temperatures conditions towards deformation structures hosting sulfide ores.

Keywords

Sudbury, geochemistry, mineralogy, pseudotachylite, impact cratering

Co-authorship Statement

The collaborative nature of this project entailed co-authorship on the integrated articles presented herein. Specifically, Peter Lightfoot is chief geologist at Vale and an adjunct professor in mineral exploration at Laurentian University. In addition to providing the sample suite and geochemical data set used in this study, Dr Lightfoot assisted with providing access to mine and surface field sites for mapping and sampling purposes. His advice and support has been invaluable to this project and the two manuscripts herein. Samples were collected by several members of the Vale mine and brownfield exploration team over the course of three summer sampling seasons. John Weirich was a former post-doctoral fellow at the University of Western Ontario, before moving to the Planetary Science Institute in Tucson, Arizona. Dr Weirich developed the geochemical mixing model and aided its integration and interpretation in this study. Dr Osinski and Dr Linnen supervised the project and contributed to the writing of both articles.

Acknowledgements

Firstly, I would like to thank Dr Gordon ‘Oz’ Osinski who first gave me the opportunity to move across the Atlantic to Canada to start a new and exciting chapter in my life. Thank you for all the incredible experiences over the last couple of years, from descending 2 km underground to visit one of the largest sulfide deposits in North America, to driving across the U.S.A. to summit cinder cone volcanoes in Arizona! I’m also very grateful to Dr Robert Linnen who has provided invaluable support and guidance with my research over the last two years, and encouraged me to peruse various conference and funding opportunities. I would also like to thank Dr. Patricia Corcoran, Dr. Brian Hart and Dr. Paul Ragona for agreeing to be my thesis examination committee.

The scope of this project would not have been possible without the support and guidance of the Vale brownfield exploration team at Sudbury. In particular, I am indebted to Peter Lightfoot for his guidance and support throughout this project, and for arranging a summer position at the exploration office, where I gained valuable industry experience. I would also like to thank Lisa Gibson, Alex ‘Sandy’ Gibson, Jason Letto, Rob Pelkey, Clarence Pickett Enrick Tremblay and Michael MacBurnie for their support and assistance during my time at Vale and with my research, as well as to Shawna Wabberi and Huw Wright for their support with surface sampling. Thanks also to the rest of the exploration team for making it a great summer, especially Clayton Pearson, Ryan Humphries, Erin Joseph and Ian Fieldhouse.

I’m also grateful to the funding provided by a fellowship from the Society of Economic Geologists Canada Foundation. I’m also grateful for funding received from the Gordon G. Suffel Scholarship for Graduate Studies in Applied Economic Geology and a scholarship from SRK Consulting Canada. Additional funding for geochemical analysis and conference attendance was provided through an NSERC Engage Grant to Dr Osinski, and NSERC Discovery Grants to Dr Linnen and Dr Osinski.

I would also like to thank my family for their continuing support in my decision to relocate to Canada, especially to Chris and Fran, for following me over the ocean to live in California, where I can escape during the Canadian winters. Thanks to all my geology friends who have made this experience so much fun, especially Laura, Anika, Tessa, Peter, Shamus, Mary, Andrea, Becca, Patrick, Jess, Jon, Adam, Ryan and Marcus to name but a few. Thanks also the entire SEG London Student Chapter and CPSX crew.

Table of Contents

Abstract	i
Keywords	i
Co-authorship Statement	ii
Acknowledgements	iii
List of Tables.....	vii
List of Equations	viii
List of Figures	ix
List of Abbreviations.....	xiv
1 Introduction.....	1
1.1 Impact Cratering	2
1.2 Sudbury Regional Geology	4
1.2.1 Sudbury Breccia	9
1.2.2 Ni-Cu-PGE Mineralization	11
1.2.3 Metamorphic and Hydrothermal History	15
1.3 Introduction to the Thesis	17
1.4 References	18
2 Reconstructing the geochemical signature of Sudbury Breccia, Ontario, Canada:	
Implications for its formation and trace metal content	32
2.1 Introduction	32
2.2 Geological Setting	33
2.3 Sample Selection and Local Geology.....	38
2.3.1 Creighton Embayment.....	39
2.3.2 West Murray Area.....	39
2.3.3 Manchester Offset Dike	40
2.3.4 McCreehy East 153 Ore Deposit.....	40

2.4	Methodology.....	41
2.4.1	Mixing Model Specifications	43
2.5	Petrography.....	45
2.6	Geochemical Results and Modelling Parameters	49
2.7	Results of Principal Component Analysis	51
2.8	Results of Mixing Models	51
2.8.1	Manchester Offset Dike	52
2.8.2	South Pump Lake	53
2.8.3	Old Creighton Town.....	53
2.8.4	West Murray Area.....	53
2.8.5	Creighton Deep	54
2.8.6	McCreedy 153 East Ore Body	54
2.9	Discussion.....	58
2.9.1	Allochthonous versus Authochthonous origin for Sudbury breccia	58
2.9.2	The origin of trace metals within the Sudbury breccia	61
2.10	Conclusions	64
2.11	References	65
3	Contrasting mineralogical and geochemical characteristics of Sudbury breccia adjacent to footwall Cu-Ni-PGE sulfide in the Crighton and Coleman deposits.....	80
3.1	Introduction	80
3.2	Geological Setting	81
3.2.1	Regional Geology.....	81
3.2.2	Metamorphic History	83
3.2.3	Sudbury Breccia	85

3.2.4 Sulfide and Hydrothermal Mineral Paragenesis.....	85
3.3 Local Geology	87
3.3.1 Coleman Mine	87
3.3.2 Creighton Mine	87
3.4 Sample Selection	89
3.5 Methodology.....	90
3.6 Mineralogy and Petrography	93
3.6.1 Samples adjacent to the McCreedy East 153 Ore Deposit.....	93
3.6.2 Samples Adjacent to the Creighton Deep Ore Deposit	95
3.7 Results	97
3.7.1 Major and trace element results for biotite.....	103
3.7.2 Major and trace element results for chlorite.....	103
3.7.3 Major and trace element results for amphibole	105
3.7.4 Major and trace element results for ilmenite and magnetite	107
3.7.5 Major and trace element results for titanite.....	108
3.7.6 In-situ U-Pb dating of titanite.....	109
3.8 Discussion.....	109
3.8.1 Mineralogy and Geochemical Variations at Creighton Mine	109
3.8.2 Mineralogy and Geochemical Variations at Coleman Mine	113
3.8.3 Comparisons between Creighton and Coleman Mine.....	118
3.9 Conclusion.....	120
3.10 References	121
4Conclusion:	133

4.1 Recommendations for future work	136
4.2 References	137
5 Curriculum Vitae	140

List of Tables

Table 2-1: Location names, number of samples (Sudbury Breccia and host) collected, NAD-27 co-ordinates of sample sites and a summary of the footwall host lithologies proximal to the Sudbury Breccia outcrops.	39
Table 2-2 Representative Sudbury breccia analyses and equivalent mixing model results and statistics. Italicized elements were used as elements of interest (X_{eoi}) in the mixing model (see methodology).	57
Table 3-1: Electron Microprobe and LA-ICP-MS operating conditions with calculated detection limits.	92
Table 3-2: Representative Titanite and Biotite Analyses from Creighton Mine	98
Table 3-3: Representative Titanite and Biotite Analyses from Coleman Mine.....	99
Table 3-4: Representative Amphibole Analyses from Coleman and Creighton Mine	100
Table 3-5: Representative Chlorite Analyses from Coleman Mine.....	101
Table 3-6: Average Ilmenite and Magnetite Analyses from Coleman Mine.....	102

List of Equations

Equation 2-1: The criteria that the mixing model applies when modelled the breccia results using the end-member components (A, B, C and D), which are compared against the actual measured breccia samples. Criteria 2 is an independent variable, whereas as criteria 3, which uses the elements of interest (EOI) is a dependent variable). A_i, B_i, C_i and D_i must ≥ 0 in criteria 1.	43
Equation 2-2: The Chi-test equation used to validate the precision of the mixing model by comparing the model geochemical results with the original Sudbury breccia results that the model is attempting to replicate.....	44
Equation 2-3: The roundness or circularity factor equation, calculated by comparing the area (A) with the perimeter (P) of the object of interest.....	48
Equation 3-1: Alteration of ferro-actinolite and albite to ferro-hornblende and quartz	111
Equation 3-2: Alteration of ferro-hornblende, anorthite and magnetite to ferro-tschermakite, clinozoisite, quartz and rutile.....	112
Equation 3-3: Alteration of Fe-augite, ilmenite and quartz to titanite and ferro-actinolite	107
Equation 3-4: Chlorite geothermometer equation developed by Kranidiotis and Maclean (1987).....	108
Equation 3-5: Alteration of biotite, quartz and anorthite to epidote, chlorite and feldspar	110
Equation 3-6: Alteration of actinolite-tremolite, ilmenite and anorthite to titanite, chlorite, quartz and magnetite	110

List of Figures

Figure 1.1: Schematic cross sections through an impact crater during the contact compression, excavation and modifications stages, highlighting the different locations of excavated, displaced and melted material. The left column depicts the formation of a smaller (<2 – 4 km), simple crater, whereas the right depicts the processes that create a complex crater, analogous to the Sudbury impact structure (from Osinski and Pierazzo 2013).	3
Figure 1.2: Geology of the Sudbury region, with the 30 x 60 km, elliptical Sudbury Igneous Complex at the centre, with radial and concentric offsets dikes extending out from the melt sheet. The North Range is primarily Archean granites and gneisses, whereas the South Range is comprised Paleoproterozoic metavolcanics and metasedimentary rocks. The Grenville orogenic front occupies the South East corner of the region (from Coulter 2016).....	5
Figure 1.3: Outline of the Sudbury Igneous Complex highlighting examples of active and historic contact, footwall, offset dike and breccia belt deposits, as well as each of the known offset-dikes in the surrounding footwall (modified after Coulter 2016 and Ames and Farrow 2007).....	8
Figure 1.4: Examples of ‘pseudotachylitic’ impact breccia from Highway 24, Creighton Township, Sudbury (A) and Leeukop Quarry, Parys Sector, South Africa (B). These images demonstrate the comparable nature of Sudbury breccia and Vredefort pseudotachylite at these two large (>200 km radius) impact structures (Vredefort image from Thomas 2013).....	10
Figure 1.5: Drill core examples of (A) pyrrhotite + pentlandite contact-style mineralization from Creighton Mine, (B) sharp-walled vein mineralization of chalcopyrite + cubanite, with inclusions of footwall material and (C) stringers and disseminations of chalcopyrite + millerite with an epidote + chlorite + magnetite alteration zone from Coleman Mine.	12
Figure 1.6: Cross section through the SIC-Footwall contact showing the relationship between embayment- and sublayer-hosted contact style ores and more fractionated, Sudbury breccia hosted chalcopyrite+cubanite (Cp+Cb) footwall veins, towards the terminations of which bornite+millerite (Bn+Mlt) and LSHPM mineralization are occasionally found (modified after Rousell and Brown 2009).	14

Figure 2.1: Geological map of the Sudbury Basin, showing the location of the Sudbury Igneous Complex, Superior Province and Huronian footwall units, and post impact Whitewater Group. Sample locations are: 1. McCreedy East 153 Ore Body; 2. Creighton Mine, Old Creighton Town and South Pump Lake; 3. Manchester Offset Dike; 4. Murray West Zone; 5. Halfway Lake (modified after Coulter 2016). 34

Figure 2.2: Flow chart demonstrating the IDL mixing model process, from the input of 3-4 end-member components (including quartz diorite: Q.D.), through to the output and interpretation of P-values based on the χ^2 test. For the equations please refer to the methodology section. Eq. 3 is a dependent variable on the results of Eq. 1 and Eq. 2, which are independent variables..... 43

Figure 2.3: A: Field image of Sudbury breccia outcrop at, South Pump Lake showing lithic fragments of granite and transported metasedimentary rocks, in a dark grey, fine-grained matrix. B: Thin section in plane polarized light (PPL) showing the texture of Sudbury breccia from Halfway Lake. The field of view illustrates the very fine-grained matrix hosting quartz and feldspar lithic fragments and green chlorite patches. C: Thin section of Sudbury breccia in PPL from the Creighton Embayment in the South Ranges, showing a coarser-grained matrix, with brown biotite and rare titanite D: Sub-grain quartz rotation (outlined in yellow) around the margins of a lithic fragment within Sudbury breccia. E: Example of the image analysis process using imageJ™ software. Clasts were identified and outlined using a semi-automatic method producing a binary image; F: following manual adjustments such as removal of the epidote vein, the image is then analysed to produce quantitative values for the clasts, such as roundness..... 46

Figure 2.4: A: Thin section in PPL and B: thin section in (XPL) of flow-banded, vitric Sudbury breccia at the margins of Sudbury breccia veins from the Halfway Lake outcrop. C: Thin section in XPL illustrating flow banded, vitric Sudbury breccia from Halfway Lake, at the contact between host gneiss (red arrow) and darker, coarser breccia matrix towards the center of the vein (yellow arrow). D: Thin section in PPL of chlorite-titanite vein (yellow arrow) in altered gneiss adjacent to Sudbury breccia from Halfway Lake, which may represent devitrified melt material..... 47

Figure 2.5: A comparison of the roundness of clasts for five samples collected from three localities in the North and South Range of the Sudbury basin. The results indicate that the average roundness of

clasts from the three localities exceeds 0.4, indicative of clast entrainment in a high temperature, pseudotachylitic melt, rather than a cataclastic breccia. Roundness factors are determined based on the perimeter versus the area of each clast (see Eq. 3). 49

Figure 2.6: Immobile elements and REE from Sudbury breccia and adjacent, unbrecciated footwall lithologies, normalised to the local offset dike, which serve as proxies for an early undifferentiated impact melt. A. Sudbury breccia from Old Creighton Town shows no evidence of a melt contribution, which would ‘pull’ the geochemical signature down towards the composition of the offset dikes. B. At the McCreedy East 153 zone the relationships are more complex; most Sudbury breccia rests between the mafic and felsic gneiss footwall end members, but some samples show an enrichment that may be attributable to a primary melt sheet contribution. 50

Figure 2.7 REE chondrite normalized plot (Sun and McDonough 1989) that compares two models of Sudbury breccia from the Manchester Offset Dike locality. The breccia modelled with a quartz diorite component has a poorer correlation with the measured breccia signature, compared to the model run using only the local footwall lithologies, quartzite and Sudbury Gabbro. Averages for footwall lithologies are shown. 52

Figure 2.8: Incompatible trace element diagrams of end-member host rocks and measured and modelled Sudbury breccia, normalised to the closest quartz diorite offset dyke. Rare earth and incompatible element diagrams cover (A) South Pump Lake, (B) Old Creighton Town, (C) Creighton Deep, (D) the Murray West Zone and (E) the McCreedy 153 East Zone. Representative host lithologies are presented along with the Range of measured and modelled Sudbury breccia results... 56

Figure 2.9: Robust PCA PC1-PC2 correlation graphs of major elements and trace metals for A: Old Creighton Town and South Pump Lake Zone, B Creighton Deep and C: McCreedy 153 East. The coordinates sit within a circle of correlation. Loadings closer to the center of the circle ($y, x = 0$) indicate that not all the variation in that component is accounted for in PC1 or PC2. Loadings with similar coordinates indicate a positive correlation for those elements (e.g. MnO, MgO and Ni). See Abdi and Williams (2010) for details on PCA correlation plots. 62

- Figure 3.1: Geological map of the Sudbury Basin, showing the location of the Sudbury Igneous Complex, Superior Province and Huronian footwall units and post impact Whitewater Group. Sample locations are: 1. Coleman Mine; 2. Creighton Mine (modified after Coulter 2016)..... 82
- Figure 3.2: Surface geology for (A) Coleman Mine and (B) Creighton Mine, including the outline of the ore zones, projected to surface. Sample localities denoted by stars, with Creighton Deep and the McCreedy 153 East sites also approximately projected to surface (modified from Ames et al., 2008)88
- Figure 3.3: Mine level plans of the hand-specimen sample localities at Coleman Mine (levels 4945 and 4550), indicating proximity to footwall Cu-Ni-PGE zones and the 1240 Ma Sudbury diabase intrusion. At Coleman Mine, hand-specimens were collected from within the mineral zones and supplemented by drill core for distal samples. Attention is drawn to the different co-ordinates, depth and orientation of the two level plans. 90
- Figure 3.4: PPL thin section images of Sudbury breccia matrix from Creighton Deep and Coleman Mine, distal (A, C) and proximal (B, D) to mineralisation, displaying the progression from ‘cold’ to ‘hot’ breccia. Backscatter SEM images of two forms of titanites observed at each mine locality. At Coleman Mine, titanite is present as a reaction rim on ilmenite-magnetite grains (E) whereas at Creighton Mine the titanite is primarily an anhedral, subtly zoned overprint on pre-existing biotite (F). Abbreviations: quartz - Qtz; feldspar – Fldspr; amphibole – Amph; titanite – Ttn; ilmenite – Ilm; magnetite – Mag; allanite – All; chalcopyrite – Cpy. 94
- Figure 3.5: (A) PPL thin section image of chlorite pseudomorphs replacing biotite in breccia matrix distal to mineralization at Coleman mine. Secondary biotite is present as a deep-red-brown, variety that can be poikiloblastic. (B) PPL images of chlorite with titanite lamellae parallel to cleavage planes in alteration selvages adjacent to footwall sulfide veins at Coleman Mine. (C) PPL image of acicular, colourless actinolite distal to mineralized zones. (D) PPL image of zoned amphibole-hornblende proximal to mineralization at Creighton mine, and nickel-bearing, blue-green ferrotschermakite enclosing remobilized sulfide grains (E). (F) PPL image from Coleman mine of the larger, anhedral amphibole clots observed in samples proximal to mineralization. See figure 3.3 for explanation of abbreviations. 96

- Figure 3.6: (A) Mg-Fe-Ni substitution series in chlorites from Coleman mine, displaying two distinct groups. Distal (orange, green) are chlorite pseudomorphs of biotite, whereas chlorites within mineralized zones (type 1 vein: red, type 2 vein: purple) (B) Octahedral vacancy chlorite geothermometer, demonstrating the difference in formation temperature in distal towards proximal chlorites. Chlorites adjacent to type 1 veins: red area, type 2 veins: blue area. 104
- Figure 3.7: Biotite from Coleman (open circles) and Creighton (filled circles) with proximity to ore from distal to mineralized samples (blue-green-yellow-red). (A) Mg/Fe in chlorites and biotites, displaying the inherited geochemistry of replacement chlorites, compared with coexisting biotites. (B) Tl/Rb vs Ni/Cr shows a relative increase in Tl content in mineralized samples, though the signature is reduced at Creighton mine. (C) Ni-Cu-Cr ternary plot demonstrating increased Ni/Cr towards ore, whereas Cu results are more scattered. (D) Whole rock geochemical data from Creighton Mine, demonstrating the decreasing Rb values with proximity to mineralization that may reflect increasing Tl substitution into biotite over K, Rb and Ce. 105
- Figure 3.8: (A) Calcic amphibole classification scheme from Leake et al. (1997) demonstrating the difference between amphibole cores (blue) and rims (green), and the similarity between the latter and amphiboles in mineralized zones (red) at Creighton mine. The grey area represents amphibole from Coleman mine. (B) Titanite analyses from Creighton mine, exhibiting the increased Al+Fe content from distal samples, ~0.5-1 km from the embayment (blue) to samples within the Creighton Deep zone (red). 106
- Figure 3.9: U-Pb Tera-Wasserburg Concordia diagrams for titanites from (A) Coleman mine (n=17) and (B) Creighton Deep (n= 25), with Monte Carlo adjusted age estimates and mean squared deviation values. 109

List of Abbreviations

Apfu: Atoms per Formula Unit.

ED-EM: Energy-Dispersive Electron-Microprobe

EMPA: Electron Microprobe Analyzer

Ga: Gigaannus or one billion years absolute time

HSFE: High Field Strength Elements

ICP-MS: Inductively-Coupled-Plasma Mass-Spectrometer

K α : Emission line results when an electron transitions from atomic K-shell to the L-shell.

L α : Emission line results when an electron transitions from atomic L-shell to the M-shell.

LA-ICP-MS: Laser-Ablation Inductively-Coupled-Plasma Mass-Spectrometrer

LSHPM: Low-Sulfide High-Precious-Meta style mineralization

LREE: Light Rare Earth Elements

Ma: Megaannus or one million years absolute time

Mpx: Mega-pixel

M.y: One million years in duration

PCA: Principal Component Analysis

PGM: Platinum-Group-Metal

PPL: Plane-polarized-light microscopy

QA-QC: Quality Assurance and Quallity Control

REE: Rare Earth Element

SIC: Sudbury Igneous Complex

VMS: Volcanogenic Massive Sulfide

WD-EM: Wavelength-Dispersive Electron-Microprobe

XPL: Cross-polarized-light microscopy

ZAF: Matrix Correction Factor

Chapter 1

1 Introduction

The 1.85 Ga Sudbury Igneous Complex, situated in central Ontario, represents one of the largest known terrestrial impact structures, as well as one of North America's most prolific mining camps, with continuous Ni-Cu-PGE mining and exploration in the region since the 1880s. Since the 1970s Sudbury breccia has increasingly been recognized as an important structural control for fractionated, Cu-PGE rich mineralization. However, the formational processes for the breccia continue to be controversial, with advocates for and in-situ shock/frictional melting process and more recently an injection model involving allochthonous impact melt material. In both cases, geochemical variations and structural observations have been used to support authochthonous and allochthonous origins. Such studies are further complicated by the difference in geological settings and post-impact metamorphism between the North and South ranges of the Sudbury basin. In order to advance exploration for Sudbury breccia-hosted footwall mineralization, a more detailed understanding of the formational processes and subsequent modification and alteration of the breccia is required. This will enable a better conception of controls on trace element and metal content in the breccia matrix, which may serve as vectoring tools towards prospective zones of mineralization.

The purpose of this investigation was to perform bulk rock and mineral geochemical analysis of Sudbury breccia from around the impact structure, in order to answer the questions posed above. This research includes ICP-MS, Fire-Assay and Lithium-Metaborate Fusion geochemical data, as well as the application of a newly developed statistical mixing model and principal component analysis, with the aim of elucidating the formational processes of Sudbury breccia and implications that this has for interpreting trace metal values in the breccia matrix as a vector towards footwall Cu-Ni-PGE deposits. In addition to identifying new vectoring tools towards prospective mineralized zones, the study also determine whether any geochemical vectors have survived post-impact alteration in the South Range and concludes with recommendations on how best to further progress our understanding on the formation and alteration of Sudbury breccia and associated footwall Cu-Ni-PGE mineralization.

1.1 Impact Cratering

It has been increasingly recognized within the planetary science community that impact cratering is a far more common and important geological phenomenon on both Earth and other solid planetary surfaces than historically considered (Osinski and Pierazzo, 2013). In addition to forming a crater, hypervelocity impact events can create ejecta blankets and uplift previously buried lithologies, and they have been associated with volcanism, landslides, climate change and tsunami events, all of which may be preserved in the geological record (Dressler and Johns, 1997; Pierazzo and Melosh, 2013). However, in the case of Earth, subsequent erosion and weathering processes have left very few pristine examples of impact craters compared with other planets and satellites within the Solar System, such as the Moon and Mars. Thus older impact structures such as Haughton, Vredefort and Sudbury can only provide a partial picture of the geological processes that occurred at the time of the crater formation, and fundamental questions remain regarding the processes involved in the formation of craters and their products, termed ‘impactites’ (Grieve and Therriault, 2013; Osinski and Pierazzo, 2013).

The formation of a hypervelocity impact crater can generally be subdivided into three stages; (1) contact and compression, (2) excavation and (3) modification (Fig. 1.1). Hydrothermal alteration has sometimes been included as a separate, fourth stage and is relevant to the Sudbury impact structure (Molnar et al., 2001; Osinski and Pierazzo, 2013). The first stage involves the initial contact between the bolide and planetary surface, which generates a compressional shock wave that propagates into both the bolide and target rock, resulting in shock metamorphism and decompression melting in the latter. This produces a variety of geological features diagnostic of impact structures, including planar deformation features, shatter cones and tektites, as well as impact melt sheets (Grieve and Therriault, 2013). In the case of the projectile, complete vaporization or melting occurs as the shock waves reach the upper, free surface and are reflected back into the bolide as a rarefaction wave (Melosh 1989; Osinski and Pierazzo, 2013). As a result, rather than the projectile, the excavation stage of the crater formation is carried out by the propagation of the radial shock wave, which results in an ‘excavation flow-field’ that produces the transient cavity (Dence 1968; Melosh 1989). Material in the upper section of the cavity is ejected out, beyond the crater rim to form ejecta deposits, whereas the lower section of the cavity experiences more localized displacement (Osinski et al., 2013). Much of the ejecta is deposited as a blanket of fine dust and fall back breccia, though some lunar crater ejecta includes pools of impact melt over the rim of the

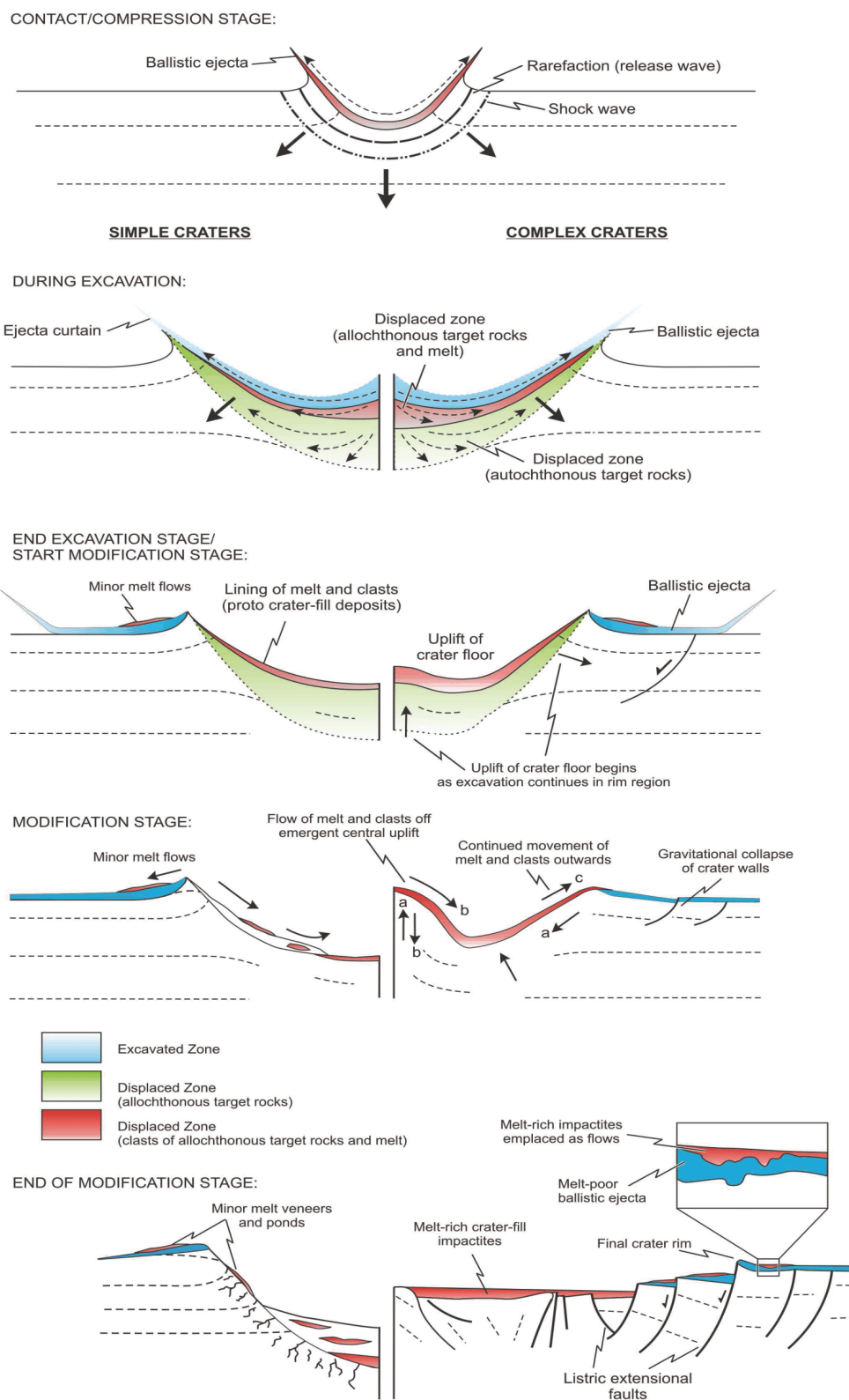


Figure 1.1: Schematic cross sections through an impact crater during the contact compression, excavation and modifications stages, highlighting the different locations of excavated, displaced and melted material. The left column depicts the formation of a smaller (<math>< 2 - 4 \text{ km}</math>), simple crater, whereas the right depicts the processes that create a complex crater, analogous to the Sudbury impact structure (from Osinski and Pierazzo 2013).

crater (Osinski et al., 2013). Following outward passage of the excavation-flow, the transient crater then experiences modification flow, which is a gravity driven reversal that attempts to close the unstable cavity (Kenkmann et al., 2013). Large impact events produce large transient cavities that are more unstable thus experiencing a more extended and drastic period of modification. Hence small ‘simple’ craters tend to retain a bowl shape, similar in appearance to the initial transient cavity, whereas cavities with a radius exceeding 2-4 kms (on Earth) will experience uplift of a central peak or ring structure and slumping of crater walls to produce collapse terranes and create a ‘complex’ crater (Melosh and Ivanov, 1999; Kenkmann et al., 2013). The development of impact breccias and the intrusion of radial and concentric impact melt-derived dikes are widely attributed to the latter crater collapse processes, which can continue for a protracted period after the impact event (Lambert, 1981; Thompson and Spray 1996; Grieve and Therriault, 2013; Kenkmann et al., 2013). Alternatively, Melosh (1979) and Melosh and Ivanov (1999) proposed that zones of impact breccia may form during the passage of the shock wave, which would generate seismic vibrations in the crater footwall. The vibrations would cause pressure fluctuations between the ambient lithostatic pressure and periods of lower pressure, during which footwall rock would behave as a viscous melt, termed ‘acoustic fluidization’. Using mathematical models Melosh (1979) demonstrated the validity of this concept in its application to explosive events, including impact cratering. Similarly, shock-heating and pressure-release during the rebound of the crater floor and/or central uplift is widely attributed to generating impact melt sheets. A similar process within the footwall could create trapped pockets of breccia melt (Reimold and Gibson 2005). In both scenarios, structural weaknesses such as fault planes and lithological contacts would serve to focus the zones of pressure fluctuation and act as preferential areas in which the pseudotachylitic melt would be generated.

1.2 Sudbury Regional Geology

The 60 x 30 km Sudbury basin is the eroded remnant of a bolide impact on the margin of the Superior Province, $1850 \pm_{-2.4}^{+1.3}$ Ma that created a complex crater with an estimated initial diameter of 200 – 250 km (Dietz, 1964; Dressler, 1984; Krogh et al., 1984; Davis, 2008; Petrus et al., 2015). The basin roughly delineates the differentiated impact melt sheet, termed the Sudbury Igneous Complex (SIC), which can be subdivided into a basal norite, overlain by quartz gabbro and granophyre units that are capped by an ‘upper contact unit’ of roof rock, termed the ‘Basal Onaping Intrusion’ (fig. 1.2) (Dietz, 1964; Naldrett and Hewins 1984;

Grieve 1994; Golightly 1994; Deutsch et al., 1995; Anders et al., 2015). Concentric and radial granodioritic intrusions, termed ‘offset-dikes’ extend outward from the SIC into the surrounding footwall rocks (Lightfoot et al., 1997a; Wood and Spray, 1998; Tuchscherer and Spray, 2002; Coulter, 2016). The differentiation of the igneous complex has been attributed to a variety of processes including fractional crystallization (Naldrett et al., 1970), viscous emulsion differentiation (Zieg and Marsh, 2005), crystallization of a density-stratified melt (Golightly 1994; Lightfoot and Keays, 2001; Keays and Lightfoot, 2004), the development of

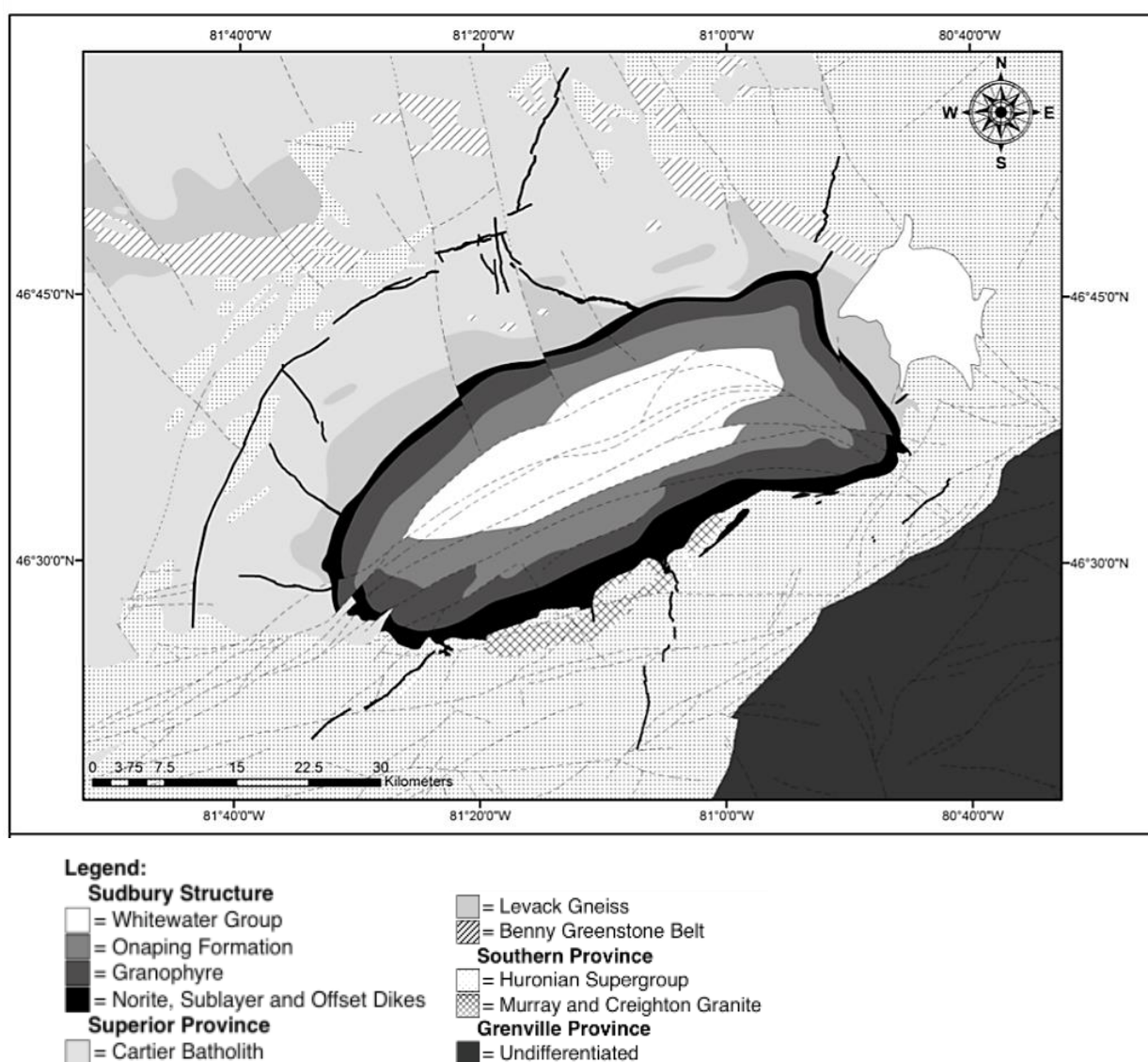


Figure 1.2: Geology of the Sudbury region, with the 30 x 60 km, elliptical Sudbury Igneous Complex at the centre, with radial and concentric offsets dikes extending out from the melt sheet. The North Range is primarily Archean granites and gneisses, whereas the South Range is comprised Paleoproterozoic metavolcanics and metasedimentary rocks. The Grenville orogenic front occupies the South East corner of the region (from Coulter 2016).

a two melt system (Chai and Eckstrand, 1994) and / or assimilation of the underlying footwall (Dickin et al., 1996). This latter process has been attributed to the formation of the sublayer; a discontinuous noritic to gabbroic, inclusion-bearing unit that is hosted in thermal erosion pits and slumping troughs in the footwall contact, termed embayments, which also served to localize sulfide melts (Lightfoot et al., 1997d; Prevec et al., 2000; Ames and Farrow, 2007; Lightfoot, 2007). Although historically grouped with the Sublayer, the offset dikes are now considered to represent an earlier component of the impact melt sheet that was emplaced into the footwall prior to the differentiation of the igneous complex (fig. 1.3) (Souch et al., 1969; Lightfoot et al., 1997a). The 2043 ± 4 Ma Vredefort impact structure, situated in South Africa, is considered analogous to the Sudbury structure, albeit slightly larger (estimated initial crater radius of ~ 300 km) and more deeply eroded (to ~ 7 km depth), and comprises impact melt units, radiating granophyre intrusions and impact breccias (Reimold and Gibson, 1996; Reimold and Gibson, 2006). As a result, Vredefort has been used as a comparison in studies of other impact structures, such as Sudbury, particularly regarding pseudotachylitic breccia, for which the South African structure is the type locality (Shand, 1916; Riller et al., 2010; Lieger et al., 2011).

The footwall lithologies of the Sudbury structure can be divided into the Superior Province of the North (including East) Range and the Southern Province, Huronian Supergroup of the South Range (fig. 2.1). The Superior Province consists of a series of high grade gneiss terranes in the north and south, with a central belt of metasedimentary and volcano-plutonic belts (Card and Ciesielski, 1986). In the vicinity of Sudbury, the Superior Province comprises the 2711 ± 7 Ma, tonalite-granodiorite Levack Gneiss Complex, from which the monzogranitic-granodioritic, 2642 ± 1 Ma, Cartier Batholith was formed by partial melting of the Levack gneiss during the Kenoran Orogeny (Krogh et al., 1984; Card and Ciesielski, 1986; Meldrum et al., 1997; Rousell and Brown, 2009). A 40 x 5 km wide segment of highly deformed metavolcanic and metasediment units, termed the Benny Greenstone Belt, runs east to west through the North Range approximately 20 km north-west of the SIC (Card and Innes, 1981). This is associated with outliers of Huronian material that extends in an arcuate belt across the North Range, from Vernon to Leinster Township. Spray and Thompson (1995) and Mungall and Hanley (2004) concluded that the outliers represent segments of the more extensive Southern Province, which were deformed prior to the impact event and then displaced by slump faulting of an extensive ring structure in the collapsing crater wall during its modification. Subsequent erosion left the down-faulted blocks as detached outliers.

However, Rousell and Long (1998) argue that the pseudotachylitic fault breccia zones cut through, rather than offset the Huronian outliers, thus refuting their formation as a crater collapse feature, and instead advocate that the outliers are preserved synclines that formed during the Penokean (1.8 – 1.7 Ga) or Blezardian (2.4 – 2.2 Ga) orogenic events.

The South Range of the SIC is composed of early Proterozoic-aged metasedimentary and metavolcanic rocks of the Huronian Supergroup, deposited during a transition period from transform rifting to a passive margin, at the edge of a Paleoproterozoic ocean (2491 ± 5 to 2219 Ma) (Krogh et al., 1996; Rousell and Brown 2009). The Huronian Supergroup at Sudbury can be roughly subdivided into two belts; an inner belt that straddles the SIC, composed of mafic and felsic extrusive and intrusive units and volcanoclastics and minor siltstones broadly termed the Elliot Lake Group, versus an outer belt of Hough and Quirke Lake Group quartz-arenites, conglomerate, arkose, mudstone and minor limestone (Card et al., 1977; Ames et al., 2008; Rousell and Brown, 2009). These units were subsequently intruded by the 2376 ± 2.3 Ma Creighton and 2477 ± 9 Ma Murray granite plutons (Krogh et al., 1996; Smith et al., 1999), which were either emplaced during crustal extension during continental rifting (Rousell and Long, 1998), or during the development of a major fold structure during the Blezardian Orogeny (2.4-2.2 Ga) (Riller and Schwerdtner 1997; Riller, 2005). Both plutons contain roof pendants and entrained rafts of Huronian material, as well as rare cases of basement derived gneissic xenoliths, brought up during emplacement. The 2217 ± 4 Ma Nipissing gabbro is another intrusive unit found in the Sudbury region, both North and South of the SIC (Noble and Lightfoot, 1992; Ames et al., 2008). Lightfoot et al. (1993) conclude that the gabbro was probably derived from mantle material that was mixed with subducted crust during the Kenoran orogeny, prior to its emplacement. Despite its relative homogeneity, Nipissing gabbro around the Worthington offset dike is compositionally distinct (e.g., it has a higher MgO content), and has been termed ‘Sudbury gabbro’ in some literature (Card and Pattison 1973). The footwall of the SIC has also been intruded by the 2452 Ma, plagioclase-phenocrystic Matachewan diabase swarm, that comprises multiple pulses of tholeiitic Fe-rich basalts that infer a source that was continuously replenished with either MORB or depleted mantle material, separate from that which created the Nipissing gabbros (Nelson, 1987). The Sudbury olivine diabase swarm was emplaced at 1238 ± 5 Ma and cross cuts the footwall, SIC and several ore deposits. The dikes occupy pre-existing brittle structures and are associated with lithospheric melting and volcanism associated with the contemporaneous Elzevirian Orogeny (1.25 – 1.19 Ga) (Shellnutt and MacRae, 2011).

Following the 1850 Ma Sudbury impact event, the Sudbury basin was overlain by Onaping Formation breccias (Grieve et al., 2010) and later interbedded mudstone and turbidite sequences of the Vermilion, Onwatin and Chelmsford Formations, which together comprise the Whitewater Group (Rousell and Brown, 2009). The Chelmsford Formation sandstones yield the youngest Rb/Sr age of 1720 ± 30 Ma (Fairbairn et al., 1968). The group represents a series of sedimentary packages that were laid down in a shallow, continental-shelf setting at the margin of the Nuna continent. The Onaping Formation has been overprinted by SIC-related hydrothermal alteration, and the Vermilion Formation hosts small (<5 million tonne) Zn-Pb-Cu VMS deposits associated with the underlying SIC (Severin and Gates 1981).

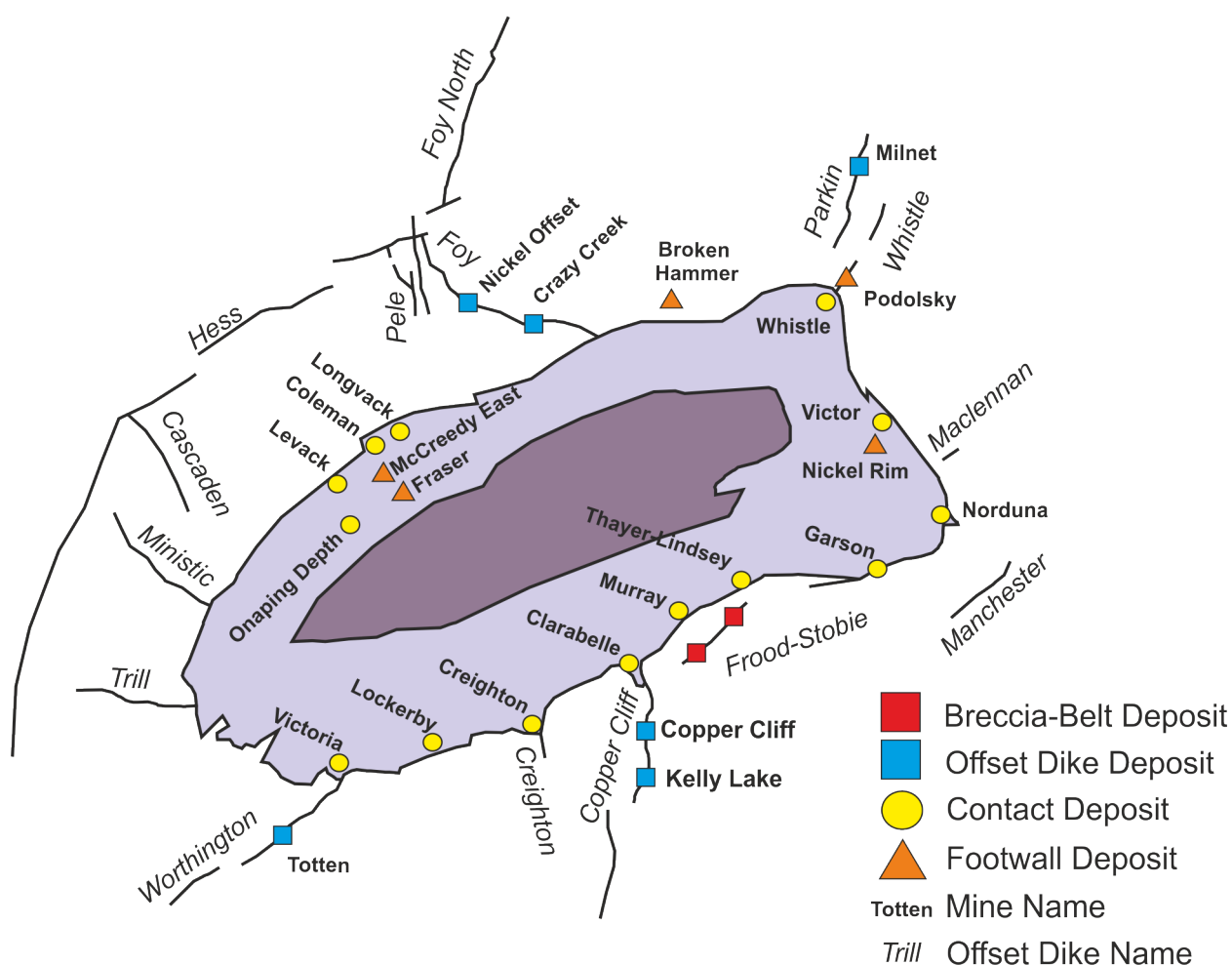


Figure 1.3: Outline of the Sudbury Igneous Complex highlighting examples of active and historic contact, footwall, offset dike and breccia belt deposits, as well as each of the known offset-dikes in the surrounding footwall (modified after Coulter 2016 and Ames and Farrow 2007).

1.2.1 Sudbury Breccia

Sudbury breccia consists of a dark grey, aphanitic matrix that hosts rounded to sub-rounded lithic clasts and mineral fragments (individual grains of footwall-derived material) of locally derived footwall material (Fig. 1.4a). The breccia is found as veins and belts up to 10's of meters wide in the footwall of the Sudbury impact structure, and is found up to 80 km from the basin at Whitefish Falls and Temagami Lake (Speers, 1957; Dressler, 1984; Parmenter et al., 2002; Rousell et al., 2003). Sudbury breccia is analogous to pseudotachylite from the Vredefort impact structure (Fig. 1.4b). It has been proposed that the more pervasive zones of brecciation represent arcuate collapse terranes, formed during the modification of the crater wall. The fault planes upon which the terranes were displaced may have experienced a continuum between initially low temperature cataclasis and comminution (i.e., mechanical grinding of a rock into powder) to higher temperature frictional melting and thermomechanical erosion (Thompson and Spray, 1996; Rousell et al., 2003; Mungall and Hanley, 2004; Spray, 2010). This is similar to the process that forms tectonic pseudotachylites in earthquake fault zones (Maddock, 1974; Di Toro and Pennacchioni, 2004; Bestmann et al., 2011); albeit forming in a single slip event and producing much more extensive zones of breccia in the case of impact events. Although Lafrance et al. (2008) and Lafrance and Kamber (2010) support a cataclastic process, they suggest that the process was in response to the passage of the shock wave (i.e., shock-induced) rather than movement along major fault planes, which appear to be notably absent in the footwall of the Sudbury structure. Alternatively, Sudbury breccia could have formed during the initial passage of the compressional shock wave, which is followed by a low pressure zone in which decompression melting, rather than cataclasis, may occur (Lambert, 1981; Reimold and Gibson 2005). The lithospheric rebound and deformation of the crater floor to produce central uplifts may also contribute to decompression melting in the footwall. Similarly, Melosh (1979) and Melosh and Ivanov (1999) proposed that impact breccias such as Sudbury breccia may form by seismic vibrations that cause the footwall rocks to melt and behave as a viscous material, a process termed 'acoustic fluidization'.

Outcrops in the South Range tend to be coarser grained and exhibit flow banding and fabric alignments compared to the North Range breccia, which is considered by Rousell et al. (2003) to be indicative of cataclasis under lower temperature conditions involving lamellar convection flow under conditions involving pre-existing fluids in the target lithologies. This is supported by trace amounts of pore fluids in the metasedimentary units of the South Range, which have been demonstrated by Magloughlin (1992) to affect strain rates within active fault zones, encouraging comminution rather than melting processes. Alternatively, the coarser grain size of the breccia matrix may be a result of the rheological differences between the largely crystalline footwall rocks of the North Range, versus the metavolcanic and metasedimentary rocks of the South Range (Kennedy and Spray, 1992) or the greater pressure-temperature conditions at the time of the impact event, prior to the uplift of the South Range by 5 – 10 kms relative to the North Range in post-impact orogenic events (see section 1.5). The South Range also experienced higher metamorphic conditions, (up to amphibolite facies) in post-impact orogenic events, compared with the greenschist facies conditions experienced in the North Range, as demonstrated by the preservation of tschermakitic hornblende at Kirkwood, Copper Cliff and Creighton Mines (Fleet et al., 1987; Magyarosi et al., 2002).

In-situ cataclasis and frictional or shock melting would be expected to produce a breccia matrix that is compositionally similar to that of the target rock from which it is derived. However, as noted in studies by Riller et al. (2010) and Lieger et al. (2011), the



Figure 1.4: Examples of ‘pseudotachylitic’ impact breccia from Highway 24, Creighton Township, Sudbury (A) and Leeukop Quarry, Parys Sector, South Africa (B). These images demonstrate the comparable nature of Sudbury breccia and Vredefort pseudotachylite at these two large (>200 km radius) impact structures (Vredefort image from Thomas 2013).

geochemistry of pseudotachylitic breccia at Vredefort and Sudbury tends to share an homogenised geochemical signature that is indicative of an allochthonous component. Instead, they propose that the breccia matrix is derived from the injection or drainage of a high temperature impact melt into low pressure, brecciated zones in the crater footwall (Randall, 2004; Lieger et al., 2009; Riller et al., 2010; Lieger et al., 2011). The initially granitic composition of the injected melt was subsequently modified by the partial assimilation of footwall rocks. The presence of igneous textures, such as 120° cooling contacts between quartz grains, in the breccia matrix is consistent with cooling from a melt, though other indicators, such as glassy inclusions formed from rapid cooling are less likely to be preserved owing to their metastable nature (Magloughlin, 1992).

1.2.2 Ni-Cu-PGE Mineralization

Sulfide mineralization was first discovered by geologists in the Sudbury region in 1856, though its significance was not recognized until the Canadian-Pacific railroad passed through the area nearly 30 years later. There have been 77 active mines in the Sudbury basin since 1883, of which two extracted Pb-Zn VMS ores situated within the Whitewater Group (Severin and Gates, 1981; Ames and Farrow, 2007). New mineralization continues to be discovered, particularly in the offset dikes and footwall environment, including the Totten depth deposit that was discovered in the mid-1990s. Ni-Cu-PGE mineralization can be broadly divided into three categories; Ni-Cu contact style, Cu-Ni-PGE footwall style and Cu-Ni-PGE offset dike-hosted (fig. 1.6). A fourth style of mineralization is hosted in the Froid-Stobie breccia belt, which runs for ~45 kms as an arcuate zone through the South Range and hosts giant (>600mt) Ni-Cu-PGE deposits. The belt was originally termed an offset dike (Souch et al., 1969) but is now considered a collapse terrane of Sudbury breccia into which magmatic sulphides and impact melt were injected to create a hybrid style deposit (Scott and Spray, 2000).

Contact style deposits were the first to be discovered, in the vicinity of the current Murray Mine in the South Range (Ames and Farrow, 2007). They are situated within sublayer material at the base of the SIC melt sheet, within embayment and trough structures, which served to localize the mono-sulfide solid solution (MSS) melt that formed during the fractional crystallization of the melt sheet (fig. 1.6). Contact ore are primarily composed of pyrrhotite > pentlandite > chalcopyrite with minor magnetite and pyrite (fig 1.5A) (Naldrett 1984). Over half of the historical resources at Sudbury are hosted within contact deposits, which include the Creighton, Murray and Coleman East Mines (Lightfoot and Keays, 2001). They are also the most nickeliferous style of mineralization with an average Cu/Ni ratio of 0.7 and total precious metals (Pt+Pd+Au) typically below 1g/t (Naldrett and Pessaran 1992). In the South Range, the activation of ductile shear zones during and after the formation of the contact ore zones has resulted in sheared contact deposits that have been remobilized into the footwall as dissemination and brecciated sulfide zones (Ames and Farrow, 2007; Mukwakwami et al., 2014). These transported contact deposits retain most of their original

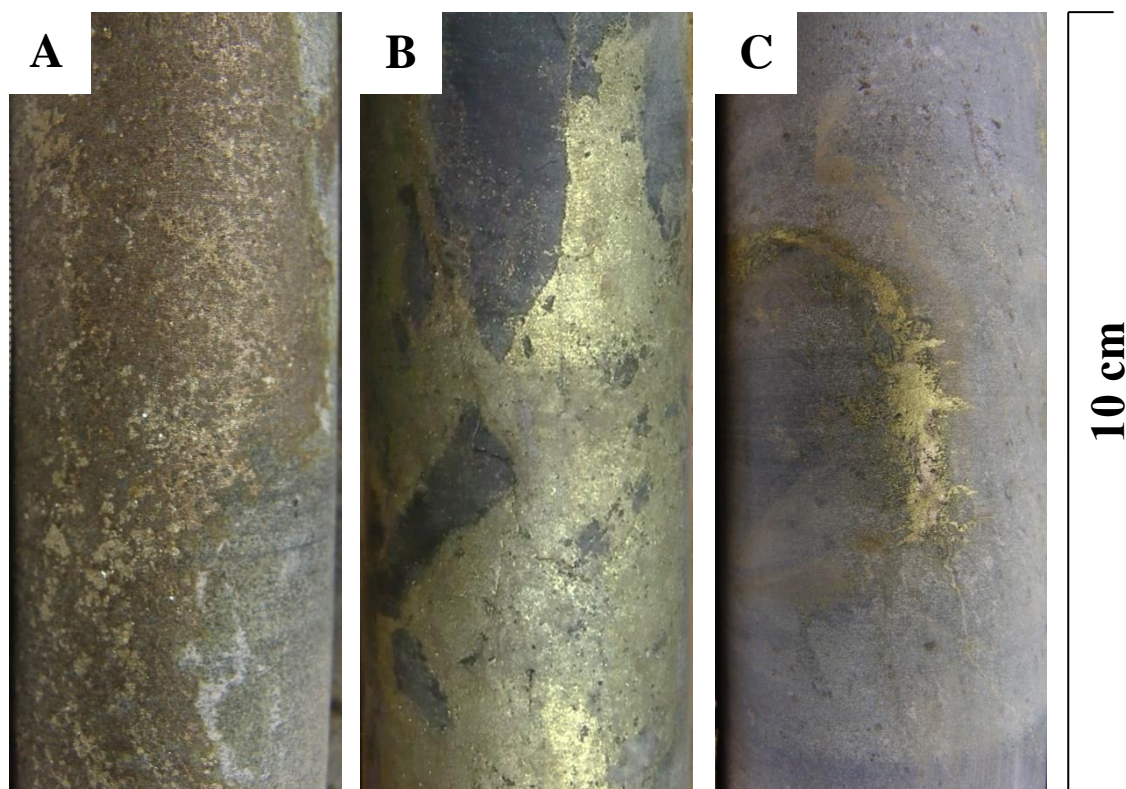


Figure 1.5: Drill core examples of (A) pyrrhotite + pentlandite contact-style mineralization from Creighton Mine, which is similar to that observed in the offset dike deposits such as at Totten mine (B) sharp-walled vein mineralization of chalcopyrite + cubanite, with inclusions of footwall material and (C) stringers and disseminations of chalcopyrite + millerite with an epidote + chlorite + magnetite alteration zone from Coleman Mine.

geochemical and mineralogical characteristics, though Cu and PGM depletion suggests at least some metal mobilization to form 'true' footwall style Cu-Ni-PGE mineralization (see below) (Mukwakwami et al., 2014). Garson Mine is the best example of a sheared contact deposit, though similar, albeit smaller examples exist at the Thayer Lindsley and Creighton Mine (Bailey et al., 2006; Dare et al., 2010).

The second type of Ni-Cu-PGE mineralization in the quartz diorite offset dikes has been discovered up to 7 km along strike from the base of the impact melt sheet. Gossanous, sub-economic material has also been reported in more distal segments of the concentric Manchester offset dike (O'Connor and Spray, 1997; Lightfoot et al., 1997b). The offset dikes can be subdivided into an inclusion free and inclusion bearing pulse, the latter of which tends to occupy the center of the intrusions and host massive to semi-massive zones and disseminations of pyrrhotite >> pentlandite > chalcopyrite (Lightfoot et al., 1997c; Tuchscherer and Spray, 2002; Ames and Farrow, 2007). As the offset dikes are connected to the main melt sheet via embayment structures, the sulfide mineralization is considered to be derived from remobilization of magmatic, contact deposits, though geochemically they are more Cu-PGM enriched (Cu/Ni ratio 1 and precious metals ~2.5 g/t) (Ames and Farrow, 2007).

Footwall style mineralization is primarily hosted in extensive zones of Sudbury breccia underlying the impact melt sheet (fig. 1.6). The breccia acted as a structural host for fractionated intermediate solid-solution (ISS) sulfide melts derived from overlying, embayment-hosted MSS contact style mineralization. This resulted in the formation of three styles of mineralizations: sharp-walled, massive chalcopyrite > cubanite > pyrrhotite > pentlandite >> magnetite + pyrite veins that are up to several meters thick (Fig 1.5B) (Abel et al., 1979; Naldrett et al., 1999; Farrow et al., 2005; Ames and Farrow, 2007; Lightfoot, 2007; Pentek et al., 2008). Although in most cases the footwall deposits are unconnected to contact deposits or embayments, there are rare examples where transitional mineralization is observed linking the two (e.g., the 9 Scoop deposit at Coleman Mine, which links the McCreeedy East contact deposits to the McCreeedy East 153 footwall deposit) (MacBurnie pers. comms. 2015). Towards the terminations of the chalcopyrite + cubanite veins is a second style of sharp-walled mineralization composed of bornite + millerite (Farrow and Watkinson, 1997; Farrow et al., 2005; Pentek et al., 2008). These Cu-rich veins tend to be < 1m thick and are considered to represent either more fractionated ISS melt that has been

transported further into the footwall (Ebel and Naldrett, 1996; Ballhaus et al., 2001) or increased interaction with fluids circulating in the footwall (Nelles, 2012). In the case of the latter, such fluids would react with the sulphides, consuming Fe and S, thereby causing the sulfide melt to crystallize a more Cu-rich assemblage. Expulsion of trace metals from the footwall veins resulted in a halogen and metalliferous halo of amphibole + chlorite + epidote within Sudbury breccia hosting sharp-walled vein systems (Abel et al., 1979; Jago et al., 1994; McCormick et al., 2002; Hanley and Mungall, 2003; Nelles, 2012). Sharp-walled mineralization typically has a Cu/Ni ratio of ~5:1 and precious metal content >7 g/t (Naldrett et al., 1999; Ames and Farrow, 2007). A third type of footwall mineralization, termed ‘low-sulfide, high-precious-metal’ (LSHPM) style is observed as blebs, stringers and disseminations of chalcopyrite >> millerite (Pt + Pd + Au >5 g/t, in some cases up to 200 g/t)

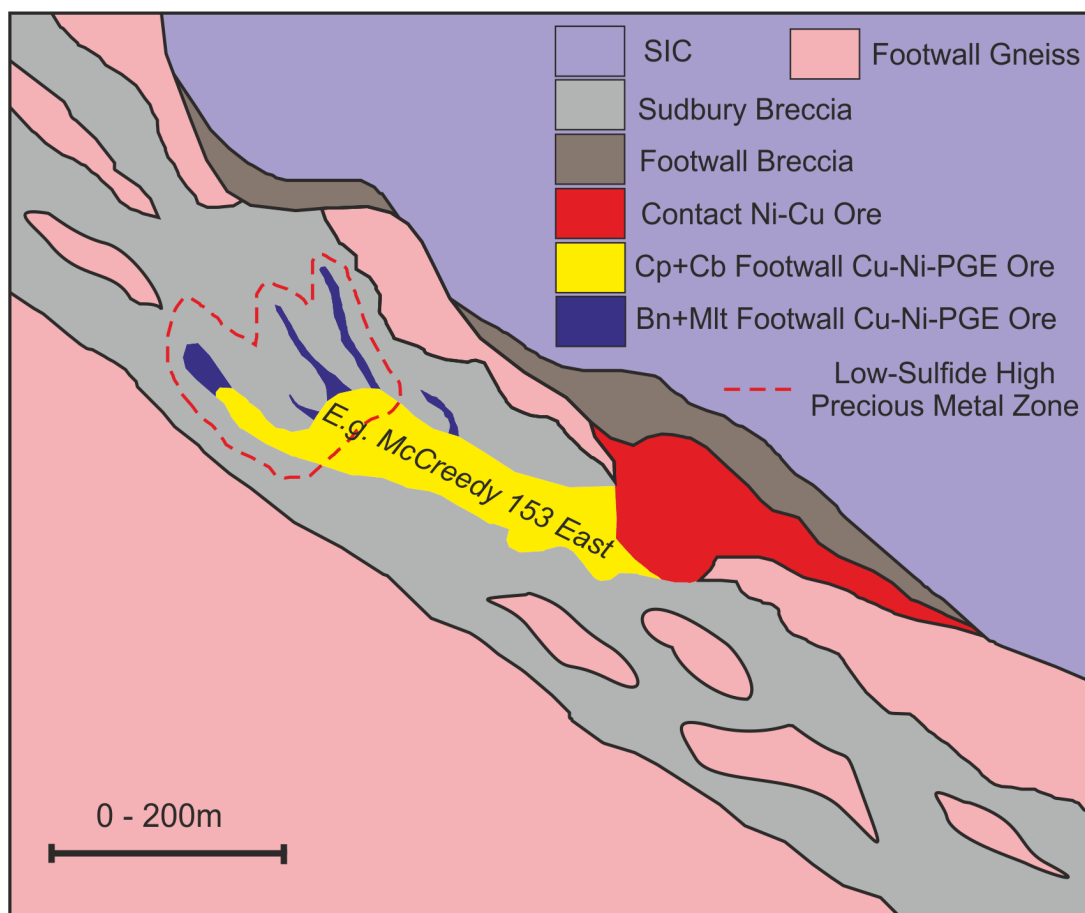


Figure 1.6: Cross section through the SIC-Footwall contact showing the relationship between embayment- and sublayer-hosted contact style ores and more fractionated, Sudbury breccia hosted chalcopyrite+cubanite (Cp+Cb) footwall veins, towards the terminations of which bornite+millerite (Bn+Mlt) and LSHPM mineralization are occasionally found (modified after Rousell and Brown 2009).

and total sulfur <3 wt.% (fig 1.5C) (Ames and Farrow, 2007; Gibson et al., 2010; Tuba et al., 2014). Precious metals tend to be found as inclusions within the sulphides, but can be found as rare, discrete trace minerals such as sperrylite (PtAs₂) and moncheite (PtTe₂) (Farrow and Lightfoot, 2002). LSHPM mineralization is spatially associated with sharp-walled veins and offset-dike sulphides, from which the PGE's were mobilized by hydrothermal-magmatic fluids either expelled from the cooling sulphide and impact melt or circulating in the footwall (Molnar et al., 1997; Marshall et al., 1999; Molnar et al., 2001; Farrow and Lightfoot, 2002; Ames and Farrow, 2007; White, 2012; Tuba et al., 2014). Although this PGE-enriched style of mineralization is highly lucrative, to date only a few purely LSHPM deposits have been mined (e.g., McCreedy West PM), the remainder being extracted as part of larger sharp-walled deposits (e.g., Podolsky, McCreedy East). In the South Range, as with contact-style deposits, there is evidence that some LSHPM occurrences have been structurally remobilized along shear faults (e.g., Denison 109 FW) (Gibson et al., 2010; White, 2012).

1.2.3 Metamorphic and Hydrothermal History

Prior to the Sudbury impact event at 1850 Ma, the target lithologies had experienced a number of metamorphic events such as the formation of the Levack Gneiss Complex at 2661 ± 2 Ma and its subsequent partial melting to form the Cartier granite at $\sim 2642 \pm 1$ Ma during the Kenoran Orogeny (Meldrum et al., 1997; Rousell et al., 1997; Ames et al., 2008). The Southern Province and Huronian units underwent folding and faulting between 2415 and 2353 Ma, associated with the Blezardian orogeny (Raharimahefa et al., 2014). Between 1900 and 1770 Ma, contemporaneous with the impact event, the region experienced greenschist to lower amphibolite facies metamorphism associated with the Penokean orogeny, to which much of the deformation of the impact structure and onset of shear zones in the South Range has been attributed (fig. 1.3) (Fleet et al., 1987; Bennet et al., 1991; Rousell et al., 1997; Bailey et al., 2004; Rousell and Brown, 2009). In addition, the development of a ~ 2 km wide thermal aureole in footwall lithologies adjacent to the impact melt sheet was concurrent with the Sudbury impact event. Partial melt textures within the aureole indicate temperatures reached up to 1000 °C (Dressler, 1984; Coats and Snajdr 1984; Prevec and Cawthorn, 2002; Pentek, 2009). Although evidence of the thermal overprint in the South Range has largely been destroyed by post-impact metamorphic activity, studies in the North Range have subdivided the aureole into three units; a distal albite + epidote hornfels (2000 – 1200 m from SIC-footwall contact), a hornblende hornfels (1100 – 350 m) and a pyroxene hornfels (>350 m). Granophyric partial melt segregations have also been observed up to 500 m into the

footwall at some localities (Pentek, 2009). During cooling of the melt sheet, magmatic and regional groundwater fluids interacted to create a high temperature ($\sim 440 - 540^{\circ}\text{C}$), saline (50 wt.% NaCl equiv.), $\text{H}_2\text{O} + \text{NaCl} \pm \text{CO}_2 \pm \text{KCl}$ fluid. Combined with hydrocarbon-rich brines derived from the cooling footwall and contact sulfide melts, these two fluids are attributed to remobilizing trace metals into the footwall and creating the hydrous, metalliferous halo around footwall mineralization observed in the North Range (Farrow and Watkinson, 1992; Marshall et al., 1999; Molnar et al., 2001; McCormick et al., 2002; Hanley et al., 2005).

The waning stages of the Penokean Orogeny were marked by a second hydrothermal system, identified as a $\sim 300 - 350^{\circ}\text{C}$, variable salinity (6 – 26 wt. % NaCl equiv.) $\text{NaCl} + \text{CO}_2 + \text{CH}_4 + \text{H}_2\text{O}$ fluid (Molnar et al., 1997; Molnar et al., 2001; Pentek, 2009). This was followed by the onset of the Yavapai-Mazatzal Orogeny at 1770 Ma that continued until ~ 1600 Ma (Rousell et al., 1997). During this period the South Range experienced greenschist to lower amphibolite grade metamorphism, based on staurolite porphyroblasts situated in the vicinity of Creighton Mine and Long Lake (Rousell et al., 1997; Ames et al., 2008; Rousell and Brown, 2009 and references therein; Raharimahefa et al., 2014). Shear zones were also reactivated and provided pathways for metamorphic fluids, as demonstrated by contemporaneous titanites hosted in faults within the Thayer-Lindsley Mine (Bailey et al., 2004). This was followed by the Chieflakian Orogeny around 1450 ± 51 Ma. As with previous orogenic events, the South Range was more extensively affected than the North Range, with greenschist to lower amphibolite facies alteration and the emplacement of hornblende diabase dikes into pre-existing fault structures such as the Murray and Creighton faults (locally termed ‘trap-dikes’) (Cochrane 1984; Fueten and Redmond, 1997; Rousell et al., 1997). Although it is the general consensus that the Penokean Orogeny resulted in the uplift of the South Range by 5 – 10 kms relative to the North Range, Fueten and Redmond (1997) argue that the later Chieflakian event created the South Range shear zone and associated displacement. Around 1238 ± 5 Ma, the North-West trending Sudbury olivine diabase dike swarm was emplaced in both the North and South Range (Krogh et al., 1987; Rousell et al., 1997). Initially considered a triple junction of radiating dikes from a central volcanic region under an extensional tectonic regime (Fahrig 1987), the intrusions are now thought to be contemporaneous with lithospheric melting and magmatism associated with the Elezvirian Orogeny and closure of the Elizvir basin (Shellnutt and MacRae, 2011). These intrusions are thought to have remobilized Ca-rich, Canadian Shield brines into brittle

structures in the Sudbury basin, including host-rock-sulfide-vein contacts, resulting in a second period of trace metal remobilization and reprecipitation (Molnar et al., 2001; Tuba et al., 2014).

The final major metamorphic event to affect the Sudbury region was a series of orogenic events often grouped as the Grenville Orogenies. These can be subdivided into the ~1250-1190 Elzevirian, Shawingian ~1140-1080, Ottawa ~1080-1020 and the 1010-980 Rigolet orogenies (Rousell et al., 1997) that resulted in the thrusting of the Mesoproterozoic Grenville Province over the Southern Province, ~30 km south of the SIC. Although the orogeny is considered to have had a limited influence on the Sudbury basin (e.g., brittle deformation of Sudbury diabase dikes) (Rousell et al., 1997; Rousell and Brown, 2009; Raharimahefa et al., 2014), there is Ar^{40}/Ar^{39} isotope evidence of a low-grade, thermal metamorphic event simultaneous with the Grenville orogeny, which influenced the Sudbury region as far north as the Benny Greenstone Belt (Thompson et al., 1998). There is also evidence of a final 5–13 Ma saline fluid associated with neotectonic brittle structures and some galena-sphalerite mineralization, though the metals are unlikely to have been derived from footwall Cu-Ni-PGE zones (Marshall et al., 1999).

1.3 Introduction to the Thesis

Chapter 2 presents the field, petrographic and whole-rock geochemical data for Sudbury breccia from a variety of field sites around the Sudbury basin. This chapter forms the basis of a paper that has been approved for publication in *Economic Geology*.

Chapter 3 details the mineralogy and mineral chemistry investigations of Sudbury breccia from Creighton Mine in the South Range and Coleman Mine from the North Range.

Combining electron microprobe analysis from the University of Western Ontario, with LA-ICP-MS elemental and U-Pb age dating work performed at Laurentian University, this study compares the changes in alteration assemblages in Sudbury breccia with proximity to footwall deposits. This chapter forms the basis for a manuscript currently in review with *Canadian Mineralogist*.

Chapter 4 highlights the primary conclusions and observations of this study, whilst putting them into the context of previous work on footwall mineralization, Sudbury breccia and impact cratering in general. There are also recommendations for future studies on the

Sudbury breccia The large datasets in both of these studies has required that most of the geochemical data is presented in separate, supplementary appendices.

1.4 References

- Abel, M.K., Buchan, R., Coats, C.J.A., and Penstone, M.E., 1979, Copper Mineralization in the Footwall Complex, Strathcona Mine, Sudbury, Ontario: *Canadian Mineralogist*, v. 17, p. 275–285.
- Ames, D., and Farrow, C., 2007, Metallogeny of the Sudbury mining camp, Ontario., in Goodfellow, W.D. ed., *Mineral Deposits of Canada: A Synthesis of Major Deposit-Types, District Metallogeny, the Evolution of Geological Provinces, and Exploration Methods*, Geological Association of Canada, Mineral Deposits Division, Special Publication, p. 329–350.
- Ames, D.E., Davidson, A., and Wodicka, N., 2008, Geology of the Giant Sudbury Polymetallic Mining Camp, Ontario, Canada.: *Economic Geology*, v. 103, p. 1057–1077.
- Anders, D., Osinski, G.R., Grieve, R.A.F., and Brillinger, D.T.M., 2015, The Basal Onaping Intrusion in the North Range: Roof rocks of the Sudbury Igneous Complex: *Meteoritics & Planetary Science*, v. 50, no. 9, p. 1577–1594.
- Bailey, J., Lafrance, B., McDonald, A.M., Fedorowich, J.S., Kamo, S., and Archibald, D.A., 2004, Mazatzal–Labradorian-age (1.7–1.6 Ga) ductile deformation of the South Range Sudbury impact structure at the Thayer Lindsley mine, Ontario: *Canadian Journal of Earth Sciences*, v. 41, no. 12, p. 1491–1505.
- Bailey, J., McDonald, A.M., Lafrance, B., and Fedorowich, J.S., 2006, Variations in Ni content in sheared magmatic sulfide ore at the Thayer Lindsley Mine, Sudbury, Ontario: *Canadian Mineralogist*, v. 44, no. 5, p. 1063–1077.
- Ballhaus, C., Tredoux, M., and Spa, A., 2001, Phase Relations in the Fe-Ni-Cu-PGE-S System at Magmatic Temperature and Application to Massive Sulphide Ores of the Sudbury Igneous Complex: *Journal of Petrology*, v. 42, no. 10, p. 1911–1926.

- Bennett, G., Dressler, B.O. and Robertson, J.A. 1991. The Huronian Supergroup and associated intrusive rocks; in *Geology of Ontario*, Ontario Geological Survey, Special Volume 4, Part 1, p.549-591.
- Bestmann, M., Pennacchioni, G., Frank, G., Göken, M., and de Wall, H., 2011, Pseudotachylyte in muscovite-bearing quartzite: Coseismic friction-induced melting and plastic deformation of quartz: *Journal of Structural Geology*, v. 33, no. 2, p. 169–186.
- Card, K.D., and Ciesielski, A., 1986, Subdivisions of the Superior Province of the Canadian Shield.: *Geoscience Canada*, v. 13, no. 1, p. 5–13.
- Card, K.D. and Innes, D.G. 1981. *Geology of the Benny area, District of Sudbury*; Ontario Geological Survey, Report 206, 117p.
- Card, K.D. and Pattison, E.F., 1973. Nipissing diabase of the Southern Province; in *Huronian stratigraphy and sedimentation*, in Young, G.M., ed., Geological Association of Canada Special Paper 12, p. 7-30.
- Card K.D., Innes D.G., Debicki R.L., 1977. *Stratigraphy, Sedimentology and Petrology of the Huronian Supergroup in the Sudbury-Espanola Area*: Ontario Division of Mines, Geoscience Study 16, 99 p.
- Chai, G., and Eckstrand, R., 1994, Rare-earth element characteristics and origin of the Sudbury Igneous Complex, Ontario, Canada: *Chemical Geology*, v. 113, p. 221–244.
- Coats, C.J.A. and Snajdr, P. 1984. Ore deposits of the North Range, Onaping–Levack area, Sudbury; in *The Geology and Ore Deposits of the Sudbury Structure*, Ontario Geological Survey, Special Volume 1, p.327-346
- Cochrane, L.B., 1984. Ore deposits of the Copper Cliff Offset; in *The Geology and Ore Deposits of the Sudbury Structure*, Pye, E.G., Naldrett, A.J. and Giblin, P.E., eds.; Ontario Geological Survey; Special Volume No. 1, p. 97-138.
- Coulter, A.B., 2016, *Recent Discoveries in the Ni-Cu-PGE bearing Trill and Parkin Offset dykes, Sudbury impact structure, Canada*: Unpublished thesis, University of Western Ontario, 152 p.

- Dare, S.A.S., Barnes, S.-J., Prichard, H.M., and Fisher, P.C., 2010, The Timing and Formation of Platinum-Group Minerals from the Creighton Ni-Cu-Platinum-Group Element Sulfide Deposit, Sudbury, Canada: Early Crystallization of PGE-Rich Sulfarsenides: *Economic Geology*, v. 105, p. 1071–1096.
- Davis, D.W., 2008, Sub-million-year age resolution of Precambrian igneous events by thermal extraction–thermal ionization mass spectrometer Pb dating of zircon: Application to crystallization of the Sudbury impact melt sheet: *Geology*, v. 36, no. 5, p. 383–386.
- Dence M. R. 1968. Shock zoning at Canadian craters: Petrography and structural implications. In *Shock metamorphism of natural materials*, edited by French B. M. and Short N. M. Baltimore: Mono Book Corp. pp. 169–184.
- Deutsch, A., Grieve, R.A.F., Avermann, M.E., Bischoff, L., Brockmeyer, P., Buhl, D., Lakomy, R., Müller-Mohr, V., Ostermann, M., and Stoffler, D., 1995, The Sudbury Structure (Ontario, Canada): a tectonically deformed multi-ring impact basin: *Geologische Rundschau*, v. 84, p. 697–709.
- Dickin, A.P., Artan, M.A., and Crocket, J.H., 1996, Isotopic evidence for distinct crustal sources of North and South Range ores, Sudbury Igneous Complex: *Geochimica et Cosmochimica Acta*, v. 60, no. 9, p. 1605–1613.
- Dietz R.S., 1964, Sudbury Structure as an Astrobleme: *The Journal of geology*, v. 72, no. 4, p. 412–434.
- Di Toro, G., and Pennacchioni, G., 2004, Superheated friction-induced melts in zoned pseudotachylytes within the Adamello tonalites (Italian Southern Alps): *Journal of Structural Geology*, v. 26, no. 10, p. 1783–1801.
- Dressler, B., 1984, The Effects of the Sudbury Event and the Intrusion of the Sudbury Igneous Complex on the Footwall Rocks of the Sudbury Structure, in Pye, E.G., Naldrett, A.J., and Giblin, P.E. eds., *Geology and Ore Deposits of the Sudbury Structure*, Ontario Geological Survey, p. 99–131.
- Dressler, B.O., and Johns, G.W., 1997, Large meteorite impacts and planetary evolution: *Geoscience Canada*, v. 24, no. 4, p. 203–204.

- Ebel, D.S., and Naldrett, A. J., 1996, Fractional crystallization of sulfide ore liquids at high temperature: *Economic Geology*, v. 91, p. 607–621.
- Fahrig WF (1987) The tectonic setting of continental mafic dyke swarms: failed arm and early passive margins. In: Halls HC, Fahrig WF (eds.) *Mafic Dyke Swarms*. Geological Association of Canada Special Paper 34:331–348
- Fairbairn, H.W., Faure, G., Pinson Jr., W.H., Hurley, P.M., 1968, Rb–Sr whole-rock age of the Sudbury lopolith and basin sediments: *Canadian Journal of Earth Sciences* 5 (3), 707–714.
- Farrow, C.E.G., Everest, J.O., King, D.M., and Jolette, C., 2005, Sudbury Cu-(Ni)-PGE systems: Refining the classification using McCreeley West mine and Podolsky project case studies, in Mungall, J.E. ed., *Exploration for Deposits of Platinum-Group Elements*, Mineralogical Association of Canada, p. 163–180.
- Farrow, C.E.G., and Lightfoot, P.C., 2002, Sudbury PGE Revisited: Towards an Integrated Model: *Canadian Institute of Mining, Metallurgy and Petroleum Special Volume*, v. 54, p. 273–297.
- Farrow, C.E.G., and Watkinson, D.H., 1992, Alteration and the Role of Fluids in Ni, Cu and Platinum-Group Element Deposition, Sudbury Igneous Complex Contact, Onaping-Levack area, Ontario: *Mineralogy and Petrology*, v. 46, p. 67–83.
- Farrow, C.G., and Watkinson, D.H., 1997, Diversity of Precious-Metal Mineralisation in Footwall Cu-Ni-PGE Deposits, Sudbury, Ontario: Implications for Hydrothermal Models of Formation: *The Canadian Mineralogist*, v. 35, p. 817–839.
- Fleet, M.E., Barnett, R.L., and Morris, W.A., 1987, Prograde Metamorphism of the Sudbury Igneous Complex: *Canadian Mineralogist*, v. 25, p. 499–514.
- Fuerten, F., and Redmond, D.J., 1997, Documentation of a 1450 Ma contractional orogeny preserved between the 1850 Ma Sudbury impact structure and the 1 Ga Grenville orogenic front, Ontario: *Bulletin of the Geological Society of America*, v. 109, no. 3, p. 268–279.

- Gibson, A.M., Lightfoot, P.C., and Evans, T.C., 2010, Contrasting Styles of Low Sulphide High Precious Metal Mineralisation in the 148 and 109 FW Zones : North and South Ranges of the Sudbury Igneous Complex , Ontario , Canada, in 11th International Platinum Symposium, Sudbury, Canada, p. 4.
- Golightly J.P., 1994, The Sudbury Igneous Complex as an Impact Melt. In Proceedings, Sudbury-Noril'sk Symposium. Edited by P.C. Lightfoot and A.J. Naldrett. Ontario Geological Survey, Special Volume 5, p. 57-64.
- Grieve R.A.F., 1994, The Impact Model of the Sudbury Structure. In Proceedings, Sudbury-Noril'sk Symposium. Edited by P.C. Lightfoot and A.J. Naldrett. Ontario Geological Survey, Special Volume 5, p. 57-64.
- Grieve, R.A.F., Ames, D.E., Morgan, J. V., and Artemieva, N., 2010, The evolution of the Onaping Formation at the Sudbury impact structure: *Meteoritics & Planetary Science*, v. 45, no. 5, p. 759–782.
- Grieve, R.A.F., and Therriault, A.M., 2013, Impactites: their characteristics and spatial distribution, in Osinski, G.R. and Pierazzo, E. eds., *Impact cratering: processes and products*, Wiley-Blackwell, p. 90–105.
- Hanley, J.J., and Mungall, J.E., 2003, Chlorine Enrichment and Hydrous Alteration of the Sudbury Breccia Hosting Footwall Cu-Ni-PGE Mineralization at the Fraser Mine, Sudbury, Ontario, Canada.: *The Canadian Mineralogist*, v. 41, p. 857–881.
- Jago B.C., Morrison G.G., Little T.L., (1994): Metal zonation patterns and microtextural and micromineralogical evidence for alkali- and halogen-rich fluids in the genesis of the Victor Deep and McCreedy East footwall copper ore bodies, Sudbury Igneous Complex. In Proceedings of the Sudbury – Noril'sk Symposium (P.C. Lightfoot & A.J. Naldrett, eds.). Ontario Geol. Surv., Spec. Vol. 5, 65-75.
- Keays, R.R., and Lightfoot, P.C., 2004, Formation of Ni-Cu-Platinum Group Element sulfide mineralization in the Sudbury Impact Melt Sheet: *Mineralogy and Petrology*, v. 82, no. 3-4, p. 217–258.
- Kenkmann, T., Collins, G.S., and Wünnemann, K., 2013, The Modification Stage of Crater Formation, in *Impact Cratering: Processes and Products*, p. 60–75.

- Kennedy, L.A., and Spray, J.G., 1992, Frictional melting of sedimentary rock during high-speed diamond drilling: an analytical SEM and TEM investigation: *Tectonophysics*, v. 204, no. 3-4, p. 323–337.
- Krogh, T.E., Davis, D.W. and Corfu, F. 1984. Precise U-Pb zircon and baddeleyite ages for the Sudbury area; in *The Geology and Ore Deposits of the Sudbury Structure, Ontario Geological Survey, Special Volume 1*, p.431-446.
- Krogh, T.E., Kamo, S.L. and Bohor, B.F. 1996. Shocked metamorphosed zircons with correlated U-Pb discordance and melt rocks with concordant protolith ages indicate an impact origin for the Sudbury Structure; in *Earth Processes: Reading the Isotope Code*, American Geophysical Union, Monograph 95, p.343-352.
- Lafrance, B., and Kamber, B.S., 2010, Geochemical and microstructural evidence for in situ formation of pseudotachylitic Sudbury breccia by shock-induced compression and cataclasis: *Precambrian Research*, v. 180, p. 237–250.
- Lafrance, B., Legault, D., and Ames, D.E., 2008, The formation of the Sudbury breccia in the North Range of the Sudbury impact structure: *Precambrian Research*, v. 165, p. 107–119.
- Lambert, P., 1981, Breccia dikes: Geological constraints on the formation of complex craters., in P.H., S. and Merrill, R.B. eds., *Proceedings of the Lunar and Planetary Science*, Lunar and Planetary Institute, p. 59–78.
- Lieger, D., Riller, U., and Gibson, R.L., 2009, Generation of fragment-rich pseudotachylite bodies during central uplift formation in the Vredefort impact structure, South Africa: *Earth and Planetary Science Letters*, v. 279, p. 53–64.
- Lieger, D., Riller, U., and Gibson, R.L., 2011, Petrographic and geochemical evidence for an allochthonous, possibly impact melt, origin of pseudotachylite from the Vredefort Dome, South Africa: *Geochimica et Cosmochimica Acta*, v. 75, no. 16, p. 4490–4514.
- Lightfoot, P.C., 2007, Advances in Ni-Cu-PGE Sulphide Deposit Models and Implications for Exploration Technologies, in Milkereit, B. ed., *Proceedings of Exploration 07: Fifth Decennial International Conference on Mineral Exploration.*, Sudbury, Canada, p. 629–646.

- Lightfoot, P.C., and Farrow, C.E.G., 2002, Geology, Geochemistry, and Mineralogy of the Worthington Offset Dike: A Genetic Model for Offset Dike Mineralization in the Sudbury Igneous Complex: *Economic Geology*, v. 97, p. 1419–1446.
- Lightfoot, P.C., and Keays, R.R., 2001, Sulfide Saturation History and Ore Genesis in the Sudbury Igneous Complex: Constraints from Main Mass, Sublayer, and Offset Geology and Geochemistry., in Eleventh Annual V.M. Goldschmidt Conference, Hot Springs, Virginia, USA, p. 1.
- Lightfoot, P.C., Morrison, G.G., Bite, A., and Farrell, P., 1997a, Geochemical Relationships in the Sudbury Igneous Complex: Origin of the Main Mass and Offset Dikes: *Economic Geology*, v. 92, p. 289–307.
- Lightfoot, P.C., Morrison, G.G., Bite, A., and Farrell, P., 1997b, Geochemical Relationships in the Sudbury Igneous Complex: Origin of the Main Mass and Offset Dikes: *Economic Geology*, v. 92, p. 289–307.
- Lightfoot, P.C., Naldrett, A.J., and Morrison, G.G., 1997c, Sublayer and Offset Dikes of the Sudbury Igneous Complex- an Introduction and Field Guide: Ontario Geological Survey, Open File Report 5965, 50 p
- Lightfoot, P.C., De Souza, H., and W., D., 1993, Differentiation and Source of the Nipissing Diabase Intrusions, Ontario, Canada: *Canadian Journal Of Earth Sciences*, v. 30, p. 1123–1140.
- Maddock, R.H., 1974, Melt origin of fault-generated pseudotachylytes: *Geology*, v. 11, p. 105–108.
- Magloughlin, J.F., 1992, Microstructural and chemical changes associated with cataclasis and frictional melting at shallow crustal levels: the cataclasite-pseudotachylyte connection: *Tectonophysics*, v. 204, p. 243–260.

- Magyarosi, Z., Watkinson, D.H., and Jones, P.C., 2002, Mineralogy of Ni-Cu-Platinum-Group Element Sulfide Ore in the 800 and 810 Orebodies, Copper Cliff South Mine, and P-T-X Conditions during the Formation of Platinum-Group Minerals: *Economic Geology*, v. 97, p. 1471–1486.
- Marshall, D., Watkinson, D., Farrow, C., Molnár, F., and Fouillac, A.-M., 1999, Multiple fluid generations in the Sudbury igneous complex: fluid inclusion, Ar, O, H, Rb and Sr evidence: *Chemical Geology*, v. 154, p. 1–19.
- McCormick, K.A., Leshner, C.M., McDonalds, A.M., Fedorowich, J.S., and R.S., J., 2002, Chlorine and Alkali Geochemical Halos in the Footwall Breccia and Sublayer Norite at the Margin of the Strathcona Embayment, Sudbury Structure, Ontario: *Economic Geology*, v. 97, p. 1509–1519.
- Meldrum, A., Abdel-Rahman, A.-F.M., Martin, R.F., and Wodicka, N., 1997, The nature, age and petrogenesis of the Cartier Batholith, northern flank of the Sudbury Structure, Ontario, Canada: *Precambrian Research*, v. 82, p. 265–285.
- Melosh, H., 1979, Acoustic fluidization: A new geologic process?: *Journal of Geophysical Research*, v. 84, pp.7513 – 7520.
- Melosh, H.J., 1989, *Impact cratering—A geologic process*: New York, Oxford University Press, 245 p
Melosh, H., 1979, Acoustic fluidization: A new geologic process?: *Journal of Geophysical Research*, v. 84, pp.7513 – 7520.
- Melosh, H.J., 2005, The Mechanics of Pseudotachylite Formation in Impact Events, in Koeberl, C. and Henkel, H. eds., *Impact Studies*, Springer, p. 55–80.
- Melosh, H.J., and Ivanov, B.A., 1999, Impact Crater Collapse: *Annual Review of Earth and Planetary Sciences*, v. 27, p. 385–415.
- Molnar, F., Watkinson, D.H., and Jones, P.C., 2001, Multiple Hydrothermal Processes in Footwall Units of the North Range, Sudbury Igneous Complex, Canada, and Implications for the Genesis of Vein-Type Cu-Ni-PGE Deposits: *Economic Geology*, v. 96, p. 1645–1670.

- Molnar, F., Watkinson, D.H., Jones, P.C., and Gatter, I., 1997, Fluid inclusion evidence for hydrothermal enrichment of magmatic ore at the contact zone of the Ni-Cu-platinum-group element 4b deposit, Lindsley mine, Sudbury, Canada: *Economic Geology*, v. 92, p. 674–685.
- Mukwakwami, J., Leshner, C.M., and Lafrance, B., 2014, Geochemistry of Deformed and Hydrothermally Mobilized Magmatic Ni-Cu-PGE Ores at the Garson Mine, Sudbury: *Economic Geology*, v. 109, p. 367–386.
- Mungall, J.E., and Hanley, J.J., 2004, Origins of Outliers of the Huronian Supergroup within the Sudbury Structure: *The Journal of Geology*, v. 112, no. 1, p. 59–70.
- Naldrett, A.J., 1984. Mineralogy and composition of the Sudbury ores; in *The Geology and Ore Deposits of the Sudbury Structure*, Ontario Geological Survey, Special Volume 1, p.309- 325
- Naldrett A.J., and Hewins R.G., 1984, The main mass of the Sudbury Igneous Complex, in, Pye, E.G., Naldrett A.J., and Giblin P.E., eds., *The geology and ore deposits of the Sudbury Structure*, Ontario Geological Survey Special Volume 1, p. 235-251.
- Naldrett, A.J., and Pessaran, A., 1992. Compositional variation in Sudbury ores and prediction of the proximity of footwall copper-PGE orebodies: *Ontario Geological Survey Miscellaneous Paper 159*, p. 47-62.
- Naldrett, A.J., Asif, M., Schandl, E., Searcy, T., Morrison, G.G., Binney, W.P., and Moore, C., 1999, Platinum-Group Elements in the Sudbury Ores: Significance with Respect to the Origin of Different Ore Zones and to the Exploration for Footwall Orebodies: *Economic Geology*, v. 94, p. 185–210.
- Naldrett, A.J., Bray, J.G., Gasparri, E.L., Podolsky, T., and Rucklidge, J.C., 1970, Cryptic variation and the petrology of the Sudbury nickel irruptive: *Economic Geology*, v. 65, p. 122–155.
- Nelles, E.W., 2012, Genesis of Cu-PGE-rich Footwall-Type Mineralization in the Morrison Deposit, Sudbury: Unpublished M.S.c. thesis, Laurentian University, Sudbury, Canada, 96 p.

- Nelson, D.O., 1987, Petrogenesis of basalts from the Archean Matachewan Dike Swarm Superior Province of Canada.: NASA/ASEE Summer Faculty Fellowship Program Report, Johnson Space Center, N88-14878. 20 p.
- Noble, S.R., and Lightfoot, P.C., 1992, U–Pb baddeleyite ages of the Kerns and Triangle Mountain intrusions, Nipissing diabase, Ontario.: *Canadian Journal of Earth Sciences*, v. 29, p. 1424–1429.
- O’Connor, J.P., and Spray, J.G., 1997, Geological Setting of the Manchester Offset Dyke within the South Range of the Sudbury Impact Structure., in *Large Meteorite Impacts and Planetary Evolution 992*, p. 38.
- Osinski, G.R., Grieve, R.A.F., and Tornabene, L.L., 2013, Excavation and Impact Ejecta Emplacement, in Osinski, G.R. and Pierazzo, E. eds., *Impact Cratering: Processes and Products*, Wiley-Blackwell, p. 43–59.
- Osinski, G.R., and Pierazzo, E., 2013, Impact cratering : processes and products, in Osinski, G.R. and Pierazzo, E. eds., *Impact Cratering: Processes and Products*, Wiley-Blackwell, p. 1–20.
- Parmenter, A.C., Lee, C.B., and Coniglio, M., 2002, “Sudbury Breccia” at Whitefish Falls, Ontario: evidence for an impact origin: *Canadian Journal of Earth Sciences*, v. 39, no. 6, p. 971–982.
- Pentek, A., 2009, Partial melting and melt segregation within the contact aureole of the Sudbury Igneous Complex (Ontario , Canada) and their significance in hydrothermal Cu-Ni-PGE mineralization of the footwall: Unpublished thesis, Eotvos Lorand University, Budapest, Hungary, 10 p.
- Pentek, A., Molnar, F., Watkinson, D.H., and Jones, P.C., 2008, Footwall-type Cu-Ni-PGE Mineralization in the Broken Hammer Area, Wisner Township, North Range, Sudbury Structure: *Economic Geology*, v. 103, p. 1005–1028.
- Petrus, J. A., Ames, D.E., and Kamber, B.S., 2015, On the track of the elusive Sudbury impact: geochemical evidence for a chondrite or comet bolide: *Terra Nova*, v. 27, no. 1, p. 9–20.

- Pierazzo, E., and Melosh, H.J., 2013, Environmental effects of impact events, in Osinski, G.R. and Pierazzo, E. eds., *Impact Cratering: Processes and Products*, Wiley-Blackwell, p. 147–156.
- Prevec, S., Lightfoot, P., and Keays, R., 2000, Evolution of the sublayer of the Sudbury Igneous Complex: geochemical, Sm–Nd isotopic and petrologic evidence: *Lithos*, v. 51, p. 271–292.
- Prevec, S.A., and Cawthorn, R.G., 2002, Thermal evolution and interaction between impact melt sheet and footwall: A genetic model for the contact sublayer of the Sudbury Igneous Complex, Canada: *Journal of Geophysical Research*, v. 107, no. B8, p. 1–14.
- Raharimahefa, T., Lafrance, B., and Tinkham, D.K., 2014, New structural , metamorphic , and U – Pb geochronological constraints on the Blezardian Orogeny and Yavapai Orogeny in the Southern Province, Sudbury, Canada: *Canadian Journal of Earth Sciences*, , no. 51, p. 750–774.
- Randall, W., 2004, Petrogenesis of Pseudotachylytes from the Sudbury Structure: Unpublished B.Sc. thesis, University of Toronto, Toronto, Canada. 39 p.
- Reimold, W.U., and Gibson, R.L., 1996, Geology and evolution of the Vredefort impact structure, South Africa: *Journal of African Earth Sciences*, v. 23, no. 2, p. 125–162.
- Reimold, W.U., Gibson, R.L., 2005, “Pseudotachylites” in Large Impact Structures: in *Impact Tectonics*, Koeberl, C. and Henkel, H. eds., Springer, pp. 1-53.
- Reimold, W.U., and Gibson, R.L., 2006, The melt rocks of the Vredefort impact structure - Vredefort Granophyre and pseudotachylitic breccias: Implications for impact cratering and the evolution of the Witwatersrand Basin: *Chemie der Erde - Geochemistry*, v. 66, no. 1, p. 1–35.
- Riller, U., 2005, Structural characteristics of the Sudbury impact structure, Canada: Impact-induced versus orogenic deformation-A review: *Meteoritics & Planetary Science*, v. 40, no. 11, p. 1723–1740.

- Riller, U.P., Schwerdtner, W.M., 1997. Mid-crustal deformation of the southern flank of the Sudbury Basin, central Ontario, Canada. *Geological Society of America Bulletin* 109, p. 841–854.
- Riller, U., Lieger, D., Gibson, R.L., Grieve, R.A.F., and Stoffler, D., 2010, Origin of large-volume pseudotachylite in terrestrial impact structures: *Geology*, v. 38, no. 7, p. 619–622.
- Rousell, D.H., and Brown, G.H., 2009, *A Field Guide to the Geology of Sudbury, Ontario* (D. H. Rousell & G. H. Brown, Eds.): Ontario Geological Survey, Sudbury Ontario.
- Rousell, D., and Long, D.G., 1998, Are Outliers of the Huronian Supergroup Preserved in Structures Associated with the Collapse of the Sudbury Impact Crater? *The Journal of geology*, v. 106, no. 4, p. 407–420.
- Rousell, D.H., Fedorowich, J.S., and Dressler, B.O., 2003, Sudbury Breccia (Canada): a product of the 1850 Ma Sudbury Event and host to footwall Cu–Ni–PGE deposits: *Earth-Science Reviews*, v. 60, p. 147–174.
- Rousell, D.H., Gibson, H.L., and Jonasson, I.R., 1997, The Tectonic, Magmatic and Mineralisation History of the Sudbury Structure: *Exploration and Mining Geology*, v. 6, no. 1, p. 1–22.
- Scott, R.G., and Spray, J.G., 2000, The South Range Breccia Belt of the Sudbury Impact Structure : *Meteoritics & Planetary Science*, , no. 35, p. 505–520.
- Severin, P.W.A. and Gates, B.I. 1981. Giant Yellowknife Mines Limited Ore Reserve Calculation Errington/Vermilion Deposits; Falconbridge Limited, Internal Report, 17p
- Shand, S.J., 1916, The Pseudotachylite of Parijs (ORange Free State) and its Relation to “Trap-Shotten Gniess” and “Flinty Crush-Rock”.: *Quarterly Journal of the Geological Society*, v. 72, p. 198–221.
- Shellnutt, J.G., and MacRae, N.D., 2011, Petrogenesis of the Mesoproterozoic (1.23 Ga) Sudbury dyke swarm and its questionable relationship to plate separation: *International Journal of Earth Sciences*, p. 3–23.

- Smith, M.D., Heaman, L.M. and Beakhouse, G.P. 1999. Constraints on the timing of felsic magmatism associated with Matachewan igneous events: Preliminary U-Pb results for the Creighton granite, Ontario; Geological Association of Canada–Mineralogical Association of Canada, Abstract Volume 24, p.119.
- Souch, B.E., and Podolsky, T., 1969, The sulphide ores at Sudbury: their particular relationship to a distinctive inclusion-bearing facies of the Nickel Irruptive: Economic Geology Monograph 4, p. 252–261.
- Speers, E.C., 1957, The Age Relation and Origin of Common Sudbury Breccia: The Journal of Geology, v. 65, no. 5, p. 497–514.
- Spray, J.G., 2010, Frictional Melting Processes in Planetary Materials: From Hypervelocity Impact to Earthquakes: Annual Review of Earth and Planetary Sciences, v. 38, no. 1, p. 221–254.
- Thomas P., 2013. The pseudotachylitic impact breccias (impact melt rocks) of the Vredefort astrobleme, Parys sector, South Africa (French): ENS Lyon, (<http://planet-terre.ens-lyon.fr/image-de-la-semaine/Img437-2013-10-14.xml>).
- Thompson, L.M., and Spray, J.G., 1996, Pseudotachylite petrogenesis: constraints from the Sudbury impact structure: Contributions to Mineralogy and Petrology, v. 125, no. 4, p. 359–374
- Souch, B.E. and Podolsky, T., 1969, The sulphide ores at Sudbury: their particular relationship to a distinctive inclusion-bearing facies of the Nickel Irruptive; in Magmatic Ore Deposits, Economic Geology, Monograph 4, p.252-261.
- Spray, J.G., and Thompson, L.M., 1995, Friction melt distribution in a multi-ring impact basin: Letters to Nature, v. 373, p. 130–132.
- Tuba, G., Molnár, F., Ames, D.E., Péntek, A., Watkinson, D.H., and Jones, P.C., 2014, Multi-stage hydrothermal processes involved in “low-sulfide” Cu(–Ni)–PGE mineralization in the footwall of the Sudbury Igneous Complex (Canada): Amy Lake PGE zone, East Range: Mineralium Deposita, v. 49, p. 7–47.

- Tuchscherer, M., and Spray, J., 2002, Geology, mineralization, and emplacement of the Foy Offset Dike, Sudbury impact structure: *Economic Geology*, v. 97, p. 1377–1397.
- White, C.J., 2012, Low-Sulfide PGE-Cu-Ni Mineralization From Five Prospects Within The Footwall Of The Sudbury Igneous by Low-Sulfide PGE-Cu-Ni Mineralization from Five Prospects with the Footwall of the Sudbury Igneous Complex , Ontario , Canada: Unpublished Ph.D. thesis, University of Toronto, Toronto, Canada. 337 p.
- Wood, C.R., and Spray, J.G., 1998, Origin and emplacement of Offset Dykes in the Sudbury impact structure: Constraints from Hess.: *Meteoritics & Planetary Science*, v. 33, p. 337–347.
- Zieg, M.J., and Marsh, B.D., 2005, The Sudbury Igneous Complex: Viscous emulsion differentiation of a superheated impact melt sheet: *Geological Society of America Bulletin*, v. 117, no. 11, p. 1427.

Chapter 2

2 Reconstructing the geochemical signature of Sudbury Breccia, Ontario, Canada: Implications for its formation and trace metal content

2.1 Introduction

Pseudotachylite was first described by Shand (1916) in the Vredefort impact structure, South Africa, as a rock that originated by in-situ melting of country rocks. In outcrop, the breccia appears as millimeter to decimeter wide veinlets and zones of dark, fine grained, aphanitic matrix hosting rounded to subrounded lithic clasts and mineral fragments (Shand, 1916; Lieger et al., 2011; Grieve and Therriault, 2013). Extensive outcrops of similar pseudotachylitic breccia, have been recognised as far as 80 km into the footwall of ~200 km diameter, 1.85 Ga Sudbury impact structure in Ontario, Canada (Speers 1957; Dietz 1964; Grieve 1994; Parmenter et al., 2002; Rousell et al., 2003; Riller et al., 2010). We use the term ‘pseudotachylitic breccia’ here as, although similar in geological setting and appearance, we have yet to constrain whether the Sudbury breccia is locally derived from in-situ lithologies. Aside from the implications for complex impact cratering models, Sudbury breccia is also associated with major Cu-Ni-PGE footwall ore systems, situated beneath embayments that host magmatic Ni-Cu sulfide contact type ore deposits (Farrow et al., 2005; Ames and Farrow, 2007; Pentek et al., 2008).

There have been several attempts to classify Sudbury breccia (e.g. Speers 1957; Müller-Mohr 1992; Rousell et al. 2003), the most recent of which subdivided the breccia into clastic, pseudotachylitic and microcrystalline varieties, which are controlled, in part, by the host lithologies and proximity to the Sudbury Igneous Complex (SIC) contact aureole (Rousell et al. 2003). Previous studies have also proposed that impact related pseudotachylitic breccias may preferentially form along planes of weakness such as pre-impact lithological contacts, structures or discrete mineral fabrics (Dressler, 1984; Lafrance et al., 2008; Lieger et al., 2009; Mungall and Hanley, 2004). Disagreements as to how to classify the variations in the appearance of Sudbury breccia and the structural controls on its emplacement form part of an underlying debate surrounding the exact formational processes of the breccia. Injection of

impact melt material derived from the melt sheet into the brecciated crater floor has previously been proposed at the ~300 km diameter Vredefort impact structure in South Africa, and may be applicable to Sudbury as well (Riller et al., 2010; Lieger et al., 2011). Alternatively, in-situ frictional melting along fault structures in the footwall during crater excavation and modification, or lower temperature fault cataclasis, have been put forward as origins for Sudbury breccia (Spray and Thompson, 1995; Rousell et al., 2003; Mungall and Hanley, 2004; Lafrance et al., 2008).

Process models for the genesis of Sudbury breccia are important from the standpoint of understanding the excavation and modification of complex impact craters, and also serve to improve our interpretation of the timing and geochemical and petrographic properties of the breccia, which may provide important tools in the search for Cu-Ni-PGE footwall mineralization. The objective of this work is to understand the process of breccia formation and the influence on its trace metal content, using a suite of samples collected from various localities in the North and South Ranges of the Sudbury Basin that are located proximal and distal to footwall mineralization. Through the application of a geochemical mixing model and principal component analysis, this study investigates the relative contributions of crustal target rocks and melt sheet, and establishes the background concentrations of metals, which can be potentially applied as a vectoring tool towards areas with anomalous metal content adjacent to footwall mineral zones.

2.2 Geological Setting

The 1850 ± 1.3/-2.4 Ma Sudbury Structure formed due to an asteroid or comet impact at the margin of the Superior Province, resulting in the formation of a crater with an estimated initial diameter of ~200 km, the eroded remains of which are represented by a 62 x 30 km basin (fig. 2.1) (Dietz 1964; Krogh et al. 1984; Dressler 1984; Ames et al., 2008; Davis, 2008; Petrus et al., 2015). The basin delineates the Sudbury Igneous Complex, which is interpreted as an impact melt sheet (Dietz 1964; Grieve 1994; Deutsch et al., 1995) from which radial and concentric, granodioritic offset dikes extend into the surrounding target rock (Lightfoot et al., 1997c; Wood and Spray, 1998; Tuchscherer and Spray, 2002). The impact melt sheet differentiated into a basal norite, overlain by quartz gabbro, granophyre and an 'upper contact unit' of roof rocks (Naldrett and Hewins, 1984; Grieve 1994; Golightly 1994; Anders et al., 2015). A number of mechanisms have been proposed for this differentiation, including fractional crystallisation (Naldrett et al., 1970), the development of a two melt

system (Chai and Eckstrand, 1994), crystallization of a density-stratified melt (Golightly, 1994; Lightfoot et al., 2001; Keays and Lightfoot, 2004), viscous emulsion differentiation (Zieg and Marsh, 2005) and/or assimilation of the underlying footwall (Dickin et al., 1996). The basal contact of the melt sheet was scoured and pitted by thermal erosion and slumping processes, which lead to the formation of embayment and trough structures into which sulfide melts were localized (Morrison 1984; Ames and Farrow, 2007). Aside from sulfide melts, the embayment structures also contain discontinuous units of noritic to gabbroic inclusion-bearing material up to 700 m thick, termed the sublayer (Lightfoot et al., 1997b; Prevec et al., 2000). Although genetically related to the overlying melt sheet, geochemical variations in the sublayer hosted in different embayment structures suggest that the unit represents the assimilation front between the melt sheet and the underlying footwall (Naldrett et al. 1986; Lightfoot et al., 1997b). Radial and concentric intrusive ‘offset dikes’ within the footwall were historically grouped with the sublayer (Souch et al. 1969), but are now considered to have been derived from undifferentiated contributions from the melt sheet, and were emplaced early in the evolution of the melt sheet (Lightfoot et al., 1997c). Although historically referred to as quartz diorite, the offset dikes are actually granodioritic in

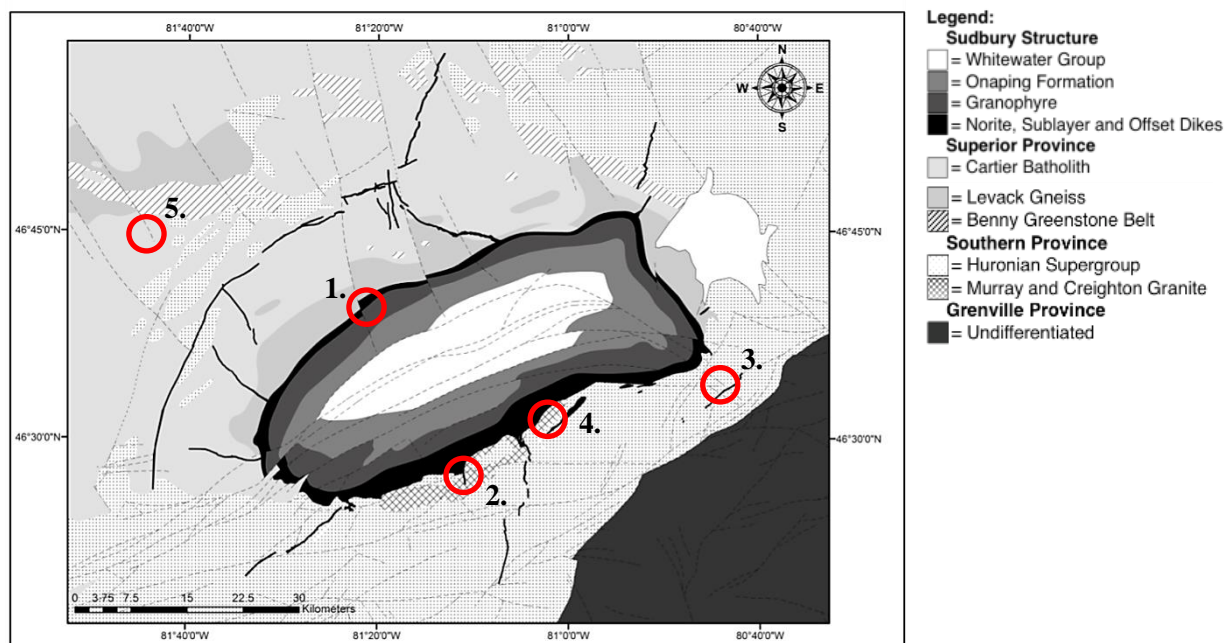


Figure 2.1: Geological map of the Sudbury Basin, showing the location of the Sudbury Igneous Complex, Superior Province and Huronian footwall units, and post impact Whitewater Group. Sample locations are: 1. McCreedy East 153 Ore Body; 2. Creighton Mine, Old Creighton Town and South Pump Lake; 3. Manchester Offset Dike; 4. Murray West Zone; 5. Halfway Lake (modified after Coulter 2016).

composition, though for consistency they will be referred to as quartz diorite here, in line with other recent papers (Lightfoot and Keays, 2001; Rickard and Watkinson, 2001; Tuchscherer and Spray, 2002). The offset dikes are considered analogous to the granophyre dikes that surround the Vredefort impact structure in South Africa, which are also believed to be impact melts (Lieger et al., 2011). Geochemical modelling by Lightfoot et al. (1997a) demonstrated that the bulk composition of the SIC main melt sheet is compositional very similar to that of the offset dikes (plus a minor ultramafic component, possibly derived from unidentified target units or a contribution from the mantle). Thus, the intrusions are considered to represent an early phase in the melt sheet prior to the differentiation of the SIC.

Overlying the Main Mass are the post-impact Onaping Formation breccias (Grieve et al., 2010) and later turbidites and mudstones of the Whitewater Group, of which the Chelmsford Formation yields the youngest Rb/Sr isochron age of 1720 ± 30 Ma (Fairbairn et al. 1968). North of the SIC, the Superior Province consists of the 2642 ± 1 Ma Cartier granites, which are believed to have been derived from partial melting of the 2711 ± 7 Ma Levack Gneiss (Krogh et al. 1984; Meldrum et al., 1997; Rousell and Brown, 2009). The South Range of the SIC is composed of early Proterozoic-aged metasedimentary and metavolcanic rocks of the Huronian Supergroup (2491 ± 5 to 2219 Ma) that were intruded by the 2376 ± 2.3 Ma Creighton and 2477 ± 9 Ma Murray granites in the South and East (Dressler, 1984; Krogh et al. 1996; Smith et al. 1999; Ames et al., 2008). The 2217 ± 4 Ma Nipissing gabbro is found in the footwall both North and South of the SIC (Noble and Lightfoot 1992; Ames et al. 2008); although Lightfoot and Farrow (2002) note that ‘Nipissing’ gabbro samples from around the Worthington offset dike are compositionally distinct (e.g., they have a higher MgO content) and they have been grouped as ‘Sudbury gabbro’ (Card and Pattison 1973).

Extensive zones of Sudbury breccia are situated in the footwall of the SIC. This breccia comprises of a dark grey, fine grained, aphanitic matrix, hosting rounded to sub-rounded lithic clasts and mineral fragments inherited from the adjacent country rock (Thompson and Spray, 1996; Rousell et al., 2003; Spray, 2010). Four theories of formation of the Sudbury breccia have been proposed. 1) frictional or shock induced melting during either the passage of the shock wave or subsequent crater collapse and modification (Thompson and Spray, 1996; Mungall and Hanley, 2004; Spray, 2010; Reimold et al., 2015); 2) lower temperature cataclasis and comminution (Lafrance et al., 2008); 3) acoustic fluidization

during pressure fluctuations caused by seismic vibrations (Melosh 1979); or 4) injection or drainage of early, superheated, impact melt into fractures in the underlying footwall immediately after the excavation of the crater (Randall, 2004; Riller et al., 2010; Lieger et al., 2011). Cataclasis (i.e., mechanical grinding of rock into powder) and frictional melting are typically viewed as two end-members of a continuous progression from initial shearing (when the rock is cold) to late stage shearing (when the rock is hot). Theory 1 supports a genesis that is similar to tectonic pseudotachylite found in earthquake fault zones (Maddock, 1974; Di Toro and Pennacchioni, 2004; Bestmann et al., 2011); albeit forming much wider zones of pseudotachylitic material in the case of the Sudbury breccia. In the cases of theories 1, 2 and 3, the composition of the breccia should be a mixture of the surrounding country rock; whereas in the case of the fourth theory, the composition of the breccia should have an allochthonous component similar to the early, undifferentiated SIC melt sheet. Theories 1 and 4 are consistent with a breccia matrix that exhibits an igneous texture, indicative of cooling from a melt. In the case of the first theory, the breccia matrix may comprise glassy or devitrified glass due to rapid cooling of friction or shock-induced melts. However, glass is not commonly preserved, and it is not an ideal indicator due to its metastable nature (Magloughlin 1992). Theory 2 is supported by rocks that exhibit mineral fabric alignment associated with shearing. Rousell (et al. 2003) notes that Sudbury breccia in the South Range tends to be coarser grained than Sudbury breccia in the North Range, which he attributes to a lower temperature, cataclastic comminution process that reflects the presence of trace amounts of pore fluids within the metasedimentary host rocks adjacent to the breccia zones. Magloughlin (1992) found that the presence of pore fluids can affect the strain rate within active fault zones, encouraging comminution rather than higher temperature frictional melting. However, pre- and syn-impact metamorphic activity approached mid-amphibole facies at Sudbury, and is likely to have expelled most of the pore-fluids prior to the impact event (Rousell et al., 1997). Alternatively, the rheological contrast between the predominantly gneissic lithologies in the North Range, versus the finer-grained, primarily metasedimentary rocks in the South Range may have affected the conditions under which the breccia formed, resulting in this textural discrepancy. A study by Kennedy and Spray (1992) was designed to establish whether the parental rock type influenced the development of pseudotachylite. They found that sandstones were less likely to generate frictional melts than siltstones and limestones. Rather, the sandstones were commonly more fractured and underwent cataclasis. Lieger et al. (2011) concluded that the matrix of the pseudotachylitic breccias surrounding the Vredefort impact structure in South Africa was originally of a

similar composition to the melt sheet derived granophyre dikes found in the footwall adjacent to the crater. Geochemical variations in the pseudotachylite were attributed to partial assimilation of host lithologies by the impact derived melt as it was transported into the footwall. In contrast, Lafrance and Kamber (2010) demonstrated that Sudbury breccia at a contact between sandstone and diabase near the SIC in the Southern Province had no contribution from the melt sheet. More recently, isotopic and geochemical studies by Reimold et al. (2015) has refuted the requirement for an impact melt component in the pseudotachylites at the Vredefort structure.

The Sudbury breccia is now recognized to be an important host to the Cu-Ni-PGE sulfide mineralization developed in the footwall of contact ore deposits located in troughs and embayments at the base of the SIC. The crystallization history of the magmatic sulfides at Sudbury is considered to involve the formation of an early monosulfide solid solution which re-crystallized to form the pyrrhotite-pentandite-chalcopyrite mineral styles at the lower contact of the SIC (Naldrett et al., 1999; Farrow et al., 2005; Ames and Farrow, 2007). The residual fractionated sulfide liquid was expelled into heavily brecciated footwall rocks, and then crystallized as an intermediate solid solution followed by mineral phases crystallizing from the residual fractionated sulfide liquid. The origin of the footwall mineralization is clearly magmatic, but there is much evidence for syn- and post-magmatic interaction between the Cu-Ni-PGE mineralization and hydrothermal fluids within the footwall that led to the remobilization of metals into the adjacent Sudbury breccia, creating a geochemical halo that is now recognized by the development of nickeliferous hydrosilicates and discrete platinum group element minerals (Hanley et al., 2005; Pentek et al., 2008; Hanley and Bray, 2009; Nelles, 2012; White, 2012).

The geochemical signature of the Sudbury breccia therefore provides important information that relates not only to the primary process of formation, but it also helps to understand the relative roles of syn-magmatic and post-magmatic hydrothermal activity in the modification of footwall mineralization at Sudbury. The observations can also be used in support of exploration of the footwall for anomalous concentrations of metals that were introduced after the breccias were consolidated.

2.3 Sample Selection and Local Geology

Six localities were identified for sampling. The locations were chosen to represent a Range in country rock compositions in North and South Range settings as well as to characterise samples located distal and proximal to footwall mineral zones (Table 2.1, Fig. 2.1). Sudbury breccia veins hosted within a single lithology were sampled so as to better distinguish in-situ versus allochthonous geochemical signatures and sampling was conducted in a variety of footwall lithologies (e.g., granites, gneisses, metasedimentary rocks) to provide a robust test of the mixing model and to relate the composition of the host rock types to the matrix of the Sudbury breccia. Sudbury breccia was subdivided based on the clast: matrix ratio, with samples with approximately >80 % matrix used in this study to minimise the influence of entrained clasts on the geochemical signature of the breccia matrix. Unbrecciated host rock samples from adjacent to the breccia zones provide a benchmark trace metal signature, against which to compare for anomalous metal contents in the Sudbury breccia located distal and proximal to footwall mineral zones. Hydrothermal veins and fractures were avoided during sampling in an effort to reduce the obvious effects of alteration on the geochemistry of the rock. A total of 87, ~1 kg samples of footwall rocks and Sudbury breccia were collected. In addition, geochemical analyses of samples from the Huronian Supergroup available in a public domain compilation by Murphy (2001) were used where sampled local lithologies and impact melt were unable to sufficiently constrain the breccia geochemistry. Geochemical data for the quartz diorite offset dikes in Lightfoot et al. (1997a) was used to establish a proxy for the composition of the early, undifferentiated impact melt sheet. Discrete geochemical variations between the eleven offset dikes have been attributed to the assimilation of local footwall lithologies by the early melt (as observed in the Sublayer) (Naldrett et al., 1986; Lightfoot et al., 1997a; Lightfoot et al. 1997b).

Table 2-1: Location names, number of samples (Sudbury Breccia and host) collected, NAD-27 coordinates of sample sites and a summary of the footwall host lithologies proximal to the Sudbury Breccia outcrops.

Sample Location	# of Samples	Co-Ordinates (UTM NAD-27)	Footwall Host Lithologies
Creighton Deep	26	486440, 5145539	Granite, granodiorite, mafic pyroclastics
Old Creighton Town	7	486357, 5144652	Granite, granodiorite,
South Pump Lake	11	485783, 5144497	Granite, granodiorite, mafic pyroclastics
Manchester Offset Dike	6	521369, 5156262	Gabbro, quartz-arenite, conglomerates
McCreedy East 153 O.B.	26	497765, 5152445	Felsic gneiss, Mafic gneiss
West Murray Area	11	469444, 5164475	Granite, granodiorite

2.3.1 Creighton Embayment

Three localities at Creighton were sampled (Creighton Deep, Old Creighton Town and South Pump Lake). Drill core from proximal to the footwall mineralization were sampled at locations with increasing distance away from the mineral zones (from 63 to 162 meters). Samples were also taken ~1 to 2 km south of the Creighton embayment. The footwall lithologies in the vicinity of Creighton Mine consist of the 2376 ± 2.3 Ma (Smith et al. 1999; Krogh et al., 1984) Creighton pluton; this is the largest of the granite intrusions found in the South Range of the Sudbury basin. The pluton intruded into metavolcanic and metasedimentary rocks of the Elsie Mountain and Stobie Formations, which comprise basalts, gabbros, metamorphosed mudstones and siltstones and minor rhyolite and dacite (Murphy, 2001; Ames et al. 2008). Enclaves and pendants of Huronian-aged country rocks and possibly basement-derived gneissic material are enclosed within domains of Sudbury breccia in the granite (Riller 2009).

2.3.2 West Murray Area

The Murray Pluton is the oldest (2477 ± 9 Ma) of three Paleoproterozoic felsic plutons present in the South Range (Krogh et al. 1996). The Murray pluton is granitic, with segregations of granodiorite and aplitic partial melting reported in some localities adjacent to

the SIC (Riller et al. 1996). Huronian metavolcanic and metasedimentary rocks from the Copper Cliff and Stobie formations are present as roof pendants above the pluton (Riller 2009; Bleeker, 2015), both of which have subsequently been intruded by Meso-Paleoproterozoic quartz diabase intrusions, that exploited pre-existing fault structures in the region, such as the Murray fault (locally termed ‘trap dikes’) (Fahrig and West 1986). Samples were taken approximately 400 m along strike from the west end of the Frood Stobie Ni-Cu-PGE ore deposit, hosted within a 45 x 0.5 km, arcuate breccia zone termed the ‘South Range Breccia Belt’ (Scott and Spray, 2000; Ames and Farrow, 2007).

2.3.3 Manchester Offset Dike

The sub-concentric Manchester offset dike, situated 5 km south of the SIC contact at Falconbridge town, extends >10 km through several stratigraphic units of the Huronian Supergroup. The Manchester Offset Dike has a higher silica content when compared with the other offset dikes, which has been attributed to assimilation of Huronian quartzo-feldspathic host rocks (Lightfoot et al., 1997a; O’Connor and Spray, 1997). Mafic Sudbury gabbro intrusions are also present in the footwall of the SIC in this area (Lightfoot and Farrow, 2002). The contacts between the offset dike and Sudbury breccia are generally sharp (Lightfoot et al., 1997a; O’Connor and Spray, 1997). Although sections of the offset dike have gossanous weathering, no economically important mineral zones are known at this time. This study focussed on a Sudbury breccia outcrop mapped by Lightfoot et al. (1997c), hosted within Huronian quartz-arenities, conglomerates and Sudbury gabbro, adjacent to the Manchester offset dike.

2.3.4 McCreedy East 153 Ore Deposit

The McCreedy 153 East footwall ore deposits form part of the Coleman-Levack mineral system. The deposit is dominated by veins of massive chalcopyrite (Cp) > cubanite (Cb) and bornite (Bn) > millerite (Mlt), which were emplaced, like the other footwall ore deposits in the North Range, as part of a fractionated sulfide melt derived from the overlying Ni-Cu contact ore bodies (Li and Naldrett, 1994; Ebel and Naldrett, 1996). The deposit is hosted in a zone of Sudbury breccia within felsic and mafic Levack gneiss (Lightfoot 2015), which is compositionally divided into tonalite-granodiorite orthogneiss, with horizons of diorite gneiss (Card 2009). The 2452^{+16}_{-9} Ma age Matachewan diabase dikes cross cut the footwall, predating the impact event; whereas later (1238 ± 4 Ma) Sudbury olivine diabase dikes cross cut both the footwall and igneous complex (Krogh et al. 1987; Heaman 1989). Samples of

drill core were collected immediately adjacent to both Cp-Cb and Bn-Mlt veins, and up to 400 m away from the veins. Additional samples were collected approximately 30 km northwest of the Levack-Coleman area, at a locality termed 'Halfway Lake', the geology of which similarly comprises Cartier granites and Matachewan intrusives. As the geochemistry of Sudbury breccia at this locality has already been evaluated by Weirich (et al., 2014) using the same mixing model as in this study, it will not be further investigated here. Instead the samples provide an important comparison of the mineralogy and textures for Sudbury breccia outside of the SIC thermal aureole (see petrography).

2.4 Methodology

Mixing models can help to establish the relative contributions of country rocks and impact melt in the formation of the matrix of the Sudbury breccia. In the model developed by Weirich (et al. 2014) optimal results are achieved when analytical precision and accuracy are 5% 2 sigma or better for all major and trace elements. Previous geochemical studies of Sudbury breccia have used X-Ray Fluorescence (XRF) or defocused electron microprobe analytical techniques to attain major element data (Thompson and Spray, 1996; Al Barazi et al., 2009; Lafrance and Kamber, 2010); whereas Lafrance (et al. 2008) used lithium metaborate and tetraborate ICP-MS technique. In the case of high-field-strength and rare earth elements, the minerals that host these elements are resistant to four acid decomposition and thus 106 samples of Sudbury breccia and host rocks, covering the six localities in both the North and South Range, were analysed using lithium-metaborate fusion ICP-MS analysis by ALS labs (ME-MS81 ultra-trace). Following preparation, 0.2g of sample is added to a lithium metaborate flux, before being mixed and fused in a furnace at ~1000°C. The resulting melt is then cooled and dissolved in 100 mL of 4 % HNO₃ and 2 % HCl₃ solution, before analysis by ICP-MS. A total of 12 duplicates and 4 standards (BHVO-2; PLO-1) were inserted into the sample suite as part of the QA-QC procedure. Supplementary data from Murphy's 2001 synthesis of Huronian geochemical data also includes analyses obtained by XRF and four acid ICP-MS.

In addition to application of the mixing model (see below), major element and trace metal (SiO₂, Al₂O₃, Na₂O, K₂O, CaO, MgO, MnO, FeO_{tot}, Ni, Cu, Cr) (Pd and Pt were not included due to the tendency for their abundances to be controlled by the nugget effect) bulk rock geochemical data of Sudbury breccia samples from McCreedy 153 East and the Creighton Embayment (South Pump Lake, Old Creighton Town and Creighton Deep) were evaluated

using the robust principal component analysis (PCA) feature on ioGAS™. Principal component analysis provides an effective means of describing essential patterns and relationships in large datasets. Robust PCA includes algorithms that allow for the removal (or down-weighting) of outliers that can adversely skew the dataset, thereby failing to capture the true variation in background data. This is achieved by replacing the standard deviation correlation matrix, used to normalize and scale the data prior to PCA, with a robust estimate. This estimate is calculated by weighting each of the samples by their robustly estimated Mahalanobis distance. Outlying samples are assigned low weights and therefore do not have as much impact on the dispersion matrix estimate. This has the effect of removing outlying samples from the correlation calculation, but then projects them onto the robustly determined principal components. PCA then transforms the ‘cloud’ of multivariate data (i.e. all the geochemical results and correlations) into a series of dimensionless eigenvectors (principal components) and their eigenvalues or magnitudes. As geochemical results are usually given in proportions (e.g. wt. %) and have a constant sum constraint, a series of additional transformations of the dataset are required in order to avoid the effects of closure. In this study, a log-ratio transformation developed by Aitchinson (1983) was applied to the data, which converts the compositional data into log-ratio vectors for PCA, the results of which are then translated back into terms relatable to the original compositional data. As highlighted by Aitchinson et al. (2002) application of PCA cannot be done a priori, instead one must have a comprehensive understanding of the samples (e.g. geological setting, controls on bulk geochemistry) prior to interpreting PCA results, in order to properly understand the implications of the correlations derived from the analysis. As such, PCA was applied after the mixing model, so that the PCA results could be interpreted within the context of whether or not the breccia requires an impact melt component. Readers are directed to Campbell (1980), Aitchinson (et al., 2002), Filzmoser and Hron (2008) and Abdi and Williams (2010) for more details on the application of correlation matrices, robust PCA and log-transformations to geochemical data.

Reflected and transmitted light microscopy was undertaken using Nikon Eclipse LV100 POL microscopes, equipped with 12 mega-pixel cameras and connected to an NIS-Element photographic software package. High resolution scans of six hand-specimen samples from Creighton, the West Murray Area and the McCreeedy 153 East were analysed using a semi-automatic quantitative image analysis process using ImageJ™, details of which can be found in Chanou et al. (2014) (Fig. 2.3 E, F).

2.4.1 Mixing Model Specifications

An IDL™ mixing model developed by Weirich et al. (in prep.) was previously used to model Sudbury breccia samples gathered from along highway 144 in the North Range (Weirich et al., 2014). The model performs a principal component decomposition of geochemical data from a selection of Sudbury breccia samples. It then attempts to reconstruct the geochemical signature of the breccia using up to four end-members by applying the following criteria:

Criteria 1: $A_i + B_i + C_i + D_i = 1$ (100 %)

Criteria 2: $A_{SiO_2} + B_{SiO_2} + C_{SiO_2} + D_{SiO_2} = SB_{SiO_2}$

Criteria 3: $A_{EOI} + B_{EOI} + C_{EOI} + D_{EOI} = SB_{EOI}$

Equation 2-1: The criteria that the mixing model applies when modelling the breccia results using the end-member components (A, B, C and D), which are compared against the actual measured breccia samples. Criteria 2 is an independent variable (i.e. SiO₂ is always set as one of the elements of interest), whereas criteria 3, which uses the elements of interest (EOI) is a dependent variable (i.e. they can be adjusted or changed between localities if necessary). A_i, B_i, C_i and D_i must ≥ 0 in criteria 1.

Where X_i are the total percentage contributions from each end member, and X_{EOI} specifically relates to the elements of interest in the input members, which must sum the same concentration as that of the measured breccia (SB_{EOI}). Equation 2 and 3 are similar, except that SB_{SiO₂} is an independent variable, whereas SB_{EOI} is a dependent variable (i.e. equation 3

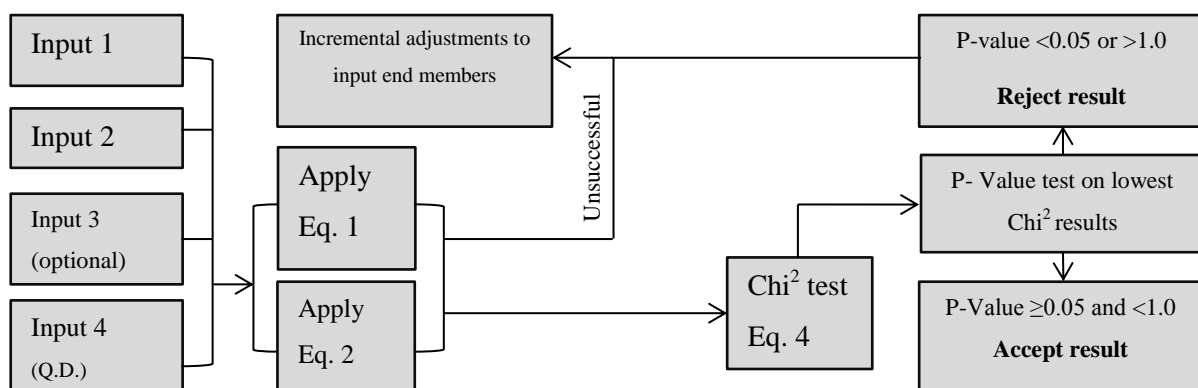


Figure 2.2: Flow chart demonstrating the IDL mixing model process, from the input of 3-4 end-member components (including quartz diorite: Q.D.), through to the output and interpretation of P-values based on the Chi² test. For the equations please refer to the methodology section. Eq. 3 is a dependent variable on the results of Eq. 1 and Eq. 2, which are independent variables.

is controlled by the values in equation 2). The input variables (X_i) for the mixing model are based on logically plausible end-member combinations that are in agreement with both geological maps (Ames et al., 2008) and observations at the sampled outcrops, the relative percentages of which are determined by the mixing model based on the elements of interest (see below). The model is limited to four end members, with one end member always set as quartz diorite from the closest offset dike (the impact melt proxy). The number of input parameters is limited to a maximum of four in order to avoid the model having too many degrees of flexibility, which can compromise statistical interpretation of the results (fig. 2.2). This also enables geologically complex localities, with more than one host rock, to be analysed (Weirich pers. comm. 2015). As the model has up to four input parameters, but applies just three equations (Eq. 1, 2 and 3) there is no deterministic solution. Instead, the model runs in a loop to determine all combinations of the two to four input end members that satisfies equations 1 and 2. Although the program will calculate a total suite of 63 elements, their relative quantities are determined based on a selected number of elements of interest (X_{EOI}), which are integrated into equation 2. In this study, the elements of interest were Al_2O_3 , SiO_2 , MgO , TiO_2 , Ce, Dy, Er, Eu, Gd, Ho, La, Lu, Nd, Pr, Sm, Tm, V, Y, Yb, Zr and Ni. This suite includes a combination of major and trace elements that should be diagnostic for each of the main rock types used as inputs for the model (e.g. gneiss, granite, and diabase). The number of elements of interest also controls the sensitivity of the mixing model and must be carefully selected. Too many X_{EOI} creates too many criteria for the program to fulfil, thus the model becomes increasingly inflexible. Conversely, too few elements will provide too many degrees of freedom for the program, affecting the validity of the model results, which are evaluated using χ^2 and P-tests. The Chi-test compares the modelled breccia with the geochemical signature of the measured breccia. The most robust modelled breccia results should have the lowest χ^2 value and are determined as follows:

$$\chi^2 = \sum \frac{(O_i - E_i)^2}{E_i}$$

Equation 2-2: The Chi-test equation used to validate the precision of the mixing model by comparing the model geochemical results with the original Sudbury breccia results that the model is attempting to replicate.

Where O_i and E_i are the observed and expected values, the latter based on the distribution of the total population of values. The P-value was calculated based on the χ^2 results, and is

a combination of several formula, which were calculated within the IDL software package (specifically the CHISQR_PDF function). Readers are directed to Barnett and Lin (2014) and others for specific details on the p-value calculation. The calculation provides a dimensionless value between 0 and 1 that can be used to determine whether or not the hypothesis (e.g. that the Chi^2 result is significant) is correct, based on a predetermined threshold value, which is normally 5 % or 0.05. P-value results between ≥ 0.05 and < 1.0 are considered acceptable (the probability of the Chi^2 result being low by chance, based on a pre-defined threshold value of > 0.05 or 5 %). P-values < 0.05 or ≥ 1.0 are indicative of either a missing input component (including alteration) restricting the result, or too many components resulting in excessive degrees of freedom in the calculation of the model breccia. The P-value is an efficient method by which to categorise models as “acceptable” or “unacceptable” and be used to indicate models that are more likely to be reproducible over repeated testing (Barnett and Lin, 2014; Werich et al., in prep.). Figure 2.2 provides a flow chart that lays out the processes of the model and how the most suitable percentage combinations of end-members are identified (i.e. low Chi^2 values and p-values between 0.05 and 0.99). Interpretation of statistic based mixing models must be done with caution, as such models will have inherent limitations. The dataset used in this study is representative of the geology of the sample localities as observed today and cannot take into account material that has been eroded away since the formation of the breccia. The mixing model is also limited by its inability to assign weighting to specific elements based on their error of precision during geochemical analysis.

2.5 Petrography

Sudbury breccia matrix from the North and South Range of the SIC has a similar macroscopic appearance, consisting of a dark grey, microcrystalline, aphanitic matrix hosting well-rounded, centimeter- to meter-sized lithic fragments, which tend to be derived from immediately adjacent host lithologies; although clasts of diabase and metasedimentary rock, transported over > 10 m were observed at South Pump Lake and the West Murray Area (Fig. 2.3A). In thin section, the breccia matrix is composed of fine-grained, aphanitic quartz and feldspar, with abundant biotite. Minor amounts of stilpnomelane, actinolite, epidote, clinozoisite, titanite, carbonate, chlorite and muscovite are also present, along with trace amounts of disseminated ilmenite, magnetite, haematite and rutile (Fig. 2.3B, C). Post-breccia-formation alteration was observed in some samples. At McCreedy East, this primarily consisted of chlorite-epidote-calcite hydrothermal veinlets, whereas at Creighton Deep some

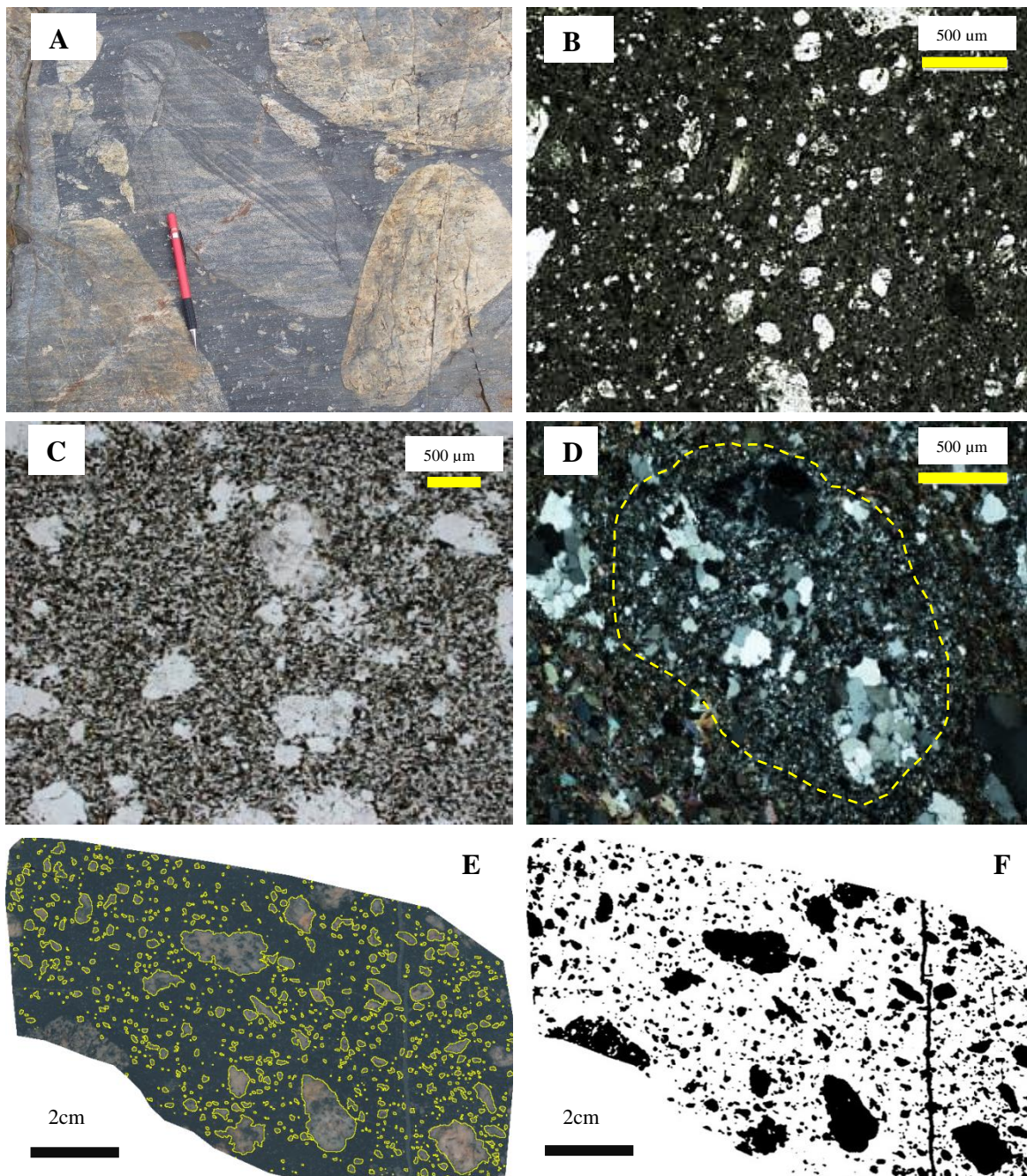


Figure 2.3: A: Field image of Sudbury breccia outcrop at, South Pump Lake showing lithic fragments of granite and transported metasedimentary rocks, in a dark grey, fine-grained matrix. B: Thin section in plane polarized light (PPL) showing the texture of Sudbury breccia from Halfway Lake. The field of view illustrates the very fine-grained matrix hosting quartz and feldspar lithic fragments and green chlorite patches. C: Thin section of Sudbury breccia in PPL from the Creighton Embayment in the South Ranges, showing a coarser-grained matrix, with brown biotite and rare titanite D: Sub-grain quartz rotation (outlined in yellow) around the margins of a lithic fragment within Sudbury breccia. E: Example of the image analysis process using imageJ™ software. Clasts were identified and outlined using a semi-automatic method producing a binary image; F: following manual adjustments such as removal of the epidote vein, the image is then analysed to produce quantitative values for the clasts, such as roundness.

of the breccia samples are strained, and the fabrics are locally associated with east-west fault structures that control the distribution of mineralization in the deep part of the Creighton Deposit. Sudbury breccia in the North Range is very similar, both in outcrop and thin section, to the fine-grained, flow banded pseudotachylites found at the Vredefort impact structure (Fig 1.4, 2.3A) (Shand, 1916; Reimold and Gibson, 2006; Lieger et al., 2011). In contrast, breccia samples from the South Range tend to be coarser-grained with greater mica content (Fig. 2.3C) (Rousell et al. 2003). Although no impact glass was directly observed in the breccia matrix, Sudbury breccia veins from Halfway Lake do exhibit vitric bands and margins (Fig. 2.4 A, B, C). We use the term “vitric” here to describe particles that resemble or may have originated from a glass. Technically, however, no glass clasts were observed in Sudbury

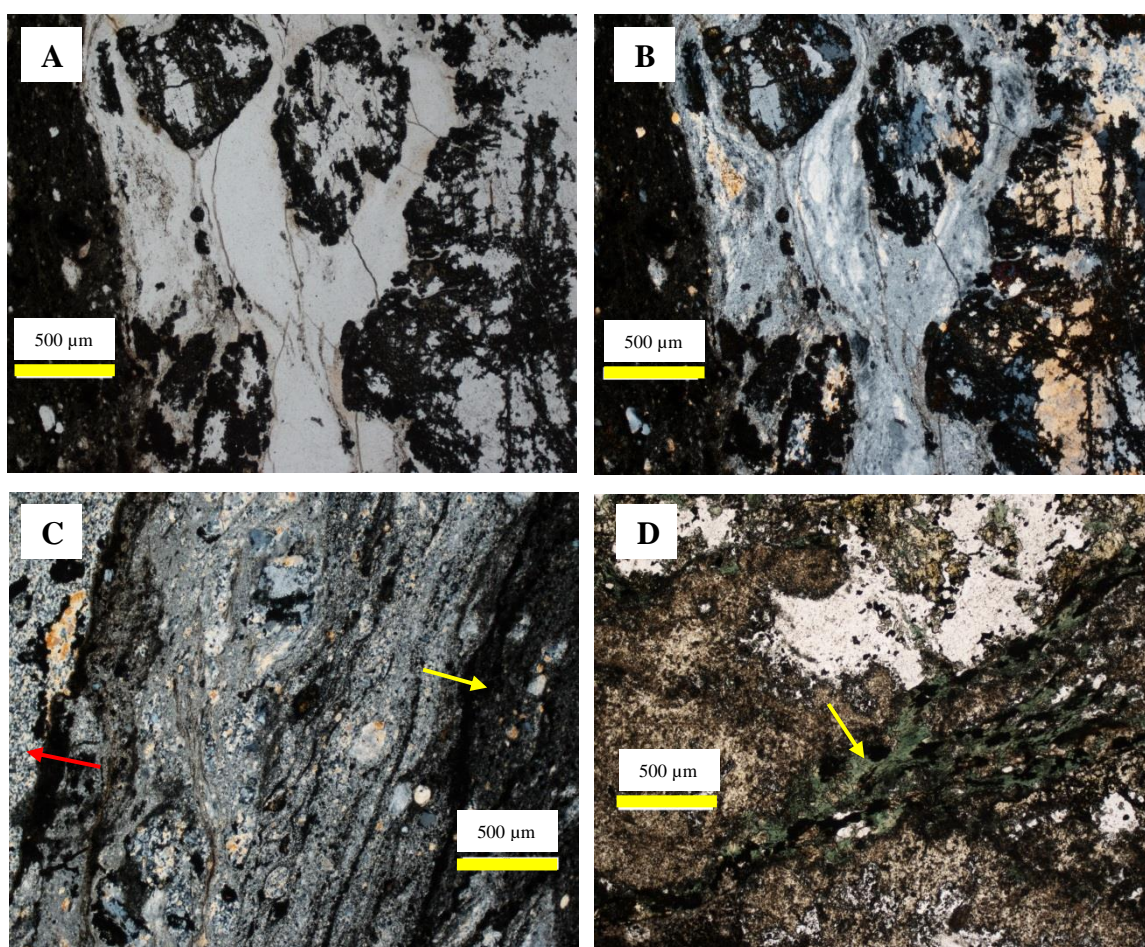


Figure 2.4: A: Thin section in PPL and B: thin section in (XPL) of flow-banded, vitric Sudbury breccia at the margins of Sudbury breccia veins from the Halfway Lake outcrop. C: Thin section in XPL illustrating flow banded, vitric Sudbury breccia from Halfway Lake, at the contact between host gneiss (red arrow) and darker, coarser breccia matrix towards the center of the vein (yellow arrow). D: Thin section in PPL of chlorite-titanite vein (yellow arrow) in altered gneiss adjacent to Sudbury breccia from Halfway Lake, which may represent devitrified melt material.

breccia, as they have been completely devitrified. The vitric bands do not exhibit any individual crystals in plane polarized light, whereas under crossed polars, stretched and contorted quartz and feldspar grains, aligned with the vein margins, were observed, implying partial melting at temperatures approaching at least 1100 °C (Spray 2010). Chloritized veinlets off-shooting from the breccia into the wall rocks, and similar contorted selvages within the matrix may also represent devitrified melts (Fig. 2.4D), similar to those observed by Randall (2004). The observation of sub-grain rotation (Fig. 2.3D), bulging quartz recrystallization and fine-grained oxide droplets within the breccia matrix from both the North and South Range also indicate that Sudbury breccia has experienced temperatures exceeding 700°C (Stipp et al., 2002; Kirkpatrick and Rowe 2013). In this study, efforts to image the lithic fragments entrained in the breccia has avoided domains showing post-impact recrystallization and alteration process that may have affected the matrix (Figs. 2.3 E, F). Lithic fragments in samples from Creighton Embayment, West Murray Area (South Range) and McCreedy 153 East zone (North Range) all have comparable complexity and roundness profiles, with >75 % of clasts at each of the three localities exhibiting a roundness factor (a dimensionless value from 0 to 1 that defines the angularity of an area of interest) exceeding 0.4 (Lin 1999) (Fig. 5). Roundness factor (a.k.a. degree of circularity or f_{circ}) is calculated based on the surface area of the clast, which is measured using the perimeter (P) and area (A) of the object of interest. As noted later in the discussion, this has important implications for the temperature conditions under which the lithic fragments were entrained in the matrix:

$$f_{circ} = \frac{4\pi A}{P^2}$$

Equation 2-3: The roundness or circularity factor equation, calculated by comparing the area (A) with the perimeter (P) of the object of interest.

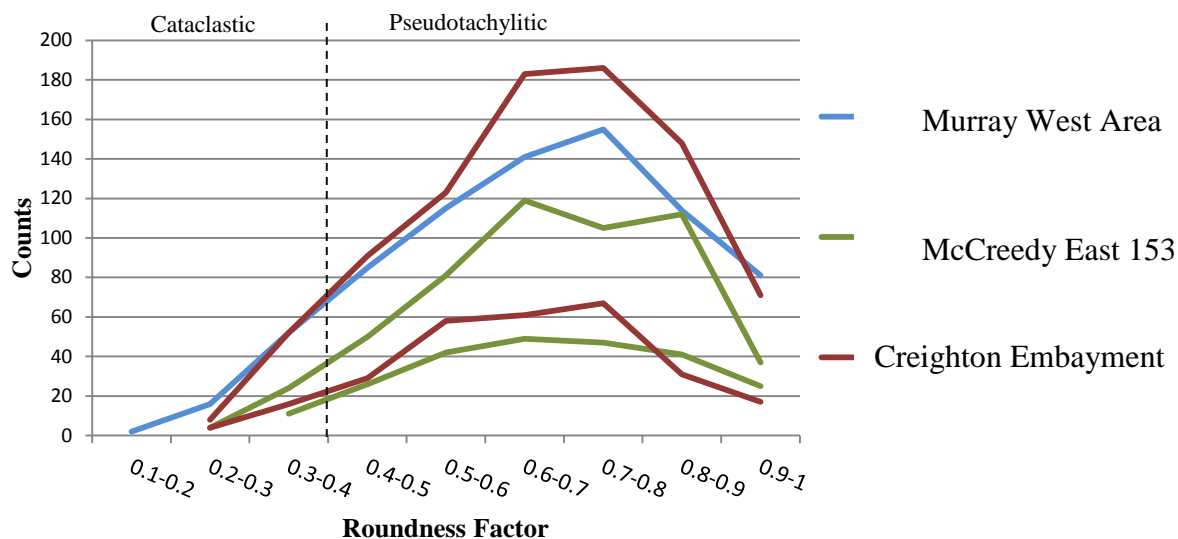


Figure 2.5: A comparison of the roundness of clasts for five samples collected from three localities in the North and South Range of the Sudbury basin. The results indicate that the average roundness of clasts from the three localities exceeds 0.4, indicative of clast entrainment in a high temperature, pseudotachylitic melt, rather than a cataclastic breccia. Roundness factors are determined based on the perimeter versus the area of each clast (see Eq. 3).

2.6 Geochemical Results and Modelling Parameters

The composition of the Sudbury breccia matrix is plotted on incompatible element diagrams normalised to the compositional average of the inclusion-free quartz diorite from the nearest offset dike (from Lightfoot et al. 1997a). These plots provide an empirical comparison of the breccia matrix to the host rock and help to identify whether a mixing relationship is viable, or whether there is a missing component that would need adding into the mixing model. The geochemical signature of the Sudbury breccia from the West Murray area is almost identical to that of the Murray granite which contains the breccia zone. For samples from the Old Creighton Town, the breccia matrix is enriched in immobile elements, compared with both the host granite and the proximal Creighton offset dike. This relationship implies that another, unidentified, end-member has contributed to the mix. A candidate for this end-member is located within <100 m of the Old Creighton Town outcrop, as a 50 x 100 m xenolith of coarse-grained material exhibiting gneissic features, including augen feldspars and gneissose banding. By comparing the geochemistry of a suite of candidate lithologies (including Levack Gneiss and Huronian Formations that may have been entrained in the Creighton pluton during emplacement) it was found that 2475 Ma migmatitic orthogneiss basement exposed adjacent to the 1250 Ma Grenville Orogenic front, provides a reasonable

end-member composition for the mix (Corfu and Easton, 2000; Murphy, 2001). A wide Range of footwall rock types are developed around the McCreedy East 153 ore body and the Creighton Deep mineral zones. The wider variety of footwall lithologies (compared with the West Murray Area and Old Creighton Town locations) may help to explain the wider Range in composition found in the Sudbury breccia matrix. However, the majority of breccia samples fall between the compositions of the host rocks (Fig. 2.6B). Likewise, the compositional average of Sudbury breccia developed adjacent to the Manchester offset dike plots between the composition of the nearby quartzite and gabbro, as does the average composition of the offset dike. The overlap between the geochemical signature of the breccia matrix and the Manchester offset dike is not diagnostic of the relative contributions from the country rocks and the offset dike. Comparison of the composition of the Sudbury breccia samples hosting 20-40 % locally derived lithic clasts versus breccia with <20 % clasts indicate a very small influence from small fragments in the breccia matrix. This is in agreement with recent studies by Weirich (et al., 2014), who observed that the removal of mineral fragments by clast-picking to create a ‘pure-matrix’ sample also had a negligible effect on the composition of the matrix, when compared with samples that had not been clast picked.

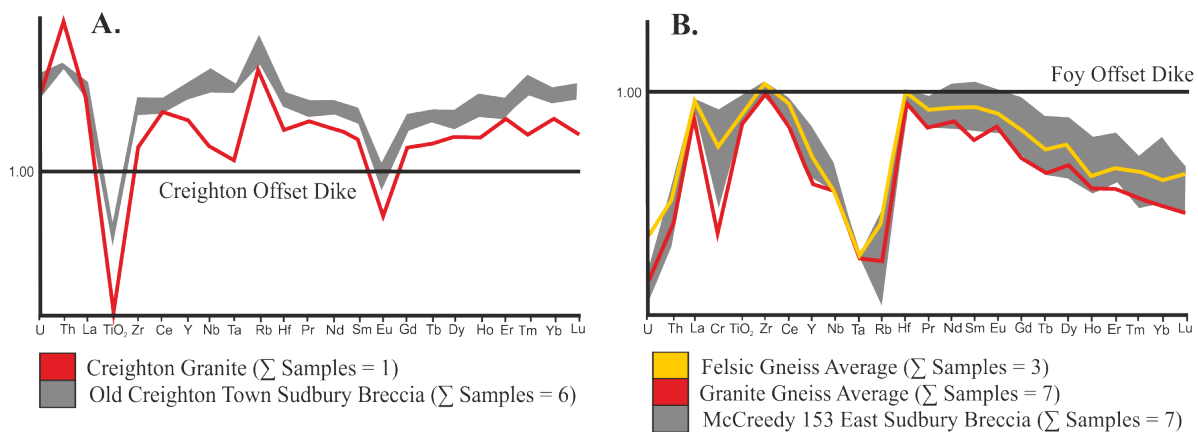


Figure 2.6: Immobile elements and REE from Sudbury breccia and adjacent, unbrecciated footwall lithologies, normalised to the local offset dike, which serve as proxies for an early undifferentiated impact melt. A. Sudbury breccia from Old Creighton Town shows no evidence of a melt contribution, which would ‘pull’ the geochemical signature down towards the composition of the offset dikes. B. At the McCreedy East 153 zone the relationships are more complex; most Sudbury breccia rests between the mafic and felsic gneiss footwall end members, but some samples show an enrichment that may be attributable to a primary melt sheet contribution.

2.7 Results of Principal Component Analysis

A total of 37 samples of Sudbury breccia from the Creighton embayment (South Pump Lake, Old Creighton Town and Creighton Deep) and McCreedy East zone were analysed using robust PCA, based on major elements and trace metals. South Pump Lake and Old Creighton Town were analysed together (Σ Sudbury breccia samples= 13) as both are distal to mineralized zones compared with Creighton Deep (Σ samples= 7) and McCreedy 153 East (Σ samples= 17). The first and second principal components (PC1-PC2) account for the most variation in the dataset and tend to reveal the most significant geochemical correlations (McCreedy East: 77.2 % of variation recorded by PC1-PC2; Creighton Deep 86.3 %; South Pump Lake + Old Creighton Town 81.8 %). Using the PC1-PC2 loadings (analogous to correlation coefficients) as co-ordinates, the PCA results can be visually plotted and interpreted in component space (Abdi and Williams 2010) (see chapter 2.9.2). Loadings furthest from the origin ($y, x = 0$) are more significant, whereas loadings closer to the origin indicate that the variation in that component is not wholly constrained by PC1-PC2 (i.e. strong correlation versus weak correlation between the selected elements). PCA results from all three localities show MgO, CaO, MnO, FeO, Cr and Ni as having strongly positive PC1 loadings versus SiO₂, which has a negative PC1 loading. At Creighton Deep and McCreedy 153 East, Al₂O₃, Na₂O and Cu exhibit a weaker correlation, which is altogether absent in more distal samples from the Creighton embayment, where Al₂O₃, Na₂O and K₂O tend to correlate with SiO₂. These observations can be quantitatively confirmed by the robust correlation matrix produced by the PCA (Table A2, A3 and A4 in the Appendix).

2.8 Results of Mixing Models

The qualitative observations noted in the previous chapter (Figs. 2.6 A, B) indicate that the local country rocks play an important part in the genesis of the matrix of the Sudbury breccia. Using mixing calculations, this section investigates whether a mixture of the country rocks can generate the observed breccia matrix, or whether an exotic melt-sheet-derived component is required. The areas selected for study are addressed in order of decreasing distance from known domains of mineralized Sudbury breccia. Results from the model were plotted and compared against measured breccia analyses in order to identify errors or discrepancies between the observed and modelled Sudbury breccia matrix. Representative geochemical results of the measured breccia versus modelled breccia are presented in Table

2-2 (country rock lithologies used to model the breccia can be found in Table A1 in the Appendix)

2.8.1 Manchester Offset Dike

Extensive outcrops of Sudbury breccia, up to 350 m wide surround the Manchester Offset Dike, which cuts the Bruce Formation quartzites and conglomerates, and pre-impact Sudbury gabbro dikes (O'Connor and Spray, 1997; Lightfoot et al., 1997c). Three breccia samples were collected, of which two were successfully modelled, but the HREE profile of the third sample did not correspond with any potential end-member combination. As previously noted, the geochemical overlap between the offset dike and footwall lithologies makes it difficult to establish the relative contributions of target rocks to the breccia matrix. To overcome this problem, the two remaining samples were run twice, firstly with a quartz diorite end-member, followed by a second run using only target lithologies. One sample did not require a contribution from the Manchester dike in either model, whereas the second sample could be

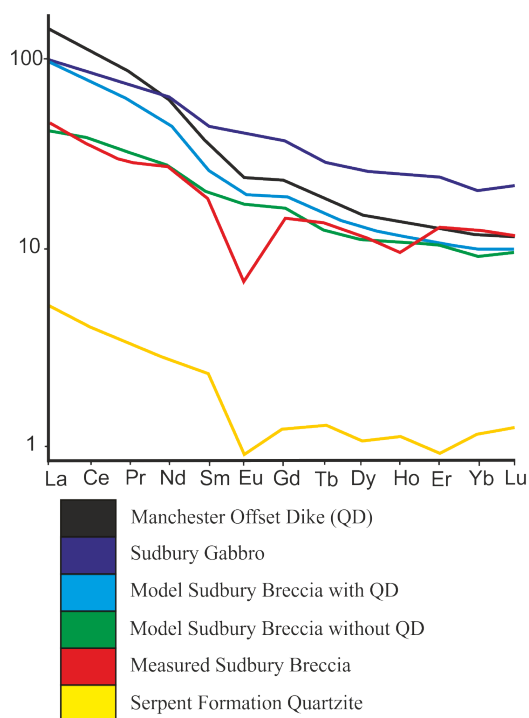


Figure 2.7 REE chondrite normalized plot (Sun and McDonough 1989) that compares two models of Sudbury breccia from the Manchester Offset Dike locality. The breccia modelled with a quartz diorite component has a poorer correlation with the measured breccia signature, compared to the model run using only the local footwall lithologies, quartzite and Sudbury Gabbro. Averages for footwall lithologies are shown.

modelled with 0–59 % quartz diorite. Empirical comparison of the two models shows that the immobile element and REE profile of the breccia modelled without quartz diorite yielded a superior fit (Fig. 2.7). In summary, the Sudbury breccia at the Manchester Offset Dike can be reconstructed from a combination of quartzite (45–57 %) and Sudbury gabbro (43–55 %), though a contribution of impact melt material cannot be ruled out.

2.8.2 South Pump Lake

Of the three localities around the Creighton Embayment, South Pump Lake is the most distal relative to the margin of the embayment. It is situated ~2 km southwest of the SIC contact. The Sudbury breccia veins cut the Creighton granite, but also contain lithic clasts of Huronian material (Fig. 2.3A) and lie close to a 6 x 1.5 km roof pendant of Elsie Mountain Formation basalt and mafic pyroclastic rocks. Two granite samples and one granodiorite sample were collected from the South Pump Lake area. Out of seven samples of breccia, five were successfully modelled with combinations of granite (19–46 %), granodiorite (18–47 %) and basalt (14–50 %) and a negligible contribution of quartz diorite (0–4 %) (Fig. 2.8A). Two Sudbury breccia matrix compositions were unsuccessfully modelled using the known end-member compositions, including quartz diorite (0% in both samples). These breccia samples may contain contributions from crustal sources that have not yet been identified, though an impact melt component can be ruled out.

2.8.3 Old Creighton Town

The Old Creighton Town Sudbury breccia outcrop is hosted entirely within the Creighton granite, 300 m south of the Creighton Embayment. A xenolithic raft of entrained granite gneiss is situated <100 m from the outcrop. Blocks of granodiorite have also been observed within outcrops of Sudbury breccia near the sample site. Based on the best fit results of modelling, the breccia at this locality consists of Creighton granite (40–70 %) and granodiorite (27–47 %) with a minor component of paragneiss from geochemical data compiled by Murphy (2001), which helps to explain the enrichment in LREE and Hf (1–13 %) (Fig. 2.8B). A contribution of quartz diorite from the Creighton offset dike (Lightfoot et al. 1997a) was not required to support the mixing model.

2.8.4 West Murray Area

The Sudbury Breccia veins at this location are hosted entirely within Murray granite. Mafic clasts observed in the breccia matrix may have been derived from quartz diabase and

Nipissing gabbro dikes that cut through the Southern Province granitoid plutons (Ames et al., 2008; Rousell and Brown, 2009). Modelling of nine Sudbury breccia samples collected from the West Murray Area require between 19–73 % Murray Granite, 0–60 % granodiorite and 2–27 % diabase (Fig. 2.8D). The quartz diorite component is 4 – 6 % in all but two samples, which require 13 and 28 %. These two outliers are split from the same outcrop as the other samples at this locality and are geochemically indistinguishable with the exception of notable depletions in La, Pr and Nd and enrichment in Rb. An experimental re-run of the program without a quartz diorite component (0%), created model breccias that were equally acceptable and with very similar geochemical signatures. Thus the high quartz diorite component may be an erroneous artifact of the mixing model attempting to account for the depleted LREE that is equally attributable to a greater diabase component, which is more likely given that the majority of samples from this site do not require an impact melt component.

2.8.5 Creighton Deep

Seven Sudbury breccia samples were collected from the footwall of the Creighton Deep ore zone within Creighton Mine, <500 m from the contact with the SIC and between 60 and 160 m from mineralized zones. The host lithologies consist of Creighton granite, granite porphyry and granodiorite, with entrained xenoliths of Elsie Mountain Formation metabasalts and gabbros. Both granitic and metabasalt fragments are present in the breccia matrix. The most successful mixing model reconstructs the breccia from a combination of a granite component (0 – 60 %), a metabasalt (2 – 93 %) and a granodiorite (1 - 64 %). Gabbro can also be included instead of metabasalt, contributing between 0 and 45 % (Fig. 2.8C). Quartz diorite from the Creighton offset dike (Lightfoot et al. 1997a) contributes 6% to one sample, but is not required in the other samples. Two samples of Sudbury breccia could not be modelled successfully. The geochemical signature of one sample is depleted in LREE compared with all of the end member rocks, including quartz diorite. The second qualitatively appears to have been successfully modelled when compared empirically with the other modelled breccia, but has a p-value <0.05, indicating a poor repeatability of the result.

2.8.6 McCreedy 153 East Ore Body

Seven samples of Sudbury breccia were collected from the country rocks containing the McCreedy East 153 ore body, which is part of the Coleman-Levack mine complex. The samples are located ~1 km from the SIC contact and trough structure hosting the Coleman

contact ore zone (Lightfoot 2015), and between 5 and 427 m from mineralized zones. The breccias are hosted in felsic gneiss, granite gneiss and mafic gneiss that form part of the Levack complex that borders the SIC-footwall contact across the North Range. Sudbury breccia samples were successfully modelled using a mixture of felsic gneiss (0–86 %), mafic gneiss (0–28 %) and granite gneiss (14–72 %) end-members from this study (Fig. 2.8E). A quartz diorite contribution from the Foy offset dike was not required to create the matrix composition of the Sudbury breccia.

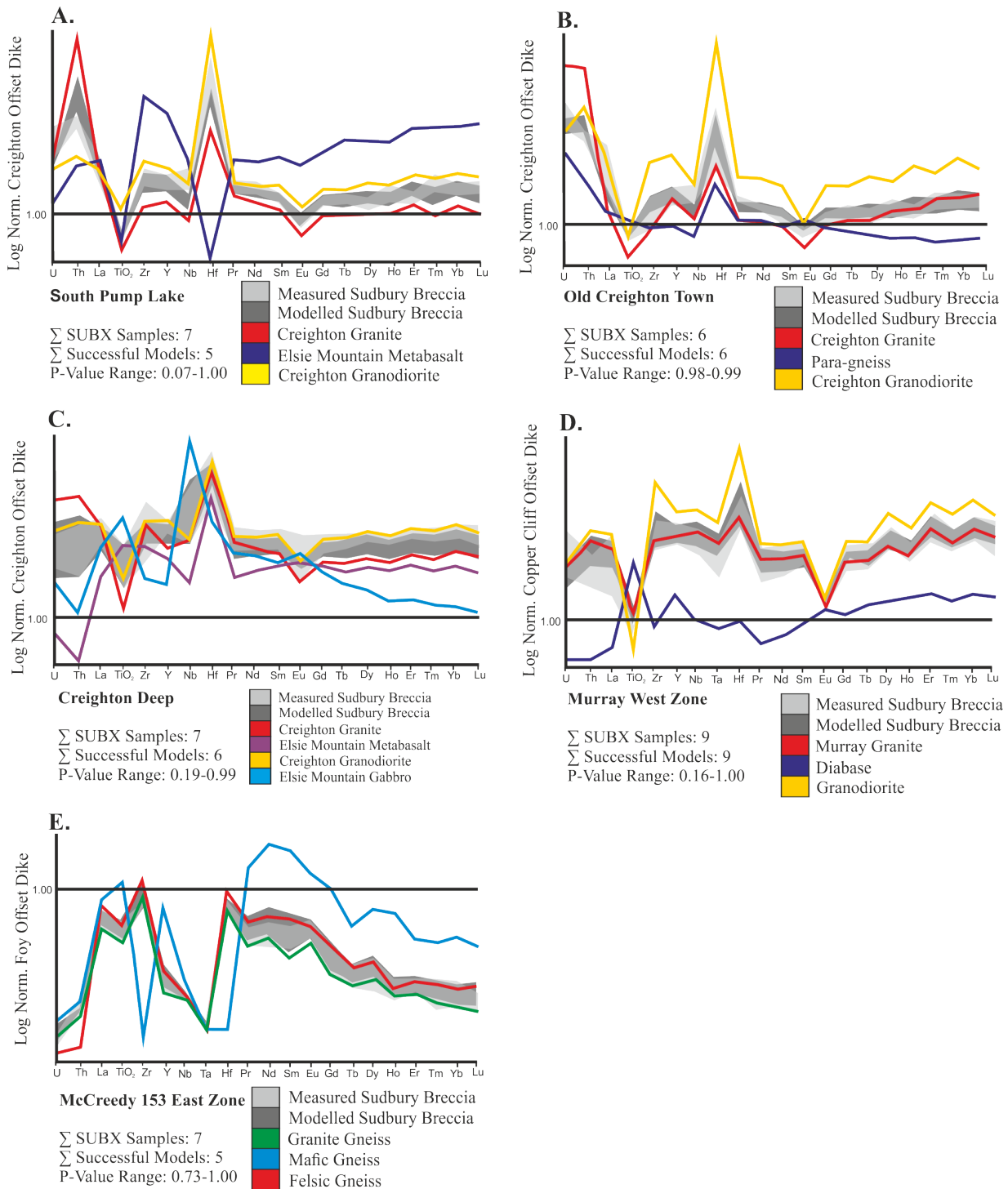


Figure 2.8: Incompatible trace element diagrams of end-member host rocks and measured and modelled Sudbury breccia, normalised to the closest quartz diorite offset dyke. Rare earth and incompatible element diagrams cover (A) South Pump Lake, (B) Old Creighton Town, (C) Creighton Deep, (D) the Murray West Zone and (E) the McCreeedy 153 East Zone. Representative host lithologies are presented along with the Range of measured and modelled Sudbury breccia results.

Table 2-2 Representative Sudbury breccia analyses and equivalent mixing model results and statistics.

Italicized elements were used as elements of interest (X_{eoi}) in the mixing model (see methodology).

	South Pump Lake		Old Creighton Town		Creighton Deep		Manchester Offset		153 McCreedy East		Murray West Zone	
	Observed	Model	Observed	Model	Observed	Model	Observed	Model	Observed	Model	Observed	Model
wt%												
<i>SiO₂</i>	<i>66.10</i>	<i>66.10</i>	<i>71.20</i>	<i>71.20</i>	<i>57.40</i>	<i>57.40</i>	<i>64.20</i>	<i>64.20</i>	<i>64.30</i>	<i>64.30</i>	<i>66.20</i>	<i>66.20</i>
<i>Al₂O₃</i>	<i>12.55</i>	<i>16.80</i>	<i>12.85</i>	<i>12.96</i>	<i>14.30</i>	<i>14.08</i>	<i>10.31</i>	<i>12.20</i>	<i>15.55</i>	<i>15.64</i>	<i>13.00</i>	<i>13.62</i>
Fe ₂ O ₃	7.32	4.81	5.17	4.01	10.05	10.06	10.20	3.58	5.20	5.31	6.13	6.60
CaO	2.27	1.37	1.71	1.93	5.99	6.24	4.58	2.70	4.64	5.13	3.36	3.40
<i>MgO</i>	<i>2.08</i>	<i>1.22</i>	<i>0.73</i>	<i>0.71</i>	<i>3.52</i>	<i>3.46</i>	<i>3.45</i>	<i>4.07</i>	<i>2.45</i>	<i>2.57</i>	<i>2.10</i>	<i>1.35</i>
Na ₂ O	2.53	2.27	2.79	2.84	3.04	2.78	2.70	5.37	4.45	4.46	2.78	3.18
K ₂ O	3.59	4.34	4.11	4.71	3.03	2.63	0.63	1.19	1.20	1.28	3.71	3.76
Cr ₂ O ₃	0.01	0.00	0.00	0.00	0.01	0.01	0.02	0.02	0.01	0.01	0.01	0.00
<i>TiO₂</i>	<i>0.49</i>	<i>0.63</i>	<i>0.42</i>	<i>0.42</i>	<i>1.04</i>	<i>1.11</i>	<i>1.87</i>	<i>1.04</i>	<i>0.56</i>	<i>0.55</i>	<i>0.60</i>	<i>0.75</i>
MnO	0.10	0.05	0.07	0.05	0.16	0.14	0.13	0.04	0.08	0.08	0.09	0.09
P ₂ O ₅	0.07	0.08	0.11	0.10	0.25	0.31	0.22	0.02	0.18	0.19	0.12	0.19
SrO	0.01	0.01	0.01	0.01	0.03	0.02	0.02	0.01	0.06	0.07	0.01	0.02
BaO	0.04	0.06	0.07	0.06	0.06	0.09	0.01	0.01	0.08	0.08	0.12	0.11
ppm												
Ba	332.00	765.09	646.00	645.91	584.00	788.48	110.31	81.60	632.00	699.23	960.00	945.32
<i>Ce</i>	<i>161.50</i>	<i>147.95</i>	<i>129.50</i>	<i>144.48</i>	<i>115.50</i>	<i>127.68</i>	<i>28.96</i>	<i>20.90</i>	<i>51.90</i>	<i>59.34</i>	<i>153.50</i>	<i>154.99</i>
Cr	40.00	79.92	20.00	15.15	100.00	91.49	78.39	110.00	70.00	72.80	70.00	22.97
Cs	15.65	6.22	10.85	4.09	2.97	2.45	0.82	1.35	0.37	0.50	6.23	3.85
<i>Dy</i>	<i>7.29</i>	<i>10.89</i>	<i>9.14</i>	<i>9.42</i>	<i>11.30</i>	<i>10.79</i>	<i>3.59</i>	<i>2.95</i>	<i>1.65</i>	<i>2.02</i>	<i>13.65</i>	<i>13.21</i>
<i>Er</i>	<i>5.13</i>	<i>7.03</i>	<i>5.92</i>	<i>6.34</i>	<i>7.20</i>	<i>6.54</i>	<i>2.18</i>	<i>2.06</i>	<i>0.80</i>	<i>0.87</i>	<i>8.54</i>	<i>8.48</i>
<i>Eu</i>	<i>1.03</i>	<i>1.53</i>	<i>1.36</i>	<i>1.31</i>	<i>1.43</i>	<i>1.94</i>	<i>1.26</i>	<i>0.39</i>	<i>1.06</i>	<i>1.14</i>	<i>1.89</i>	<i>1.96</i>
Ga	21.80	13.47	21.80	16.67	19.20	19.19	14.66	15.00	20.90	20.16	19.10	19.87
<i>Gd</i>	<i>6.90</i>	<i>10.68</i>	<i>9.19</i>	<i>9.22</i>	<i>10.00</i>	<i>10.46</i>	<i>4.15</i>	<i>2.88</i>	<i>2.55</i>	<i>3.01</i>	<i>12.80</i>	<i>12.49</i>
Hf	5.30	8.98	8.60	7.45	6.10	9.27	3.74	3.80	4.20	4.22	12.70	13.34
<i>Ho</i>	<i>1.80</i>	<i>2.10</i>	<i>2.08</i>	<i>1.85</i>	<i>2.18</i>	<i>2.03</i>	<i>0.77</i>	<i>0.53</i>	<i>0.28</i>	<i>0.31</i>	<i>2.70</i>	<i>2.59</i>
<i>La</i>	<i>105.50</i>	<i>78.68</i>	<i>69.60</i>	<i>73.27</i>	<i>56.60</i>	<i>61.48</i>	<i>12.77</i>	<i>10.50</i>	<i>27.70</i>	<i>31.17</i>	<i>83.10</i>	<i>80.22</i>
<i>Lu</i>	<i>0.80</i>	<i>1.03</i>	<i>0.94</i>	<i>0.83</i>	<i>1.09</i>	<i>0.89</i>	<i>0.30</i>	<i>0.29</i>	<i>0.09</i>	<i>0.12</i>	<i>1.28</i>	<i>1.21</i>
Nb	30.60	23.25	33.40	19.10	24.60	26.76	14.44	8.40	3.10	3.20	27.00	29.15
<i>Nd</i>	<i>55.70</i>	<i>62.87</i>	<i>58.10</i>	<i>56.39</i>	<i>54.00</i>	<i>55.77</i>	<i>16.08</i>	<i>12.30</i>	<i>21.20</i>	<i>25.67</i>	<i>68.60</i>	<i>66.81</i>
<i>Pr</i>	<i>15.90</i>	<i>16.70</i>	<i>15.10</i>	<i>15.69</i>	<i>14.05</i>	<i>14.40</i>	<i>3.77</i>	<i>2.61</i>	<i>5.97</i>	<i>6.81</i>	<i>18.60</i>	<i>18.16</i>
Rb	406.00	209.15	317.00	196.66	150.50	104.26	20.78	34.90	16.30	19.31	152.00	142.32
<i>Sm</i>	<i>8.82</i>	<i>11.62</i>	<i>10.45</i>	<i>10.56</i>	<i>11.10</i>	<i>11.73</i>	<i>3.74</i>	<i>2.76</i>	<i>3.88</i>	<i>4.40</i>	<i>13.70</i>	<i>13.71</i>
Sn	9.00	6.79	9.00	4.53	4.00	18.27	1.10	1.00	1.00	1.00	5.00	4.75
Sr	114.50	149.17	102.50	76.89	207.00	163.82	143.38	46.10	532.00	577.61	86.80	109.79
Ta	1.80	2.12	1.80	1.00	1.70	1.46	0.84	0.60	0.10	0.10	1.80	1.86
Tb	1.23	1.69	1.57	1.47	1.66	1.64	0.59	0.49	0.30	0.36	2.03	1.95
Th	30.30	32.08	29.70	37.54	13.45	12.13	2.59	6.11	3.37	2.72	18.70	21.54
<i>Tm</i>	<i>0.92</i>	<i>0.99</i>	<i>0.95</i>	<i>0.82</i>	<i>0.99</i>	<i>0.92</i>	<i>0.32</i>	<i>0.26</i>	<i>0.09</i>	<i>0.12</i>	<i>1.25</i>	<i>1.21</i>
U	8.10	6.91	6.04	4.31	3.19	2.55	0.53	1.66	0.25	0.34	5.29	4.04

<i>V</i>	95.00	76.05	25.00	27.38	142.00	120.69	215.61	133.00	81.00	87.63	63.00	59.70
<i>W</i>	1.00	2.69	4.00	5.71	1.00	1.00	1.00	1.00	<1	0.00	14.00	1.19
<i>Y</i>	48.50	63.67	55.30	52.81	63.90	56.65	18.86	15.60	7.30	8.70	73.90	72.03
<i>Yb</i>	5.92	7.32	5.92	6.15	8.00	6.50	1.91	2.01	0.61	0.72	8.55	8.45
<i>Zr</i>	169.00	326.79	312.00	298.13	224.00	336.84	131.26	141.00	176.00	169.56	445.00	476.26
Tl	10.00	0.00	0.00	9.40	10.00	0.00	0.00	<10	0.00	0.00	<10	6.07
Cd	<0.5	0.00	0.00	0.00	<0.5	0.19	0.00	<0.5	0.90	2.30	<0.5	0.01
Co	18.00	14.58	7.00	7.58	34.00	29.63	28.97	9.00	14.00	15.65	15.00	16.02
Cu	10.00	30.20	4.00	18.48	38.00	90.30	29.10	22.00	341.00	71.69	39.00	39.51
Li	110.00	16.64	60.00	17.94	40.00	13.50	5.48	<10	10.00	6.61	70.00	14.04
Mo	<1	0.51	0.00	1.04	<1	0.39	1.81	<1	<1	1.97	3.00	2.43
<i>Ni</i>	31.00	33.50	10.00	11.13	59.00	73.90	58.39	80.00	35.00	39.67	39.00	20.37
Pb	18.00	25.17	25.00	25.74	31.00	23.91	11.29	<2	408.00	243.16	23.00	32.41
Sc	14.00	12.07	6.00	5.67	19.00	18.34	18.00	14.00	8.00	9.00	11.00	11.04
Zn	143.00	84.60	96.00	69.81	184.00	125.92	80.94	6.00	99.00	116.35	112.00	127.92
Total	97.16	97.74	99.24	99.02	98.88	98.34	98.33	94.45	98.76	99.65	98.23	99.28
Average												
Chi2	24.1		2.69		6.96		7.37		2.93		2.38	
Average												
P-Value	0.12		0.99		0.97		0.98		0.99		0.99	

2.9 Discussion

2.9.1 Allochthonous versus Autochthonous origin for Sudbury breccia

Determining the relative contributions of autochthonous and allochthonous material present in Sudbury breccia has important implications for the conditions under which the matrix was generated. Previous studies have utilised major and trace element geochemistry to argue for both in situ- and impact melt contributions to the breccia matrix (Thompson & Spray 1996; Randall 2004; Lafrance et al. 2008; Riller et al. 2010; Lieger et al. 2011). Preferential melting of mafic phases (Spray, 1992; Thompson and Spray, 1996; Plattner et al., 2003), mixing of parautochthonous melt within the footwall (Reimold 1991; Reimold et al., 2015) and injection and mixing of impact melt within the footwall (Lieger et al., 2011) have also been suggested as mechanisms to explain the differences in major element concentrations between the breccia matrix and adjacent country rock. Several previous studies have already established that rheological variations between different lithologies (such as mafic and felsic units) can create planes of weakness in the target rock that are activated during the excavation and modification stages of cratering, creating fault and fracture zones which may preferentially localize pseudotachylite development (Kenkmann et

al., 2013; Dressler 1984; Thompson and Spray 1996; Mungall and Hanley 2004) and possibly create pathways for the emplacement of impact melt into the footwall (Lieber et al., 2011). Localization of the formation of Sudbury breccia at lithological and rheological contacts would create a pseudotachylite consisting of a mixture of contributions from the host rocks. This is consistent with our models for Sudbury breccia at localities that require a mixture of local mafic and felsic footwall components, such as at McCreedy 153 East and Creighton Deep.

Although it is incorrect to assume that the results of the mixing model provide evidence of the definitive relative contributions from local footwall lithologies, the results do demonstrate that there is no need to invoke an impact melt component to construct the geochemical signature of the breccia, regardless of proximity to the SIC melt sheet (Fig. 2.8). Moreover, a wholly in-situ genetic model is complicated by the presence of transported material such as diabase clasts at West Murray Area breccia and paragneiss material at Old Creighton Town. In the latter case, gneissic material is locally present as a xenolith, <100 m from the sample site, implying a localised transport mechanism during breccia formation. Similar observations were made by Schwarzman et al. (1983) and Reimold (1991) at the Vredefort impact structure, who concluded that the 50–100 m distance between in-situ mafic wall rocks and mafic clasts hosted in a cross cutting pseudotachylite vein were the result of some transport in the breccia. This can be explained by thermal expansion or injection of melt and entrained clasts into local, low pressure, extensional zones (Melosh, 2005; Riller et al., 2010; Reimold et al., 2015). Riller et al. (2010) suggests that the latter process could have driven the injection of SIC-derived impact melt into the footwall at Sudbury, though it is also consistent with transportation of locally-derived frictional melt into tensile damage zones adjacent fault planes (Fedorowich et al., 1999; Kim et al., 2004). The presence of tensile features such as en-echelon and jig-saw fractures at Old Creighton Town, similar to those reported by several authors (Speers, 1957; Fedorowich et al., 1999; Riller et al., 2010), extending outwards from a 1–2 m wide zone of Sudbury breccia that may have created low-pressure zones that served to mobilize and mix the melt in the wider, breccia-forming zone. The injection of cataclastic and pseudotachylitic material in fault damage zones has been reported in several settings, including the West Musgrave Block, Australia (Glikson and Mernagh, 1990), and the Muddy Mountain thrust fault, Nevada (Engelder, 1974).

The pooling of melt into extensional zones may also explain the accumulation of thick zones of pseudotachylitic breccia at both the Vredefort and Sudbury impact structures. Previously, Spray and Thompson (1995) proposed that a more protracted period of fault slip, on the order of kilometers, taking place over the space of several minutes during crater excavation and modification, could produce thick accumulations of in-situ melt. Lubrication of the fault zone by the initial frictional melt (and thus termination of frictional melting) could be prevented by immediate draining of pseudotachylitic melt into extension zones within and adjacent to the fault planes (Melosh, 2005), as has been demonstrated to occur in the Okanagan Valley shear zone in Southern British Columbia (Brown et al., 2015). Furthermore, recent research by Lavallée et al. (2015) has demonstrated that fault-generated frictional melts do not display standard Newtonian viscous behaviour and that under extreme slip conditions, the low viscosity melt acts more like a viscoelastic semi-solid. If the strain rate exceeds the period of viscous response, the melt can experience lubrication failure whilst continuing to behave as a mobile, low viscosity liquid (Mungall pers. comm. 2016). This would enable frictional melting to continue, with melt being transported into fracture zones away from their origin. The presence of Sudbury breccia veins with banded, vitric margins (Fig. 2.4A, B, C) may represent the zones of frictional melting, whereas veins lacking such textures could signify cooler material that has been transported into non-melt generating fractures. This may also explain the lack of displacement observed in host rocks either side of some pseudotachylite veins at both Sudbury and Vredefort, which has been noted in several studies (Zubrigg 1957; Riller et al., 2010; Lieger et al., 2011; Reimold et al., 2015).

Another group of models call on a cataclastic process rather than a melt origin for the Sudbury breccia. Pseudotachylites are, unfortunately, highly susceptible to post emplacement recrystallization and alteration processes, owing to their fine grain size and meta-stable mineralogy (Kirkpatrick and Rowe, 2013). As a result, evidence of quenching from a melt can be obliterated in a relatively short span of geologic time. Sudbury breccia is widely documented to have acted as a preferential pathway for hydrothermal fluid systems, evidenced by the presence of post-impact hydrothermal-metamorphic titanites and amphiboles (Fleet et al., 1987; Bailey et al., 2004), feldspar alteration (Thompson et al., 1998) and the spatial association between Sudbury breccia and post-impact hydrous assemblages (Farrow and Watkinson, 1992; Hanley 2002; Hanley et al., 2004). At Halfway Lake, Sudbury breccia bears a striking resemblance to pseudotachylites found in tectonic fault zones (Rousell et al. 2003; Weirich et al. 2014; Macaudiere et al., 1985; Glikson and

Mernagh, 1990) and at the Vredefort impact structure (Lieger et al. 2011) (Fig. 2.4 A, B). On the other hand, Sudbury breccia in the South Range has a coarser matrix that could be the result of formation by cataclasis (Rousell et al. 2003). Following the impact event, the South Range was uplifted by 10 to 15 km along the South Range Shear Zone (Shanks and Schwerdtner 1991; Riller, 2005). Thus the coarser Sudbury breccia from locations such as Murray and Creighton could also be a result of a greater depth of formation compared with the North Range breccia. Although the lack of a definitive melt texture in South Range Sudbury breccia is problematic for a high temperature origin, if they are cataclastic in origin (as proposed by Rousell et al. 2003) then the breccia clasts should be more angular than for a melt breccia, due to partial melting or thermomechanical erosion in the latter scenario (Magloughlin, 1992; Lin, 1999). Image analysis of lithic fragments in Sudbury breccia from McCreedy 153 East, the West Murray Area and the Creighton Embayment show similar clast surface areas, with >75 % of clasts exceeding a roundness factor of 0.4 (eq. 5) (Fig. 2.5). This suggests thermomechanical erosion in a high temperature melt setting, rather than fragmentation or comminution under cataclastic conditions (Lin, 1999). The presence of discrete oxide inclusions, sub grain rotation and bulging recrystallization textures in South Range breccias are also suggestive of a matrix that crystallised at temperatures exceeding 700 °C (Stipp et al., 2002; Kirkpatrick and Rowe, 2013). Although this temperature exceeds lower amphibolite facies, which is considered the peak grade of post-impact metamorphic overprinting in the area (Fleet et al. 1987; Magyarosi 1998), it may reflect high temperature, contact metamorphism associated with the SIC aureole (Prevec and Cawthorn, 2002). Optically continuous patches of quartz (a.k.a ‘flood quartz’) and the sub-igneous textures observed in Sudbury breccia in the McCreedy East and Victor mines has previously been attributed to thermal overprinting by the SIC (Morrison 1994) and may also account for the lack of primary melt textures in the majority of samples from this study. Further out from the SIC and associated heat aureole, melt textures, such as vitric margins, have been better preserved, as noted in Sudbury breccia at Halfway Lake and in quartz diorite at the Trill offset dike by Smith et al. (2013) and Coulter (2016).

2.9.2 The origin of trace metals within the Sudbury breccia

Sudbury breccia is considered to have acted as a structural weakness in the footwall into which evolved ISS sulfide melts were emplaced. This was followed by a partial redistribution of metals into the breccia by fluids expelled from the cooling sulfide melt and subsequent hydrothermal remobilization of fluids by regional meteoric fluid systems in the footwall

(Abel et al., 1979; Coats and Snajdr, 1984; McCormick and McDonald, 1999; Hanley and Mungall, 2003; Hanley et al., 2005; White, 2012). Several studies on Sudbury breccia immediately adjacent to footwall Cu-Ni-PGE sulfide veins have noted its relative enrichment in metals compared with the adjacent footwall lithologies, particularly for Cu, Au, Pt and Pd (Morrison et al., 1994; Ames and Farrow, 2007).

Anomalous metal concentrations further away from the ore zones are difficult to reconcile with expulsion or remobilization of metals from sulfide melts. For example, Sudbury breccia near the Manchester Offset Dike has relatively elevated concentrations of up to 80 ppm Ni and 32 ppm Cu, despite the lack of a significant known mineral zone in the area. The geochemical modelling presented in the previous section implies that the trace metal content in Sudbury breccia could be partially derived from local country rocks. The robust principal component analysis of Sudbury breccia samples from the Creighton embayment and McCreehy 153 localities reveals a correlation between MgO, MnO, FeO, Ni, Cr \pm CaO versus SiO₂ \pm Al₂O₃, K₂O that likely reflects the relationship between breccia matrix derived from

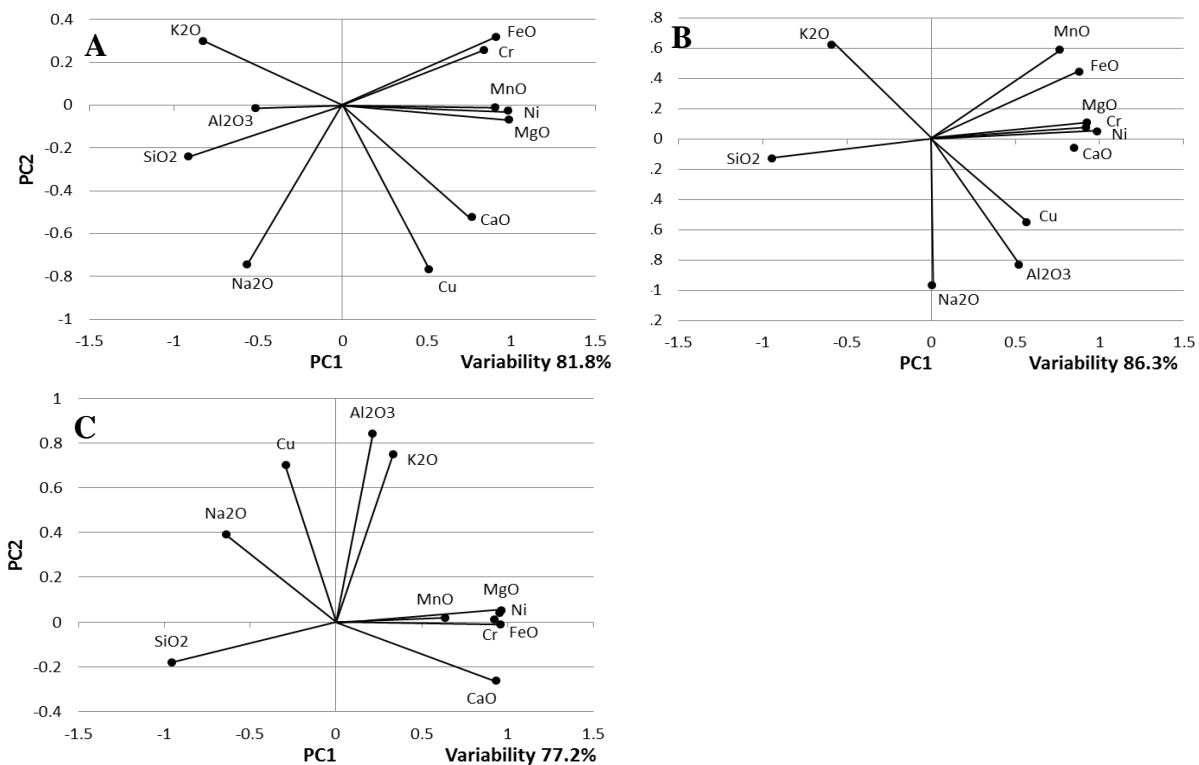


Figure 2.9: Robust PCA PC1-PC2 correlation graphs of major elements and trace metals for A: Old Creighton Town and South Pump Lake Zone, B Creighton Deep and C: McCreehy 153 East. The coordinates sit within a circle of correlation. Loadings closer to the center of the circle ($y, x = 0$) indicate that not all the variation in that component is accounted for in PC1 or PC2. Loadings with similar coordinates indicate a positive correlation for those elements (e.g. MnO, MgO and Ni). See Abdi and Williams (2010) for details on PCA correlation plots.

more siliceous rocks versus more mafic rocks (Fig. 2.9A, B, C). Thus there appears to be a particularly strong association between Ni, Cr and the assimilation of mafic lithologies in the footwall. In the case of the Manchester sample site, Sudbury gabbro, a ubiquitous lithology in the South Range, provides the most suitable local metal source, in an area largely made up of quartz-feldspathic metasedimentary rocks. Studies by Al Barazi et al. (2009) on Sudbury breccia in the South West of the Sudbury basin, adjacent to the Worthington Offset Dike, also concluded that, aside from an impact melt component, Nippising (Sudbury) gabbro provided the best source for metal enrichments in the breccia. A degree of host lithology control on the breccia metal content is also demonstrated at Creighton Deep, where a Sudbury breccia sample with a Cu content of 97 ppm, (the average Cu concentration from this locality was 22 ppm), was found to include lithic fragments of altered metabasalt hosting discrete, very fine grained disseminated chalcopyrite and bornite. The general absence of mafic clasts in the breccia matrix can be explained by the preferential assimilation of mafic units, owing to the lower shear yield strength or thermal conductivity of minerals commonly associated with such rocks (e.g. biotite and amphibole) (Spray, 1992; Spray, 2010). In light of this, it would be expected that mafic footwall lithologies would have a significant influence on the geochemistry and trace metal content of Sudbury breccia, even in localities where it is a relatively minor component.

Compared with Ni and Cr, Cu in more distal breccia samples does not show a strong correlation with other elements (Fig. 2.9A). However, within mineralized zones at Creighton Deep and McCreedy 153 East, there is a second order principal component correlation (PC2) between Cu, Al_2O_3 and Na_2O , inferring that Cu is controlled by a different process than that of the other trace metals (Fig. 2.9B, C). One explanation could be the occurrence of fine-grained disseminations of Cu-sulfide inclusions within sheet- and sorosilicates, such as chlorite, epidote and illite, which has previously been reported in aureoles surrounding ultramafic-mafic Ni-Cu-PGE intrusions and Cu-Au porphyry systems (Ahn et al., 1997; Suarez et al., 2009). It is possible that there is a similar association at Sudbury, resulting from hydrothermal interaction with the ore zones following their emplacement. For example, in Sudbury breccia from the McCreedy East 153 zone, post-mineralization, epidote-chlorite veinlets and biotite alteration patches are observed hosting subhedral, disseminated pyrite>>chalcopyrite grains. These post-impact epidote veinlets are associated with orthomagmatic- and basement-derived fluids and have been attributed to the localised remobilization of metals out of footwall ore zones (Molnar et al., 2001; Campos-Alvarez et

al., 2010; Tuba et al., 2014) and may explain the elevated Cu concentrations in felsic gneisses adjacent to sulfide veins in the 153 ore zone (up to 826 ppm Ni and 1240 ppm Cu), compared to distal host rock (8–50 ppm Cu). Combining the PCA results with the mixing model results indicates that the metal content of the breccia appears to be a continuum between assimilation of Ni-Cr bearing mafic units from the footwall and an aureole of silicate hosted, Cu inclusions that has developed near to the mineral zones, possibly reflecting hydrothermal remobilization.

2.10 Conclusions

Our observations do not support an impact melt injection model; instead they indicate that, rather than a wholly in-situ or autochthonous impact melt origin, Sudbury breccia is the product of a more dynamic, parautochthonous melt mixing process. Its geochemistry, combined with field observations, points towards the presence of a localised transport mechanism, such as thermal expansion or pressure driven injection into tensile zones adjacent to fault planes. The presence of vitric margins on some breccia veins, away from the thermal aureole of the SIC, combined evidence of thermomechanical erosion of lithic fragments and high temperature quartz recrystallization textures, appears to rule out a cataclastic origin. Rather, we suggest that the breccia was formed from a high temperature melt. In general, there is evidence of thermal overprinting and recrystallization of Sudbury breccia adjacent to the SIC, which has obliterated any evidence of impact glass or melt in the breccia matrix. More specifically, the coarser texture of breccia throughout the South Range may be attributed to a combination of orogenic overprinting and original formation at a much greater depth than breccias in the North Range.

The data we present for samples from distal and proximal to sulfide mineral zones has identified two sources for trace metal concentrations in the Sudbury breccia. At localities distal to the ore zones, Ni and Cr can be derived wholly from preferential assimilation of metal-bearing mafic units. However, closer to ore bearing zones, our results are in agreement with previous work, in which there appears to be a halo of hydrothermally altered, metalliferous Sudbury breccia, related to remobilized metals associated with the footwall ore zones. Thus care must be exercised when evaluating trace metals in Sudbury breccia for exploration purposes, in particular, comparison with local mafic units is advised in order to set a background trace metal value prior to determining the degree of metal enrichment/depletion in the breccia matrix.

2.11 References

- Abel, M.K., Buchan, R., Coats, C.J.A., and Penstone, M.E., 1979, Copper Mineralization in the Footwall Complex, Strathcona Mine, Sudbury, Ontario: *Canadian Mineralogist*, v. 17, p. 275–285.
- Ahn, J.H., Xu, H., and Buseck, P.R., 1997, Transmission Electron Microscopy of Native Copper Inclusions in Illite: *Clay and Clay Materials*, v. 45, no. 2, p. 295–297.
- Aitchinson, J., 1983, Principal component analysis of compositional data: *Biometrika*, v. 70, no. 1, p. 57–65.
- Aitchison, J., Barcelo-Vidal, C., Martin-Fernandez, J.A. and Pawlowsky-Glahn, V., 2000: Log-ratio analysis and compositional distance, *Mathematical Geology*, v. 32, p. 271-275.
- Ames, D., and Farrow, C., 2007, Metallogeny of the Sudbury mining camp, Ontario., in Goodfellow, W.D. ed., *Mineral Deposits of Canada: A Synthesis of Major Deposit-Types, District Metallogeny, the Evolution of Geological Provinces, and Exploration Methods*, Geological Association of Canada, Mineral Deposits Division, Special Publication, p. 329–350.
- Ames, D.E., Davidson, A., and Wodicka, N., 2008, Geology of the Giant Sudbury Polymetallic Mining Camp, Ontario, Canada.: *Economic Geology*, v. 103, p. 1057–1077.
- Anders, D., Osinski, G.R., Grieve, R.A.F., and Brillinger, D.T.M., 2015, The Basal Onaping Intrusion in the North Range: Roof rocks of the Sudbury Igneous Complex: *Meteoritics & Planetary Science*, v. 50, no. 9, p. 1577–1594.
- Al Barazi, S., Riller, U., and Hecht, L., 2009, Geochemistry of Pseudotachylites in Target Rocks of the Sudbury Impact Structure, Ontario, Canada, [abs] 72nd Annual Meteoritical Society Meeting, Nancy, France, 2009, Abstract 5397.

- Bailey, J., Lafrance, B., McDonald, A.M., Fedorowich, J.S., Kamo, S., and Archibald, D.A., 2004, Mazatzal–Labradorian-age (1.7–1.6 Ga) ductile deformation of the South Range Sudbury impact structure at the Thayer Lindsley mine, Ontario: *Canadian Journal of Earth Sciences*, v. 41, no. 12, p. 1491–1505.
- Barnett, I., and Lin, X., 2014, Analytic p-value calculation for the higher criticism test in finite-d problems: *Biometrika*, v. 101, no. 4, p. 964–970.
- Bestmann, M., Pennacchioni, G., Frank, G., Göken, M., and de Wall, H., 2011, Pseudotachylite in muscovite-bearing quartzite: Coseismic friction-induced melting and plastic deformation of quartz: *Journal of Structural Geology*, v. 33, no. 2, p. 169–186.
- Brown, S.R., Andrews, G.D.M., Russell, J.K., and Gibson, H.D., 2015, Rheological and structural constraints on the accumulation of 'thick' pseudotachylites *Petrology Geochemistry & Petrogenesis Outcrop data*, American Geophysical Union, San Francisco, USA, 2015, (<http://fallmeeting.agu.org/2012/files/2012/12/AGU-poster-pseudotachylite-v.3.pdf>) .
- Campbell, N.A. (1980). Robust procedures in multivariate analysis. I: Robust covariance estimation; *Applied Statistics*, v. 29, p 231-237.
- Campos-Alvarez, N.O., Samson, I.M., Fryer, B.J., and Ames, D.E., 2010, Fluid sources and hydrothermal architecture of the Sudbury Structure: Constraints from femtosecond LA-MC-ICP-MS Sr isotopic analysis of hydrothermal epidote and calcite: *Chemical Geology*, v. 278, no. 3-4, p. 131–150.
- Card, K.D. and Pattison, E.F., 1973. Nipissing diabase of the Southern Province; in Huronian stratigraphy and sedimentation, in Young, G.M., ed., Geological Association of Canada Special Paper 12, p. 7-30.
- Chai, G., and Eckstrand, R., 1994, Rare-earth element characteristics and origin of the Sudbury Igneous Complex, Ontario, Canada: *Chemical Geology*, v. 113, p. 221–244.

- Chanou, A., Osinski, G.R., and Grieve, R.A.F., 2014, A methodology for the semi-automatic digital image analysis of fragmental impactites: *Meteoritics & Planetary Science*, v. 49, no. 4, p. 621–635.
- Coats, C.J.A. and Snajdr, P., 1984, Ore deposits of the North Range, Onaping-Levack area, in Pye, E.G., Naldrett, A.J., Giblin, P.E., eds., *The geology and ore deposits of the Sudbury structure: Ontario Geological Survey Special Volume 1*, p. 327–346.
- Corfu, F., and Easton, R.M., 2000, U-Pb evidence for polymetamorphic history of Huronian rocks within the Grenville front tectonic zone east of Sudbury, Ontario, Canada: *Chemical Geology*, v. 172, p. 149–171.
- Coulter, A.B., 2016, Recent Discoveries in the Ni-Cu-PGE bearing Trill and Parkin Offset dykes, Sudbury impact structure, Canada: Unpublished M.Sc. thesis, London, Canada, University of Western Ontario, 152 p.
- Davis, D.W., 2008, Sub-million-year age resolution of Precambrian igneous events by thermal extraction–thermal ionization mass spectrometer Pb dating of zircon: Application to crystallization of the Sudbury impact melt sheet: *Geology*, v. 36, no. 5, p. 383–386.
- Dence M.R., 1971, Impact Melts: *Journal of Geophysical Research*, v. 23, p. 5552-5565
- Deutsch, A., Grieve, R.A.F., Avermann, M.E., Bischoff, L., Brockmeyer, P., Buhl, D., Lakomy, R., Müller-Mohr, V., Ostermann, M., and Stoffler, D., 1995, The Sudbury Structure (Ontario, Canada): a tectonically deformed multi-ring impact basin: *Geologische Rundschau*, v. 84, p. 697–709.
- Dickin, A.P., Artan, M.A., and Crocket, J.H., 1996, Isotopic evidence for distinct crustal sources of North and South Range ores, Sudbury Igneous Complex: *Geochimica et Cosmochimica Acta*, v. 60, no. 9, p. 1605–1613.
- Dietz R.S., 1964, Sudbury Structure as an Astrobleme: *The Journal of Geology*, v. 72, no. 4, p. 412–434.

- Dressler, B., 1984, The Effects of the Sudbury Event and the Intrusion of the Sudbury Igneous Complex on the Footwall Rocks of the Sudbury Structure, in Pye, E.G., Naldrett, A.J., and Giblin, P.E. eds., *Geology and Ore Deposits of the Sudbury Structure*, Ontario Geological Survey, p. 99–131.
- Ebel, D.S., and Naldrett, a. J., 1996, Fractional crystallization of sulfide ore liquids at high temperature: *Economic Geology*, v. 91, p. 607–621.
- Engelder, J.T., 1974, Cataclasis and the Generation of Fault Gouge: *Geological Society of America Bulletin*, v. 85, p. 1515–1522.
- Fahrig, W.F., and West, T.D. 1986. Diabase dyke swarms of the Canadian Shield. *Geological Survey of Canada, Map 1627A*
- Fairbairn, H.W., Faure, G., Pinson Jr., W.H., Hurley, P.M., 1968, Rb–Sr whole-rock age of the Sudbury lopolith and basin sediments: *Canadian Journal of Earth Sciences* 5 (3), 707–714.
- Farrow, C.E.G., and Watkinson, D.H., 1992, Alteration and the Role of Fluids in Ni , Cu and Platinum-Group Element Deposition, Sudbury Igneous Complex Contact, Onaping-Levack area, Ontario: *Mineralogy and Petrology*, v. 46, p. 67–83.
- Farrow, C.E.G., Everest, J.O., King, D.M., and Jolette, C., 2005, Sudbury Cu-(Ni)-PGE systems: Refining the classification using McCreedy West mine and Podolsky project case studies, in Mungall, J.E. ed., *Exploration for Deposits of Platinum-Group Elements*, Mineralogical Association of Canada Short Course 35, Oulu, Finland, p. 163–180.
- Filzmoser, P., and Hron, K., 2008, Correlation Analysis for Compositional Data: *Mathematical Geosciences*, v. 41, p. 905–919.
- Fleet, M.E., Barnett, R.L., and Morris, W.A., 1987, Prograde Metamorphism of the Sudbury Igneous Complex: *Canadian Mineralogist*, v. 25, p. 499–514.

- Glikson, A.Y., and Mernagh, T.P., 1990, Significance of pseudotachylite vein systems, Giles basic/ultrabasic complex, Tomkinson Ranges, western Musgrave Block, central Australia: *Journal of Australian Geology and Geophysics*, v. 11, p. 509–519.
- Golightly J.P., 1994, The Sudbury Igneous Complex as an Impact Melt. In *Proceedings, Sudbury-Noril'sk Symposium*. Edited by P.C. Lightfoot and A.J. Naldrett. Ontario Geological Survey, Special Volume 5, p. 57-64.
- Grieve, R.A.F., and Therriault, A.M., 2013, Impactites: their characteristics and spatial distribution, in, G.R., Pierazzo, E., eds., *Impact cratering: processes and products*, Wiley-Blackwell p. 90–105.
- Grieve, R.A.F., Ames, D.E., Morgan, J. V., and Artemieva, N., 2010, The evolution of the Onaping Formation at the Sudbury impact structure: *Meteoritics & Planetary Science*, v. 45, no. 5, p. 759–782.
- Hanley, J.J., and Bray, C.J., 2009, The Trace Metal Content of Amphibole as a Proximity Indicator for Cu-Ni-PGE Mineralisation in the Footwall of the Sudbury Igneous Complex, Ontario, Canada: *Economic Geology*, v. 104, p. 113–125.
- Hanley, J.J., and Mungall, J.E., 2003, Chlorine Enrichment and Hydrous Alteration of the Sudbury Breccia Hosting Footwall Cu-Ni-PGE Mineralization at the Fraser Mine, Sudbury, Ontario, Canada: *The Canadian Mineralogist*, v. 41, p. 857–881.
- Hanley, J.J., Mungall, J.E., Bray, C.J., and Gorton, M.P., 2004, The Origin of Bulk and Water Soluble Cl and Br Enrichments in Ore Hosting Sudbury Breccia in the Fraser Copper Zone, Strathcona Embayment, Sudbury, Ontario, Canada: *The Canadian Mineralogist*, v. 42, p. 1777–1798.
- Hanley, J.J., Mungall, J.E., Pettke, T., Spooner, E.T.C., and Bray, C.J., 2005, Ore metal redistribution by hydrocarbon–brine and hydrocarbon–halide melt phases, North Range footwall of the Sudbury Igneous Complex, Ontario, Canada: *Mineralium Deposita*, v. 40, no. 3, p. 237–256.

- Heaman, L.M. 1989. U-Pb dating of mafic dyke swarms: what are the options?, [abs] International Association of Volcanology and Chemistry of the Earth's Interior, Continental Magmatism, New Mexico Bureau of Mines and Mineral Resources, Bulletin 131, Abstract p.125.
- Kenkmann, T., Collins, G.S., and Wünnemann, K., 2013, The Modification Stage of Crater Formation, in, G.R., Pierazzo, E., eds., Impact cratering: processes and products, Wiley-Blackwell, p. 60–75.
- Kennedy, L.A., and Spray, J.G., 1992, Frictional melting of sedimentary rock during high-speed diamond drilling: an analytical SEM and TEM investigation: *Tectonophysics*, v. 204, no. 3-4, p. 323–337.
- Keays R.R., and Lighfoot P.C., 2004, Formation of Ni-Cu-PGE sulphide mineralisation in the Sudbury Impact Melt Sheet: *Mineralogy and Petrology*, v. 82, no. 3. P. 217-258
- Kim, Y.S., Peacock, D.C.P., and Sanderson, D.J., 2004, Fault damage zones: *Journal of Structural Geology*, v. 26, p. 503–517.
- Kirkpatrick, J.D., and Rowe, C.D., 2013, Disappearing ink: How pseudotachylites are lost from the rock record: *Journal of Structural Geology*, v. 52, p. 183–198.
- Krogh, T.E., Corfu, F., Davis, D.W., Dunning, G.R., Heaman, L.M., Kamo, S.L., Machado, N., Greenough, J.D. and Nakamura, E. 1987. Precise U-Pb isotope ages of diabase dikes and mafic to ultramafic rocks using trace amounts of baddeleyite and zircon; in *Mafic Dike Swarms*, Geological Association of Canada, Special Paper 34, p.147-152.
- Krogh, T.E., Davis, D.W. and Corfu, F. 1984. Precise U-Pb zircon and baddeleyite ages for the Sudbury area; in *The Geology and Ore Deposits of the Sudbury Structure*, Ontario Geological Survey, Special Volume 1, p.431-446.

- Krogh, T.E., Kamo, S.L. and Bohor, B.F. 1996. Shocked metamorphosed zircons with correlated U-Pb discordance and melt rocks with concordant protolith ages indicate an impact origin for the Sudbury Structure; in *Earth Processes: Reading the Isotope Code*, American Geophysical Union, Monograph 95, p.343-352.
- Lafrance, B., and Kamber, B.S., 2010, Geochemical and microstructural evidence for in situ formation of pseudotachylitic Sudbury breccia by shock-induced compression and cataclasis: *Precambrian Research*, v. 180, p. 237–250.
- Lafrance, B., Legault, D., and Ames, D.E., 2008, The formation of the Sudbury breccia in the North Range of the Sudbury impact structure: *Precambrian Research*, v. 165, p. 107–119.
- Lavallée, Y., Hirose, T., Kendrick, J.E., Hess, K.-U., and Dingwell, D.B., 2015, Fault rheology beyond frictional melting: *Proceedings of the National Academy of Sciences*, v. 112, no. 30, p. 9276–9280.
- Li, C., and Naldrett, A.J., 1994, A numerical model for the compositional variations of Sudbury sulfide ores and its application to exploration: *Economic Geology*, v. 89, p. 1599–1607.
- Lieger, D., Riller, U., and Gibson, R.L., 2009, Generation of fragment-rich pseudotachylite bodies during central uplift formation in the Vredefort impact structure, South Africa: *Earth and Planetary Science Letters*, v. 279, p. 53–64.
- Lieger, D., Riller, U., and Gibson, R.L., 2011, Petrographic and geochemical evidence for an allochthonous, possibly impact melt, origin of pseudotachylite from the Vredefort Dome, South Africa: *Geochimica et Cosmochimica Acta*, v. 75, no. 16, p. 4490–4514.
- Lightfoot P.C., 2015, Structural Controls on Nickel Sulfide Mineralization at Sudbury, Thompson and Voisey's Bay: *Prospectors and Developers Conference*, Toronto, Canada 2015.

- Lightfoot, P.C., and Farrow, C.E.G., 2002, Geology, Geochemistry, and Mineralogy of the Worthington Offset Dike: A Genetic Model for Offset Dike Mineralization in the Sudbury Igneous Complex: *Economic Geology*, v. 97, p. 1419–1446.
- Lightfoot, P.C., and Keays, R.R., 2001, Sulfide saturation history and ore genesis of the Sudbury Igneous Complex: Constraints from main mass and offset geochemistry [abs.]: 11th Annual Goldschmidt Conference, Roanoke, Virginia, 2000, Abstracts with Proceedings. (CD-ROM)
- Lightfoot, P.C., Doherty, W., Farrell, K.P., Keays, R.R., Moore, M., and Pekeski, D., 1997a, Geochemistry of the Main Mass, Sublayer, Offsets and Inclusions from the Sudbury Igneous Complex, Ontario: Ontario Geological Survey Open File Report 5959, p. 231.
- Lightfoot, P.C., Morrison, G.G., Bite, A., and Farrell, P., 1997b, Geochemical Relationships in the Sudbury Igneous Complex: Origin of the Main Mass and Offset Dikes: *Economic Geology*, v. 92, p. 289–307.
- Lightfoot, P.C., Naldrett, A.J., and Morrison, G.G., 1997c, Sublayer and Offset Dikes of the Sudbury Igneous Complex- an Introduction and Field Guide: Ontario Geological Survey, Open File Report 5965, 50 p.
- Lightfoot P.C., Keays R.R., and Doherty W., 2001, Chemical Evolution and Origin of Nickel Sulfide Mineralization in the Sudbury Igneous Complex, Ontario, Canada: *Economic Geology*, v. 96, p. 1855-1875.
- Lin, A., 1999, Roundness of clasts in pseudotachylites and cataclastic rocks as an indicator of frictional melting: *Journal of Structural Geology*, v. 21, p. 473–478.
- Macaudiere, J., Brown, W.L. & Ohnenstetter, D., 1985. Microcrystalline textures resulting from rapid crystallization in a pseudotachylite melt in a meta-aNorthosite. *Contributions to Mineral Petrology*, v. 89, pp.39–51
- Maddock, R.H., 1974, Melt origin of fault-generated pseudotachylites: *Geology*, v. 11, p. 105–108.

- Magloughlin, J.F., 1992, Microstructural and chemical changes associated with cataclasis and frictional melting at shallow crustal levels: the cataclasite-pseudotachylite connection: *Tectonophysics*, v. 204, p. 243–260.
- Magyarosi Z., 1998, *Metamorphism of the Proterozoic Rocks Associated with the Sudbury Structure*: Unpublished M.Sc. thesis, Ottawa, Canada, Carleton University, 118 p.
- McCormick, K.A., and McDonald, A.M., 1999, Chlorine-bearing amphiboles from the Fraser mine, Sudbury, Ontario, Canada: description and crystal chemistry: *The Canadian Mineralogist*, v. 37, p. 1385–1403.
- Meldrum, A., Abdel-Rahman, A.-F.M., Martin, R.F., and Wodicka, N., 1997, The nature, age and petrogenesis of the Cartier Batholith, northern flank of the Sudbury Structure, Ontario, Canada: *Precambrian Research*, v. 82, p. 265–285.
- Melosh, H., 1979, Acoustic fluidization: A new geologic process?: *Journal of Geophysical Research*, v. 84, pp.7513 – 7520.
- Melosh, H.J., 1989, *Impact cratering—A geologic process*: New York, Oxford University Press, 245 p
- Melosh, H.J., 2005, The Mechanics of Pseudotachylite Formation in Impact Events, in Koeberl, C. and Henkel, H. eds., *Impact Studies*, Springer, p. 55–80.
- Miyahshiro A., 1973, *Metamorphism and Metamorphic Belts*: Springer, 492 p.
- Molnar, F., Watkinson, D.H., and Jones, P.C., 2001, Multiple Hydrothermal Processes in Footwall Units of the North Range, Sudbury Igneous Complex, Canada, and Implications for the Genesis of Vein-Type Cu-Ni-PGE Deposits: *Economic Geology*, v. 96, p. 1645–1670.
- Morrison G.G., 1984, Morphological features of the Sudbury structure in relation to an impact origin: *Ontario Geological Survey Special Volume 1*, p. 513-522.

- Morrison G.G., Jago B.C., White T.L., 1994, Footwall mineralization of the Sudbury Igneous Complex, in Lightfoot P.C. and Naldrett A.J., eds., Proceedings of the Sudbury-Noril'sk Symposium. Ontario Geological Survey, Special Volume 5, p. 57-64.
- Müller-Mohr, V., 1992, Breccias in the basement of a deeply eroded impact structure, Sudbury, Canada: *Tectonophysics*, v. 216, p. 219–226.
- Mungall, J.E., and Hanley, J.J., 2004, Origins of Outliers of the Huronian Supergroup within the Sudbury Structure: *The Journal of Geology*, v. 112, no. 1, p. 59–70.
- Murphy, E.I., 2001, Geology, Metamorphism and Geochemistry of Rocks of the Southern and Grenville Provinces in the Vicinity of the Grenville Front, Timmins Creek Area, Near Sudbury, Ontario: Ontario Geological Survey, Open File Report 6041, 132 p.
- Naldrett A.J., and Hewins R.G., 1984, The main mass of the Sudbury Igneous Complex, in, Pye, E.G., Naldrett A.J., and Giblin P.E., eds., *The geology and ore deposits of the Sudbury Structure*, Ontario Geological Survey Special Volume 1, p. 235-251.
- Naldrett, A.J., Bray, J.G., Gasparrini, E.L., Podolsky, T., and Rucklidge, J.C., 1970, Cryptic variation and the petrology of the sudbury nickel irruptive: *Economic Geology*, v. 65, p. 122–155.
- Naldrett, A.J., Rao, B.V. and Evensen, N.M., 1986, Contamination at Sudbury and its role in ore formation, in *Metallogeny of Basic and Ultra- basic Rocks*: Gallagher, M.J., Ixer, R.A., Neary, C.R. and Pritchard, H.M. eds. Special Publication of the Institute of Mining and Metallurgy, London, p.75-92.
- Naldrett, A.J., Asif, M., Schandl, E., Searcy, T., Morrison, G.G., Binney, W.P., and Moore, C., 1999, Platinum-Group Elements in the Sudbury Ores: Significance with Respect to the Origin of Different Ore Zones and to the Exploration for Footwall Orebodies: *Economic Geology*, v. 94, p. 185–210.
- Nelles, E.W., 2012, Genesis of Cu-PGE-rich Footwall-Type Mineralization in the Morrison Deposit, Sudbury: Unpublished M.Sc. thesis, Sudbury, Canada, Laurentian University, 96 p.

- Noble, S.R., Lightfoot, P.C., 1992, U–Pb baddeleyite ages of the Kerns and Triangle Mountain intrusions, Nipissing diabase, Ontario. *Canadian Journal of Earth Sciences*. 29, 1424–1429.
- O'Connor, J.P., and Spray, J.G., 1997, Geological Setting of the Manchester Offset Dyke within the South Range of the Sudbury Impact Structure. [abs.] *Large Meteorite Impacts and Planetary Evolution*, 1997, Sudbury, Canada, Abstracts, p. 38.
- Pentek, A., Molnar, F., Watkinson, D.H., and Jones, P.C., 2008, Footwall-type Cu-Ni-PGE Mineralization in the Broken Hammer Area, Wisner Township, North Range, Sudbury Structure: *Economic Geology*, v. 103, p. 1005–1028.
- Parementer, A.C., Lee, C.B. and Conigli, M., 2002, “Sudbury Breccia” at Whitefish Falls, Ontario: evidence for an impact origin, *Canadian Journal of Earth Sciences*, v. 39, no. 6, p. 971-982.
- Petrus, J. a., Ames, D.E., and Kamber, B.S., 2015, On the track of the elusive Sudbury impact: geochemical evidence for a chondrite or comet bolide: *Terra Nova*, v. 27, no. 1, p. 9–20.
- Plattner, U., Markl, G., and Sherlock, S., 2003, Chemical heterogeneities of Caledonian (?) pseudotachylites in the Eidsfjord Anorthosite, North Norway: *Contributions to Mineralogy and Petrology*, v. 145, p. 316–338.
- Prevec, S.A., and Cawthorn, R.G., 2002, Thermal evolution and interaction between impact melt sheet and footwall: A genetic model for the contact sublayer of the Sudbury Igneous Complex, Canada: *Journal of Geophysical Research*, v. 107, no. 8, p. 1–14.
- Prevec, S., Lightfoot, P., and Keays, R., 2000, Evolution of the sublayer of the Sudbury Igneous Complex: geochemical, Sm–Nd isotopic and petrologic evidence: *Lithos*, v. 51, p. 271–292.
- Randall, W., 2004, *Petrogenesis of Pseudotachylites from the Sudbury Structure*:

Unpublished B.Sc. thesis, Toronto, Canada, University of Toronto, 39 p.

- Reimold, W.U., and Gibson, R.L., 2006, The melt rocks of the Vredefort impact structure - Vredefort Granophyre and pseudotachylitic breccias: Implications for impact cratering and the evolution of the Witwatersrand Basin: *Chemie der Erde - Geochemistry*, v. 66, no. 1, p. 1–35.
- Reimold, W.U., Wannek, D., Hoffmann, M., Hansen, B.T., Hauser, N., Schulz, T., Siegert, S., Thirlwall, M., Zaag, P.T., and Mohr-Westheide, T., 2015, Vredefort Pseudotachylitic Breccia and Granophyre (Impact Melt Rocks): Clues to their Genesis from New Field, Chemical and Isotopic Investigations: [abs] *Bridging the Gap III*, Freiburg, Germany, 2015, Abstract 1035.
- Rickard, J.H., and Watkinson, D.H., 2001, Cu-Ni-PGE Mineralization within the Copper Cliff Offset Dike, Copper Cliff North Mine, Sudbury, Ontario : Evidence for Multiple Stages of Emplacement: *Exploration and Mining Geology*, v. 10, no. 1-2, p. 111–124.
- Riller, U., 2005, Structural characteristics of the Sudbury impact structure, Canada: Impact-induced versus orogenic deformation-A review: *Meteoritics & Planetary Science*, v. 40, no. 11, p. 1723–1740.
- Riller, U., 2009, Felsic Plutons, in *A Field Guide to the Geology of Sudbury Ontario*, Ontario Geological Survey Open File Report 6243, p11-13
- Riller, U., Cruden, A.R. and Schwerdtner, W.M. 1996. Magnetic fabric and microstructural evidence for a tectono- thermal overprint of the Murray pluton, central Ontario, Canada; *Journal of Geology*, v.18, p.1005-1016.
- Riller, U., Lieger, D., Gibson, R.L., Grieve, R.A.F., and Stoffler, D., 2010, Origin of large-volume pseudotachylite in terrestrial impact structures: *Geology*, v. 38, no. 7, p. 619–622.
- Rousell, D.H., and Brown, G.H., 2009, *A Field Guide to the Geology of Sudbury, Ontario*: Ontario Geological Survey, Open File Report 6243, 223p.

- Rousell, D.H., Fedorowich, J.S., and Dressler, B.O., 2003, Sudbury Breccia (Canada): a product of the 1850 Ma Sudbury Event and host to footwall Cu–Ni–PGE deposits: *Earth-Science Reviews*, v. 60, p. 147–174.
- Rousell, D.H., Gibson, H.L., and Jonasson, I.R., 1997, The Tectonic, Magmatic and Mineralisation History of the Sudbury Structure: *Exploration and Mining Geology*, v. 6, no. 1, p. 1–22.
- Schwarzman, E.C., Meyer, C.E., and Wilshire, H.G., 1983, Pseudotachylite from the Vredefort Ring, South Africa, and the origins of some lunar breccias.: *Geological Society of America Bulletin*, v. 94, p. 926–935.
- Scott, R.G., and Spray, J.G., 2000, The South Range Breccia Belt of the Sudbury Impact Structure : *Meteoritics & Planetary Science*, no. 35, p. 505–520.
- Shand, S.J., 1916, The Pseudotachylite of Parijs (ORange Free State) and its Relation to “Trap-Shotten Gniess” and “Flinty Crush-Rock”: *Quarterly Journal of the Geological Society*, v. 72, p. 198–221.
- Shanks, W.S. and Schwerdtner, W.M. 1991. Structural analysis of the central and southwestern Sudbury Structure, Southern Province, Canadian Shield; *Canadian Journal of Earth Sciences*, v.28, p.411-430.
- Smith, D.A., Bailey, J., and Pattison, E.F., 2013, Discovery of New Offset Dykes and Insights into the Sudbury Impact Structure, [abs] *Large Meteorite Impacts and Planetary Evolution V*, 2013, Sudbury, Canada, Abstract 3090.
- Souch, B.E. and Podolsky, T., 1969, The sulphide ores at Sudbury: their particular relationship to a distinctive inclusion-bearing facies of the Nickel Irruption; in *Magmatic Ore Deposits*, *Economic Geology*, Monograph 4, p.252-261.
- Speers, E.C., 1957, The Age Relation and Origin of Common Sudbury Breccia: *The Journal of Geology*, v. 65, no. 5, p. 497–514.

- Spray, J.G., 1992, A physical basis for the frictional melting of some rock-forming minerals: *Tectonophysics*, v. 204, p. 205–221.
- Spray, J.G., 2010, Frictional Melting Processes in Planetary Materials: From Hypervelocity Impact to Earthquakes: *Annual Review of Earth and Planetary Sciences*, v. 38, no. 1, p. 221–254.
- Spray, J.G., and Thompson, L.M., 1995, Friction melt distribution in a multi-ring impact basin: *Letters to Nature*, v. 373, p. 130–132.
- Stipp, M., Stünitz, H., Heilbronner, R., and Schmid, S.M., 2002, The eastern Tonale fault zone: A “natural laboratory” for crystal plastic deformation of quartz over a temperature Range from 250 to 700 °C: *Journal of Structural Geology*, v. 24, p. 1861–1884.
- Suarez, S., Nieto, F., and Velasco, F., 2009, Copper inclusions in chlorite from the Aguablanca Ni-Cu-PGE sulfide deposit (SW Spain): *Revista de la Sociedad Espanola de Mineralogia*, v. 11, p. 173–174.
- Thompson, L.M., and Spray, J.G., 1996, Pseudotachylite petrogenesis: constraints from the Sudbury impact structure: *Contributions to Mineralogy and Petrology*, v. 125, no. 4, p. 359–374.
- Thompson, L.M., Spray, J.G., and Kelley, S.P., 1998, Laser probe argon-40/argon-39 dating of pseudotachylite from the Sudbury Structure: Evidence for postimpact thermal overprinting in the North Range: *Meteoritics & Planetary Science*, v. 33, p. 1259–1269.
- Di Toro, G., and Pennacchioni, G., 2004, Superheated friction-induced melts in zoned pseudotachylites within the Adamello tonalites (Italian Southern Alps): *Journal of Structural Geology*, v. 26, no. 10, p. 1783–1801.

- Tuba, G., Molnár, F., Ames, D.E., Péntek, A., Watkinson, D.H., and Jones, P.C., 2014, Multi-stage hydrothermal processes involved in “low-sulfide” Cu(–Ni)–PGE mineralization in the footwall of the Sudbury Igneous Complex (Canada): Amy Lake PGE zone, East Range: *Mineralium Deposita*, v. 49, p. 7–47.
- Tuchscherer, M., and Spray, J., 2002, Geology, mineralization, and emplacement of the Foy Offset Dike, Sudbury impact structure: *Economic Geology*, v. 97, p. 1377–1397.
- Weirich, J.R., Osinski, G.R., Pentek, A., and Bailey, J., 2014, Geochemistry of Sudbury Breccia in the North Range of the Sudbury Impact Structure, Canada., [abs] 45th Lunar and Planetary Science Conference, Woodlands, Texas, USA, 2014, Abstract 1819.
- White, C.J., 2012, Low-Sulfide PGE-Cu-Ni Mineralization From Five Prospects Within The Footwall Of The Sudbury Igneous by Low-Sulfide PGE-Cu-Ni Mineralization from Five Prospects with the Footwall of the Sudbury Igneous Complex , Ontario , Canada: Unpublished Ph.D thesis, Toronto, Canada, University of Toronto, 337 p.
- Wood, C.R., and Spray, J.G., 1998, Origin and emplacement of Offset Dykes in the Sudbury impact structure: Constraints from Hess.: *Meteoritics & Planetary Science*, v. 33, p. 337–347.
- Zieg, M.J., and Marsh, B.D., 2005, The Sudbury Igneous Complex: Viscous emulsion differentiation of a superheated impact melt sheet: *Geological Society of America Bulletin*, v. 117, no. 11, p. 1427.
- Zurbrigg, H.F., 1957, The Frood–Stobie Mine: Structural Geology of Canadian Ore Deposits: Canadian Institute of Mining and Metallurgy Congress Volume 2. CIM, Montreal, Canada, pp. 341–349

Chapter 3

3 Contrasting mineralogical and geochemical characteristics of Sudbury breccia adjacent to footwall Cu-Ni-PGE sulfide in the Crighton and Coleman deposits

3.1 Introduction

Footwall sulfide systems situated beneath the 1.85 Ga Sudbury Igneous Complex (SIC) represent fractionated sulfide melts that were transported from overlying, embayment-hosted, contact-style magmatic Ni-Cu deposits, into extensive zones of underlying Sudbury breccia (Morrison, 1984; Farrow et al., 2005; Ames and Farrow, 2007). The Sudbury breccia consists of centimeter to meter-scale veins of a dark grey, fine-grained, aphanitic matrix hosting locally-derived lithic fragments (Thompson and Spray, 1996; Rousell et al., 2003). There is evidence that hydrothermal magmatic fluids modified existing contact and/or footwall sulfide mineralization to form a wider footprint of disseminated, ‘low-sulfide’ high-precious-metal style (LSHPM) mineralization within zones of Sudbury breccia (Gibson et al., 2010; White, 2012; Tuba et al., 2014). Several investigations strived to constrain the nature and extent of the geochemical aureoles adjacent to the ‘footwall’ Cu-Ni-PGE mineralization through studies on the mineralogy and chemistry of the breccia (Farrow and Watkinson, 1992; Li and Naldrett, 1993; McCormick and McDonald, 1999; Molnar et al., 2001; Hanley and Mungall, 2003; Pentek, 2009; Nelles, 2012; White, 2012). These studies reveal systematic changes in the chemistry of mineral assemblages relative to the position of the known mineral zones. They may provide vectors towards footwall-style mineralization and they can provide insights on the composition of the fluids and the hydrothermal, magmatic or metamorphic processes (Caritat et al., 1993; Che et al., 2013; Warren et al., 2015; Wilkinson et al., 2015; Williamson et al., 2016). However, despite the larger volume of contact-style mineralization relative to footwall-style (~8:1), there is a notable absence of an extensive hydrothermal stain, disseminated sulfide halo or mineral vector within rocks adjacent to Ni-Cu contact-deposits. The exception is the presence of small, discontinuous patches of LSHPM zones and some structurally remobilized examples of contact-style ore (e.g., Garson and Crean Hill Deposits) (Lightfoot 2007; Gibson et al., 2012).

In the case of footwall-style mineralization, between ~150-700 m from mineralized-zones, both the relative abundances of hydrosilicates (e.g. amphiboles, chlorites, biotites) and their halogen and trace metal contents increase in the matrix of Sudbury breccia (Li and Naldrett, 1993; McCormick and McDonald, 1999; Hanley and Mungall, 2003; Hanley et al., 2004; Hanley and Bray, 2009; White, 2012). These variations may serve as a vector towards areas that are more prospective for footwall mineralization, although the exact relationship between the fractionated Cu-Ni-PGE sulfide melt and the hydrous mineral alteration assemblage remains poorly understood (Hanley and Mungall, 2003; Hanley and Bray, 2009; Leshner et al., 2009). With the exception of a study by White (2012), the majority of recent investigations on geochemical and mineralogical variations in the Sudbury breccia have been confined to the North and East Range of the Sudbury basin (in particular the Coleman-Levack embayment). This is largely because the higher metamorphic grade in the South Range, which peaked at a lower amphibolite facies during the 1.84 – 1.85 Ga Penokean Orogeny (Fleet et al., 1987), has thwarted efforts to develop linkages between hydrothermal and magmatic processes.

The goal of this work is to compare the mineral assemblages and mineral chemistry of Sudbury breccia, collected proximal and distal to zones of known footwall mineralization at Coleman Mine in the North Range with that developed proximal to footwall mineral zones at Creighton Mine in the South Range. This study builds upon previous research to identify key elemental and mineralogical vectors towards mineral zones in the North and South Ranges and to constrain the P-T conditions experienced by Sudbury breccia during and following the emplacement of sulfide zones. A special emphasis of this study is to apply recent research results on the application of titanite and chlorite in vectoring to mineral zones and understanding the geothermobarometry of mineral zones (Suarez et al., 2009; Li et al., 2010; Wilkinson et al., 2015; Xu et al., 2015; Yavuz et al., 2015).

3.2 Geological Setting

3.2.1 Regional Geology

The 30 x 60 km Sudbury Basin represents the eroded remains of an impact structure with an estimated initial diameter of ~200 – 250 km, which was a result of a bolide impact at the southern margin of the Superior Province at 1850 ± 1.3/-2.4 Ma (Fig. 3.1) (Dietz, 1964; Dressler, 1984; Krogh et al. 1984; Davis, 2008; Petrus et al., 2015). The basin consists of a

differentiated impact melt sheet (Naldrett and Hewins, 1984; Grieve 1994; Golightly 1994), overlain by the Onaping Formation (Grieve et al., 2010; Anders et al., 2015) and later turbidites and sedimentary rocks of the (1720 ± 30 Ma) Whitewater Group (Fairbairn et al., 1968). The basal contact between the igneous complex and the footwall is marked by discontinuous units of inclusion bearing, noritic-gabbroic material termed the Sublayer, which is thought to represent the assimilation front of the melt sheet into the footwall (Naldrett et al. 1986; Lightfoot et al., 1997; Prevec et al., 2000). The footwall of the SIC is broadly divided into the North (including East) and South Range. The North Range lies within the Superior Province and overlies the 2642 ± 1 Ma Cartier granites, which is thought

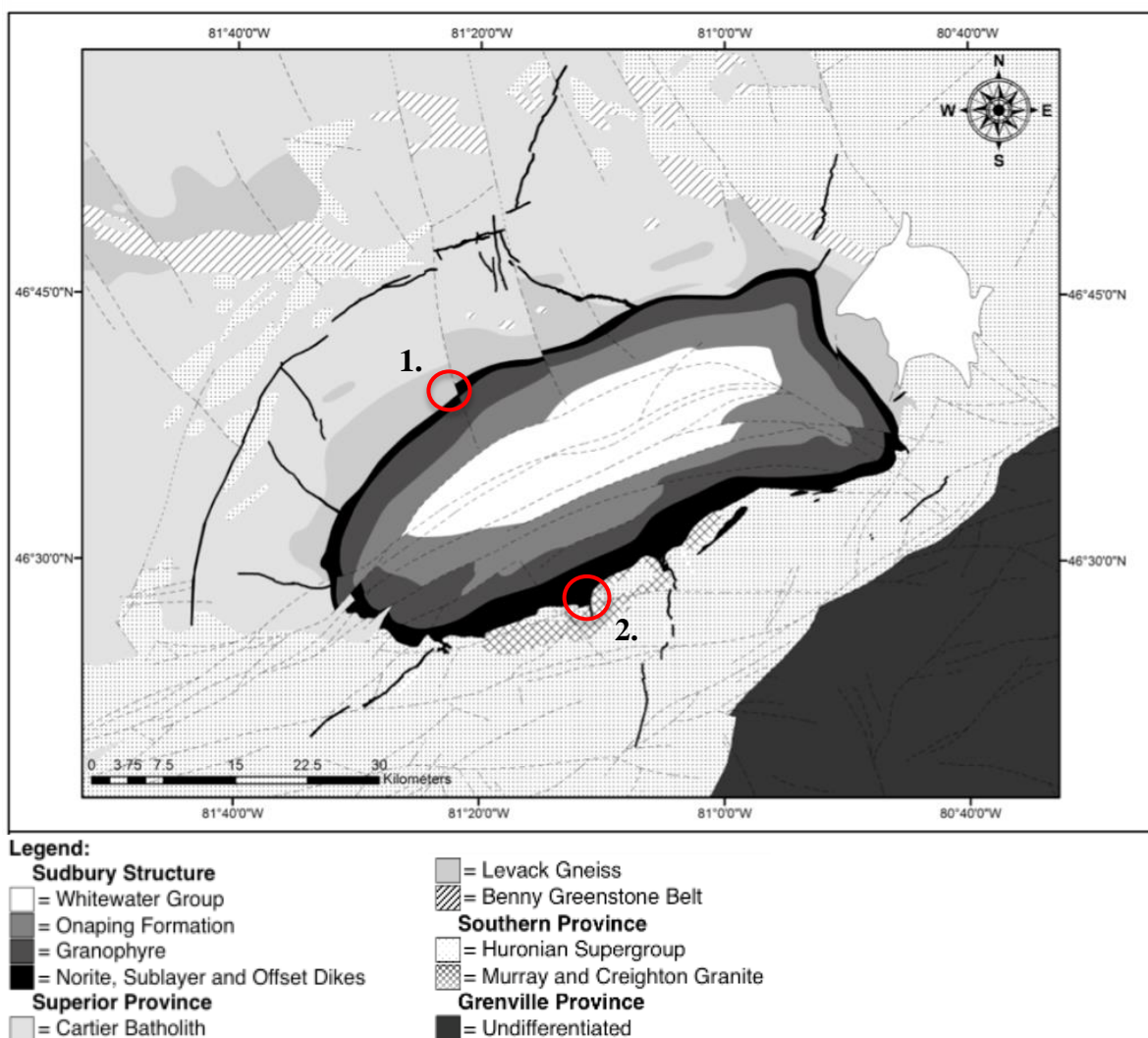


Figure 3.1: Geological map of the Sudbury Basin, showing the location of the Sudbury Igneous Complex, Superior Province and Huronian footwall units and post impact Whitewater Group. Sample locations are: 1. Coleman Mine; 2. Creighton Mine (modified after Coulter 2016).

to have been derived from partial melting of the 2711 ± 7 Ma Levack Gneiss Complex (Krogh et al. 1984; Meldrum et al., 1997; Rousell and Brown, 2009). The South Range comprises early Paleoproterozoic metasedimentary and metavolcanic rocks of the Huronian Supergroup (2491 to 2219 ± 5 Ma) that were subsequently intruded by the 2376 ± 2.3 Ma Creighton and 2477 ± 9 Ma Murray granites (Dressler, 1984; Krogh et al. 1996; Smith et al. 1999; Ames et al., 2008). The 2217 ± 4 Ma Nipissing gabbro is present in both the North and South Range (Noble and Lightfoot 1992; Ames et al. 2008).

3.2.2 Metamorphic History

The Sudbury region experienced several pre-impact metamorphic events, including the formation of the Levack Gneiss Complex (2661 ± 2 Ma) and the 2415-2343 Ma Blezardian Orogeny (Meldrum et al., 1997; Ames et al., 2008 and references therein; Rousell and Brown, 2009; Raharimahefa et al., 2014). The rocks that crystallized from the impact melt sheet, plus the Sudbury breccia and younger Whitewater Group and 1265 Ma Sudbury diabase dikes are the only rock units that provide reliable indications of the metamorphic conditions that post-date the 1850 Ma impact event. Much of the deformation and metamorphism in the South Range, including the South Range shear zone, has been attributed to the 1900-1770 Ma Penokean Orogeny. This peaked at lower amphibolite facies in rocks now located near the contact between the SIC and Southern Province, and progressed to greenschist facies in the North Range (Fleet et al., 1987; Bennet et al., 1991; Rousell et al., 1997; Bailey et al., 2004; Rousell and Brown, 2009). This was followed by the Yavapai-Mazatzal Orogeny between 1770-1600 Ma, which may have reactivated some of the shear zones in the South Range, evidenced by the presence of shear zone-hosted titanites in the Thayer-Lindsley Mine with U-Pb ages of 1658 ± 68 Ma (Bailey et al., 2004; Ames et al., 2008). The peak metamorphic conditions in the South Range during the Yavapai-Mazatzal Orogeny indicate upper greenschist to lower amphibolite facies, based on syn-foliation growth of staurolite porphyroblasts observed at some localities in the Creighton to Long Lake area (Rousell and Brown, 2009 and references therein; Raharimahefa et al., 2014). Around 1450 ± 51 Ma the South Ranges experienced another period of greenschist to amphibolite facies alteration, associated with the Chieflakian Orogeny. The deformation of the Sudbury Structure has been attributed to this orogenic event, which included the reactivation (or even formation) of the South Range shear zone and associated uplift of the South Range by approximately 5 – 10 kms (Fueten and Redmond, 1997). This tectonic event has also been attributed to the earlier Penokean orogeny (Rousell et al., 1997). The Chieflakian orogeny was followed by the

emplacement of the Sudbury diabase dike swarm around 1238 ± 5 Ma, associated with lithospheric melting and magmatism during the closing of the Elzevir basin (Shellnutt and MacRae, 2011). Finally, a series of orogenic events occurred between 1250 and 980 Ma, which can be subdivided into the ~1250-1190 Elzevirian, Shawingian ~1140-1080, Ottawa ~1080-1020 and the 1010-980 Rigolet orogeny (Rousell et al., 1997). The Grenville Orogenies resulted in the over-thrusting of the Mesoproterozoic Grenville Province on the Southern Province south of the SIC. Although these orogenic events are considered to have had only a minor influence in the Sudbury basin, such as the intrusion and subsequent brittle deformation of some Sudbury diabase dikes (Rousell et al., 1997; Rousell and Brown, 2009; Raharimahefa et al., 2014), Ar_{40}/Ar_{39} dating of feldspars in Sudbury breccia from the North Range indicate a low-grade thermal metamorphic event of ~10 My in duration occurred during the Grenville orogeny, which influenced the region as far north as the Benny Greenstone Belt (Thompson et al., 1998).

The footwall lithologies, including Sudbury breccia, adjacent to the SIC also experienced varying degrees of contact metamorphism. Studies by Dressler (1984), Coats and Snajdr (1984), Prevec and Cawthorn (2002) and Pentek (2009) mapped a contact metamorphic aureole extending approximately 2,000 m into the footwall of the SIC in the North Range, with textures indicating temperatures reaching up to 1,000 °C. The contact aureole is divided into albite-epidote hornfels (2,000-1,200 m from SIC-footwall contact), hornblende hornfels (1,100-350 m) and pyroxene hornfels (>350 m), with partial melt segregations observed up to 500 m into the footwall. Morrison (1994) initially proposed that recrystallization textures and coarsening grain size in the Sudbury breccia matrix could serve as a potential vector towards areas of high heat flow and footwall mineralization for both the North and South Range. However, more recent studies have confirmed that the recrystallization textures are common to Sudbury breccia in the North Range and not necessarily indicative of mineralized zones (Hanley and Mungall, 2003). The Sudbury breccia does display localized, subtle recrystallization adjacent to footwall mineral zones; evidence for this includes the crystallization of secondary minerals, such as poikiloblastic biotite and the development of a granoblastic, sub-igneous texture (MacBurnie 2016 per. comms.). The majority of Cu-Ni-PGE footwall deposits are situated within <700 m of the SIC contact (Golightly 2009), and so they reside within the thermal aureole of the SIC.

3.2.3 Sudbury Breccia

The Sudbury breccia is a pseudotachylitic impact breccia found up to 80 km away from the SIC. It forms irregular veins and zones ranging from millimeters up to tens of meters wide, consisting of dark grey, fine grained, aphanitic matrix hosting locally derived, rounded to sub-rounded lithic fragments and mineral fragments of footwall material (Parmenter et al., 2002; Rousell et al., 2003). The processes that formed Sudbury breccia remain uncertain, with competing theories invoking; in-situ, high temperature, frictional melting (Thompson and Spray, 1996; Fedorowich et al., 1999), lower temperature cataclasis during excavation and modification of the transient crater (Lafrance and Kamber, 2010), or injection or drainage of super-heated impact melt into the brecciated footwall (Lieger et al., 2009; Riller et al., 2010). Recent studies confirm an in situ melt origin for Sudbury breccia without any involvement of melt contributions from the SIC (Weirich et al., 2015; O'Callaghan et al. in press)

3.2.4 Sulfide and Hydrothermal Mineral Paragenesis

The Sudbury breccia and associated country rocks provided an important structural control on the emplacement of intermediate solid solution (ISS)-rich sulfide melts that were derived by fractional crystallization of monosulfide solid solution (MSS) contact mineralization at the base of the nearby melt sheet (Keays and Crockett, 1970; Naldrett et al., 1994, 1999; Farrow et al., 2005; Ames and Farrow, 2007). This resulted in the development of veins and disseminations of chalcopyrite ± cubanite ± pentlandite ± pyrrhotite and bornite ± millerite, which are termed type 1 and type 2 veins respectively herein. Type 2 veins are primarily developed at the terminations of type 1 veins and are found as thinner (< 1m) veinlets that appear to have experienced greater interaction with fluids in the footwall (Farrow et al., 2005; Stout et al., 2010; Nelles, 2012). A third type of footwall mineralization, termed 'low-sulfide, high-precious-metal'-style (LSHPM) is also hosted within the Sudbury breccia as irregular stringers, disseminations and stockwork veins of chalcopyrite, millerite and precious-metals-bearing-minerals (e.g., moncheite [Pt.Pd][Te,Bi]₂) (Farrow et al., 2005; Stewart and Lightfoot 2010). There is no general consensus on the formation of LSHPM-style mineralization, with concepts proposing; (1) hydrothermal modification of sharp-walled, Cu-rich veins (Hanley et al., 2011; White 2010; Nelles 2012), (2) expulsion of early, metal bearing fluids from cooling contact-style deposits, prior to emplacement of sharp-walled vein systems (Farrow and Watkinson 1997; Molnar et al., 2001; Farrow et al., 2005;

Pentek et al., 2008; Tuba et al., 2014) or (3) the transportation of late, fractionated, Cu-PGE enriched magmatic fluids into the footwall (Keays and Lightfoot 2004). In the South Range there is also evidence of a structurally-remobilized LSHPM-style of mineralization hosted within shear zones (e.g., the Denison 109 FW zone) (Gibson et al., 2011).

Previous studies on mineralogy, geochemistry and stable isotopes (Sr, Cl, O, H) in Sudbury breccia, the melt sheet and overlying Onaping intrusion roof rocks, and Whitewater Group have identified the presence of several distinct hydrothermal events that may have interacted with sulfide mineralization (Li and Naldrett 1993; McCormick and MacDonald 1999; McCormick et al., 2002; Hanley and Mungall 2003; Hanley and Bray 2004; Campos-Alvarez et al., 2010; Hanley et al., 2011; Tuba et al., 2014). The earliest event (~1850 Ma) was the mixing of magmatic fluids derived from SIC with regional ground waters and metamorphic fluids in the footwall to produce a 440 – 540°C, saline (50 wt.% NaCl equiv.), $\text{H}_2\text{O} + \text{NaCl} \pm \text{CO}_2 \pm \text{KCl}$ fluid. This was concurrent with the exsolution of a $\text{CH}_4 \pm \text{C}_2\text{H}_6 \pm \text{C}_2\text{H}_2 \pm \text{C}_3\text{H}_8$, hydrocarbon-rich, saline brine from the cooling sulfide veins (Hanley et al., 2005). Both of these fluids interacted with the sulfide mineralization, remobilizing and reprecipitating some precious metals into dissemination and veinlets within Sudbury breccia and has been attributed to forming the metalliferous and halogen-rich mineral assemblages, including stilpnomelane, chlorite, epidote and pyrosmalite (Farrow and Watkinson, 1992a; Molnar et al., 1997; Marshall et al., 1999; McCormick and McDonald, 1999; Molnar et al., 2001; Hanley et al., 2005; Pentek et al., 2008; Hanley and Bray, 2009). This was followed by a regional, 300 – 350°C, $\text{NaCl} + \text{CO}_2 + \text{CH}_4 + \text{H}_2\text{O}$ fluid with variable salinity (6 – 26 wt.% NaCl equiv.), linked with the waning stages of the 1.7 – 1.8 Ga Penokean orogeny, though there is no evidence of mineralization associated with this fluid (Molnar et al., 1997; Marshall et al., 1999; Molnar et al., 2001). Late, Ca-rich, 150 – 250°C, shield brines also interacted with the sulfide mineralization, resulting in metal remobilization and the formation of epidote-chlorite assemblages, for which the 1.24 Ga Sudbury diabase swarm has been proposed as a heat source (Molnar et al., 2001; Dare et al., 2010; Tuba et al., 2014). The youngest fluid was saline (> 16 wt.% NaCl equiv.) and was associated with galena-sphalerite-calcite-quartz veins locally observed in neotectonic fractures within footwall ore zones, that have Rb-Sr age dates of 5 – 13 Ma but these do not appear to have affected pre-existing footwall mineralization (Marshall et al., 1999).

3.3 Local Geology

3.3.1 Coleman Mine

Coleman Mine is situated in the Coleman-Levack Embayment, which forms the richest known system of mineralization in the North Range (fig. 3.2A). Both Ni-Cu contact sulfide and Cu-Ni-PGE footwall sulfide mineralization are mined at Coleman mine, with a transition zone of fractionated sulfide melt linking some of the footwall deposits directly to the embayment hosted contact deposits (Lightfoot, 2015, 2016). Footwall rocks consist of tonalite-granodiorite orthogneiss and horizons of diorite gneiss of the Levack Gneiss Complex, with later cross cutting (2446 ± 3 Ma) Matachewan and Sudbury (1238 ± 4 Ma) diabase dikes (Heaman 1989; Krogh et al., 1987; Card, 2009; Ames et al. 2008). Two major north-south structures, termed the Fecunis and Bob's Lake faults delineate the east and west boundaries of the Levack embayment. Both extend into the footwall and are believed to pre-date the SIC, with subsequent reactivation following the impact event (Rousell et al. 2009; White 2012). This study focuses in particular on the McCreedy 153 East ore body, which represents a typical footwall Cu-Ni-PGE sulfide footwall deposit, comprising type 1 (chalcopyrite + pyrrhotite) and type 2 (bornite + millerite) veins, with disseminations and stockwork veins of Pd-Pt-Au, hosted within extensive zones of Sudbury breccia beneath the embayment (Ames and Farrow, 2007; Stout et al., 2010; Dare et al., 2014b; Lightfoot 2016). Both type 1 and 2 veins are commonly observed with a thin (<0.5 m) green-black, chlorite + epidote + pyrosmalite alteration selvage (see below). The McCreedy East 153 ore body is connected to the Levack #4 contact mineral zone via the 9 Scoop mineral zone that comprises transitional styles of mineralization that are Cu- and PGE-rich. The underlying footwall contains a number of discrete narrow veins of chalcopyrite + millerite + pentlandite that occupy the space between the base of 9 Scoop and the north boundary of the 153 deposit.

3.3.2 Creighton Mine

The Creighton ore body is one of the largest and longest-producing mines in the Sudbury basin (Farrow and Lightfoot, 2002; Lightfoot 2016). The footwall rocks comprise granite and granodiorite of the Creighton pluton, Huronian Elsie Mountain Formation metabasalts and altered, pre-impact quartz diabase dikes (fig. 3.2B) (Fahrig and West, 1986; Dressler 1984; Ames et al. 2008). Enclaves and pendants of Huronian-aged country rocks and possible

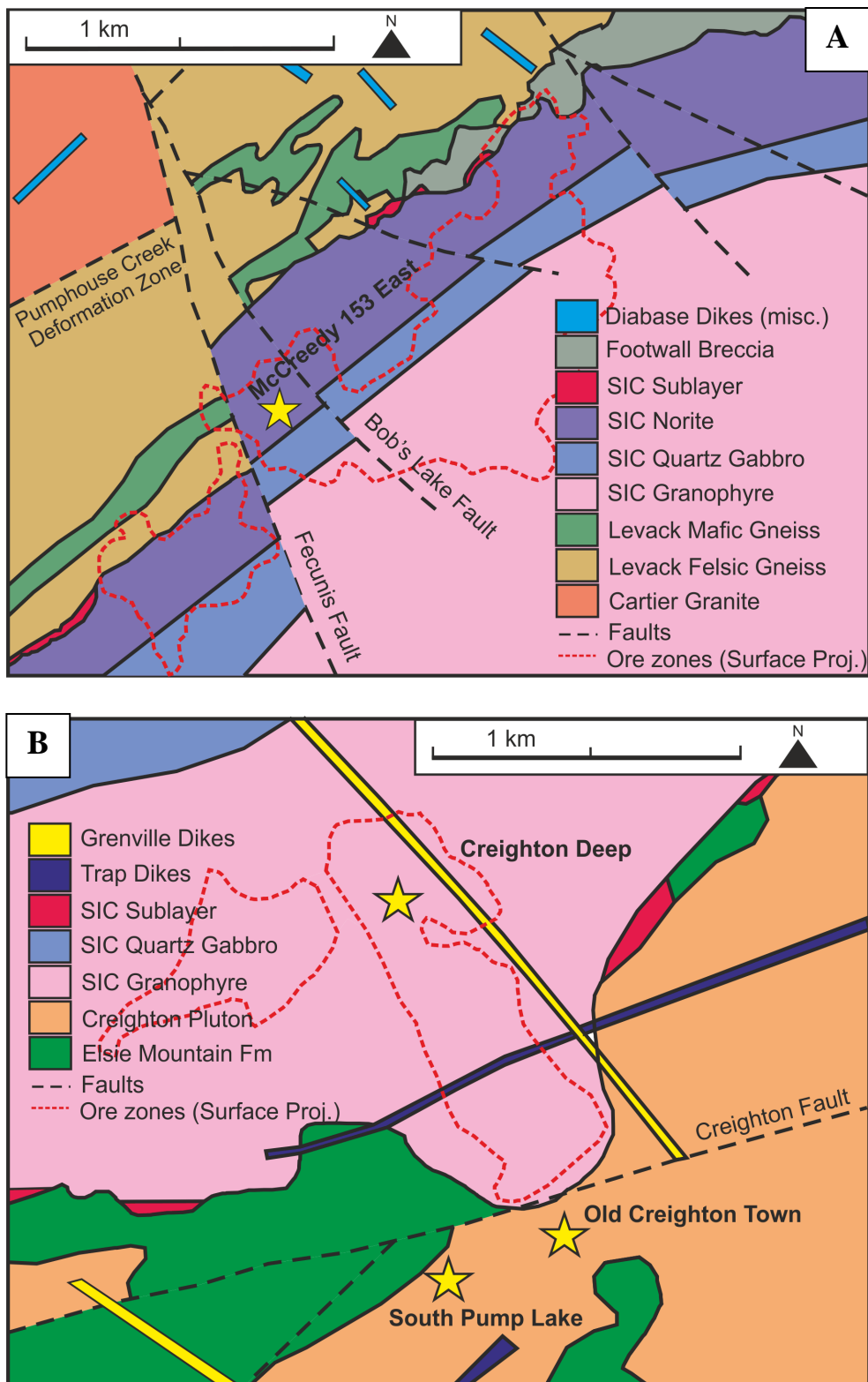


Figure 3.2: Surface geology for (A) Coleman Mine and (B) Creighton Mine, including the outline of the ore zones, projected to surface. Sample localities denoted by stars, with Creighton Deep and the McCreeedy 153 East sites also approximately projected to surface (modified from Ames et al., 2008)

basement-derived gneissic material can also be found enclosed within the granite (Riller 2009; O'Callaghan et al., 2016 in press). The Creighton deposit consists of contact type Ni-Cu sulfide mineralization, occupying a branched main embayment ~0.5 km wide and extending to depths exceeding 3 km (Rousell and Brown, 2009; Dare et al., 2010). The near-surface part of the deposit contains important examples of footwall mineralization, these comprise disseminated and vein types of mineralization as well as large ore deposits like the 126 ore body (Lightfoot et al., 1997). There are also several ore bodies that have been modified and/or remobilized by post-impact shear zones that cut through the South Range, like those developed at Garson Mine (Farrow and Lightfoot, 2002; Dare et al., 2010; Snelling et al., 2013; Mukwakwami et al., 2014). However, there is no evidence of a late hydrothermal halo or mineral vector within the melt sheet norite and gabbro overlying the Creighton deposit (Lightfoot 2007). This study focuses in particular on the 'Creighton Deep' mineral zones, which are situated at 2012 m (6600 feet) to 2420 m (7940 feet) depth. At Creighton Deep, the mineralization style shifts from a contact hosted ore body (400 OB) to a mineral zones hosted entirely within Sudbury breccia situated in the footwall beneath the SIC (e.g. the 403, 320, 420, and other zones documented in Lightfoot, 2015).

3.4 Sample Selection

A total of 112, ~1 kg samples were collected from three localities in the Sudbury basin, covering both host rocks and Sudbury breccia at the Coleman and Creighton Mines. Sampling was conducted in such a way as to include Sudbury breccia specimens representative of the alteration selvages developed adjacent to the sulfide veins. Additional material was collected at spaced intervals away from the mineral zones to allow for mineralogical comparison of distal versus proximal samples of Sudbury breccia.

A total of 29 drill core and hand specimen samples of Sudbury breccia and 19 samples of footwall gneiss were collected from the McCreedy 153 footwall deposit in Coleman Mine, stepping out from <0.5 m to ~425 m from mineralized zones (Fig.3.2). Drill core sampling at Creighton Deep totaled 28 ~1kg footwall rock samples and 23 ~1kg samples of Sudbury breccia with varying amounts of matrix to lithic fragments. Samples Ranged from <0.5 m to 319 m from mineralization. Hand specimen samples were also collected at Old Creighton Town, approximately 415 m into the footwall south of the Creighton embayment. Eleven ~1kg samples of Sudbury breccia were collected, as well as 2 samples of adjacent Creighton granite.

3.5 Methodology

Reflected and transmitted light microscopy was undertaken using Nikon Eclipse LV100 POL microscopes, equipped with 5 Mpx and 12Mpx cameras, connected to NIS-Element photographic software package. Major element analyses for biotite, amphibole, chlorite, titanite and oxide mineral chemistries were obtained using the University of Western Ontario's JEOL JXA-an 8530F field emission electron microprobe, in the Earth and Planetary Materials Analysis (EPMA) Laboratory, which is capable of wavelength (WD-EM) and energy dispersive (ED-EM) x-ray spectroscopy, producing geochemical data and element maps for individual minerals and specific regions of the thin section. WD-EM results were ZAF corrected, with specific overlap correction applied to some elements such as V-Ti (ratio of counts at V peak vs. counts on Ti peak, measured directly on pure Ti standard) to take into account the peak overlap between Ti $K\alpha$ and V $K\alpha$. Similar corrections were also applied for V-Cr, and Cr-Mn. Previously, the process for analysing fluorine has been hampered by the overlap between the $FK\alpha$ and $FeL\alpha$ peaks (Potts and Tindle, 1989; Witter and Kuehner,

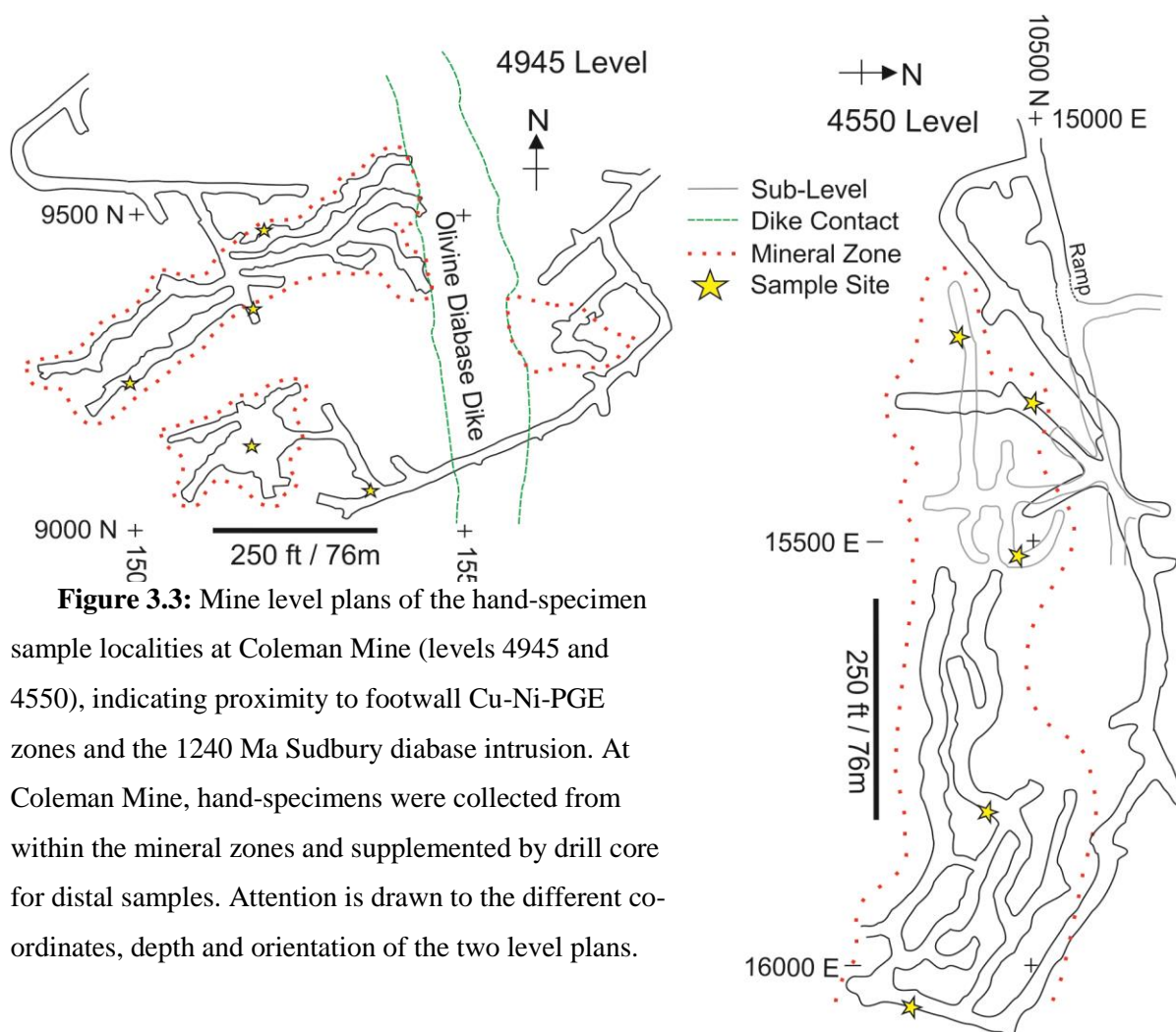


Figure 3.3: Mine level plans of the hand-specimen sample localities at Coleman Mine (levels 4945 and 4550), indicating proximity to footwall Cu-Ni-PGE zones and the 1240 Ma Sudbury diabase intrusion. At Coleman Mine, hand-specimens were collected from within the mineral zones and supplemented by drill core for distal samples. Attention is drawn to the different coordinates, depth and orientation of the two level plans.

2004). However, advances in the resolution of electron microprobes means that the F / Fe peak overlap has been negated, which was confirmed in this study by analysis of F / Fe bearing standards using the LDE1 crystal at 1.5kv. In addition, F was the first element analysed with WDS for each mineral, thus minimising the effects of F migration away from the target region due to beam heating. Three separate recipes were used during the microprobe analysis (amphibole-biotite; titanite; oxides; chlorite). Specific details on the spectrometers, L-values, counts and standards can be found in table 3-1.

Trace metal analysis and U-Pb age dating was conducted at the Geoscience Laboratories, Ontario Geological Survey, Sudbury, using laser ablation-inductively coupled plasma-mass spectrometry (LA-ICP-MS) (see table 3.1). In order to average out zonation or discrete inclusions in the target minerals and to avoid total ablation through the 30µm polished thin section, transect analyses of the minerals was conducted. Calibration of the analyte was performed on standard basalt glass (GSE-1G). Quality control standards NIST-610, NIST-612 and ATH0 were used to evaluate the accuracy of the results. The average Al₂O₃ wt%, determined by WD-EM in biotite, titanite and chlorite from the two sample localities respectively, was used as an internal standard. ³⁹K and ⁴⁶Ti were monitored to identify whether partially-chloritized biotite (a decrease in ³⁹K counts), or ilmenite inclusions in titanite (an increase in ⁴⁶Ti) were encountered during the transect analysis. Data reduction was performed using Igor Pro Iolite™ software, which allows selection of portions of each mineral analysis signal that have consistent count rates, reducing the risk of contamination by inclusions or fractures. U-Pb isotope geochronology was conducted by LA-ICP-MS time resolved analysis of ²³⁸U, ²⁰⁴Pb, ²⁰⁶Pb, ²⁰⁷Pb, ²⁰⁸Pb, ⁴³Ca, ⁵¹V, ⁶⁵Cu, ⁹⁰Zr, ²⁰²Hg and ²³²Th isotopes in titanite grains from the two sample localities, mounted on polished, 30µm thin sections. Each spot analysis consisted of a 60s of data acquisition with a 48µm spot size, 5 Hz repetition rate and scan velocity of 4000µm/s. Every ten titanite measurements were followed by analyses of NIST SRM 610, standard zircon FCT and standard titanites BLR-1 and OLT-1. U, Th and Pb concentrations were calibrated using ⁴³Ca as the internal calibration for titanites, with NIST SRM 610 as the reference material. FCT, OLT-1 and BLR-1 were used as external standards for U-Pb fractionation correction of the spot analyses. A total of 42 spot analyses of titanite were collected, before common lead corrections were applied. ²⁰⁷Pb/²⁰⁶Pb and ²⁰⁶Pb/²³⁸U ratios and ages were calculated using the Igor Pro Iolite™ software and Isoplot/Ex v. 4.15., with the relative standard deviations set at 2σ. Bulk rock samples were sent for whole rock geochemical analysis by lithium-metaborate fusion ICP-MS details of which details can be found in chapter 2 and in the appendices data.

Table 3-1: Electron Microprobe and LA-ICP-MS operating conditions with calculated detection limits.

WD- Electron Microprobe		LA-ICP-MS	Trace Element	(U-Pb)
Model	JEOL JXA-an 8530F	ICP-MS Model	Australian Scientific Instruments RESOLution M-50	
		LA Model	Thermo X-Series II	
Beam Conditions	15 kV, 20 - 100 nA	Wavelength	193 nm	
Spot Size	1-5 μm	Pulse Duration	20 ns	
	100s for V, Ni, 50s for Cu, 40s for Cl	Repetition Rate	8 Hz	5Hz
		Shield Torch Used?	Yes	
Count Time	15s for F 20s all other elements	Dwell Time	10 ms	
		Detector Mode	Dual, pulse counting to analogue transitions ~2 Mcps	
Corrections	ZAF	Beam Width	19-36 μm	36-48 μm
Crystals	LDE1, TAP, LIF, PETH, PETL, LIFH,	Energy Density	5 J/cm ²	6 J/cm ²
Analysis Type	Wavelength - Dispersive Spot Analysis	Forward Power	1450 watts	1480 watts
		Scanning Mode	Peak Hopping	
		Dwell Time per isotope	10s	30s
		Primary Calibration standard	NIST-SRM-610	OLT1
		Secondary QC control	NIST SRM-612, GOR132, KL2, ATH0, MLB3, FCT	
		Internal Standard	Al ₂ O ₃ (determined by WD-EM)	
		Gas Flow	He (650 ml/min), N ₂ (6 ml/min), Ar (800 ml/min)	
		Data reduction scheme	VAge_UComPbine	
Elements (Detection Limits in ppm calculated to 3 σ)	SiO ₂ (774), Al ₂ O ₃ (301), Na ₂ O (319), K ₂ O (106), MgO (365), FeO (567), MnO (653), NiO (630), CaO (143), Nb ₂ O ₅ (56), U (47), Th (47), Cl (76), F (3960), TiO ₂ (202)	Element, isotope and average detection limits in ppm (Pettke calculation)	Ti_47 (3.86), V_51 (1.20), Cr_52 (4.00), Ni_60 (2.94), Cu_65 (2.08), Zn_66 (1.87), As_75 (8.95), Rb_85 (3.95), Y_89 (0.31), Nb_93 (0.24), Pd_106 (2.39), Cd_111 (0.68), Ce_140 (0.04), Ta_181 (0.01), Tl_205 (0.04), Th_232 (0.11), U_238 (0.10)	

3.6 Mineralogy and Petrography

The Sudbury breccia matrix from the North and South Range typically has a similar macroscopic appearance, consisting primarily of a dark grey, microcrystalline, aphanitic matrix with entrained millimeter- to meter-sized clasts. Cataclastic varieties, with flow banded textures are also locally reported in the South Range and most distal outcrops of Sudbury breccia (Rousell et al., 2003), but they are not an important variant in the footwall and are not included in this study. Clasts are derived from the immediately adjacent footwall, and they can be subdivided into lithic fragments and smaller, individual mineral grains. Lithic fragments in the studied sample suite are consistently rounded to sub-rounded, an observation that is interpreted to be indicative of thermomechanical erosion in a high temperature melt, rather than lower temperature cataclasis, which should produce more angular clasts (Lin, 1999; O’Callaghan et al., in press). Mineral grains are sub-rounded to angular and, as with the larger lithic fragments, tend to be felsic in composition (i.e. predominantly quartz and feldspars). Mafic clasts and grains are notably absent, even where the breccia veins cut through diabases, or diorite gneisses. This is attributed to the preferential comminution of minerals commonly associated with mafic phases (e.g., pyroxenes and micas), which have lower fracture toughness and thermal conductivity (Spray, 2010). Closer to the SIC, the breccia matrix tends to exhibit recrystallization as a result of thermal metamorphism. This is primarily manifested as a coarsening in grain size to a sub-igneous texture (Fig. 3.3A, B, C, D) and, in some cases, alteration to a green-grey color. Aside from the increased presence of discrete disseminated sulfides, there is no definitive macroscopic features within the thermal aureole of the SIC to differentiate between breccia proximal and distal to mineralization.

3.6.1 Samples adjacent to the McCreedy East 153 Ore Deposit

Microscopically, the Sudbury breccia matrix distal to the SIC in the North Range is very fine-grained to vitric, with no discernible crystals and it commonly displays flow banding or compositional zonation at the vein margins (Fig. 3.3C). We use the term “vitric” here to describe particles that resemble or may have formed from a glass. However, no glass clasts were observed in the Sudbury breccia, as one would expect complete devitrification by subsequent hydrothermal and metamorphic activity, producing fine grained quartz, feldspars and hydrosilicates such as chlorite. Thin (<20 cm wide) chlorite selvages off-shooting from Sudbury breccia zones, which may represent devitrified melt, were observed both in this study and by Randall (2004). Contorted and partially melted quartz and feldspar within the matrix at the margins of Sudbury breccia zones indicate that temperatures

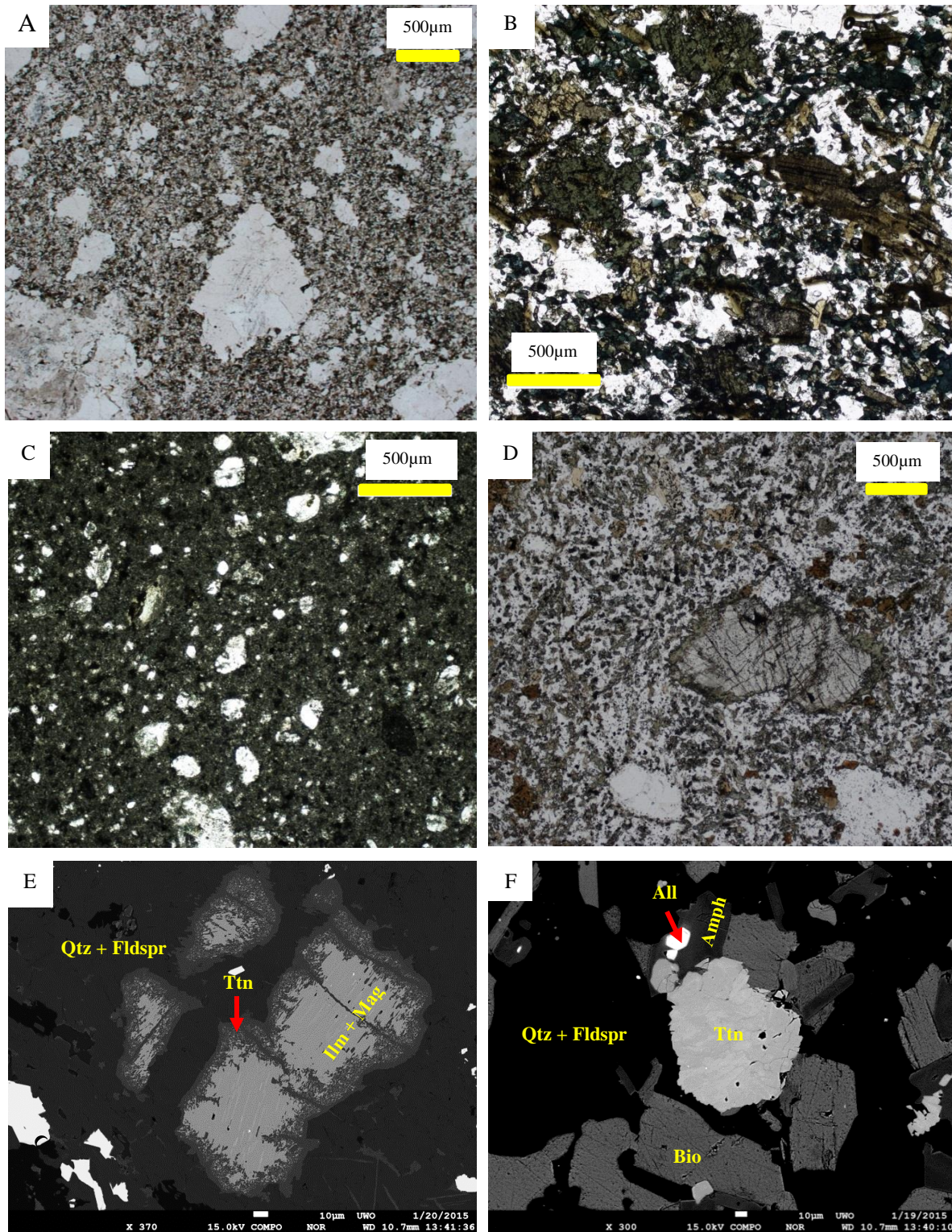


Figure 3.4: PPL thin section images of Sudbury breccia matrix from Creighton Deep and Coleman Mine, distal (A, C) and proximal (B, D) to mineralisation, displaying the progression from ‘cold’ to ‘hot’ breccia. Backscatter SEM images of two forms of titanites observed at each mine locality. At Coleman Mine, titanite is present as a reaction rim on ilmenite-magnetite grains (E) whereas at Creighton Mine the titanite is primarily an anhedronal, subtly zoned overprint on pre-existing biotite (F). Abbreviations: quartz - Qtz; feldspar - Fldspr; amphibole - Amph; titanite - Ttn; ilmenite - Ilm; magnetite - Mag; allanite - All; chalcopyrite - Cpy.

exceeding 1000°C (Spray, 2010; O'Callaghan et al. in press). With decreasing distance from the SIC, the matrix shows greater degrees of recrystallization and alteration, with the growth of biotite, epidote, and amphiboles in a groundmass primarily comprised quartz, orthoclase and plagioclase (Fig. 3.3D). The selvages of intensely altered, dark green-black Sudbury breccia are immediately adjacent (< 0.5 meters) to the sharp-walled sulfide veins.

Biotite is present primarily as platy, subhedral, light brown grains that exhibit increasing degrees of chloritization with proximity to mineralization (Fig. 3.4A, B). Within ~20 m of sulfide veins the primary biotite is almost entirely replaced by chlorite and a secondary, deep-red-brown, anhedral, poikiloblastic biotite is developed. The alteration selvage adjacent to sulfide veins also hosts a primary, radial chlorite variety that is spatially associated with the sulfide veins. The remainder of the altered matrix consists of quartz, sericitized feldspars, calcite, epidote, pyrosmalite $[(\text{Fe},\text{Mn})_8\text{Si}_6\text{O}_{15}(\text{OH},\text{Cl})_{10}]$ and rare pyroxene. Amphibole was primarily observed as very fine, colorless to green, acicular grains. Proximal to mineral zones, in addition to acicular varieties, amphibole is also observed as a continuum between partial replacement rims to complete overprinting of pre-existing pyroxenes by green, anhedral to subhedral clusters of actinolite-tremolite (Fig. 3.4C, 3.4F). Within the thin, more intense alteration selvage, amphibole appears to have been entirely replaced by epidote and a third chlorite species that forms ragged, anhedral clots that host titanite exsolution lamellae (Fig. 3.3B). Fe-oxides (ilmenite-magnetite) are generally very fine-grained clusters that increase in abundance towards mineral zones. Within <100 m of mineralized zones, ilmenite exhibits <5 μm magnetite exsolution lamellae and titanite alteration rims (Fig. 3.3E), an assemblage also noted by Gasparri and Naldrett (1972) and McCormick et al. (2002a). The almost complete absence of ilmenite in more distal samples has previously been attributed to complete replacement by titanite and/or magnetite. These observations are generally in agreement with previous studies (Farrow and Watkinson, 1992b; Morrison 1994; McCormick and McDonald, 1999; Hanley and Mungall, 2003; Hanley and Bray, 2009).

3.6.2 Samples Adjacent to the Creighton Deep Ore Deposit

Compared with the North Range, Sudbury breccia matrix at Creighton Deep is coarser grained, regardless of proximity to mineralization or the SIC (Fig. 3.3A, B). This may be a result of the different rheological conditions in the South Range or formation at greater depth, prior to post-impact uplift (Rousell et al. 2003). Sudbury breccia matrix in distal samples

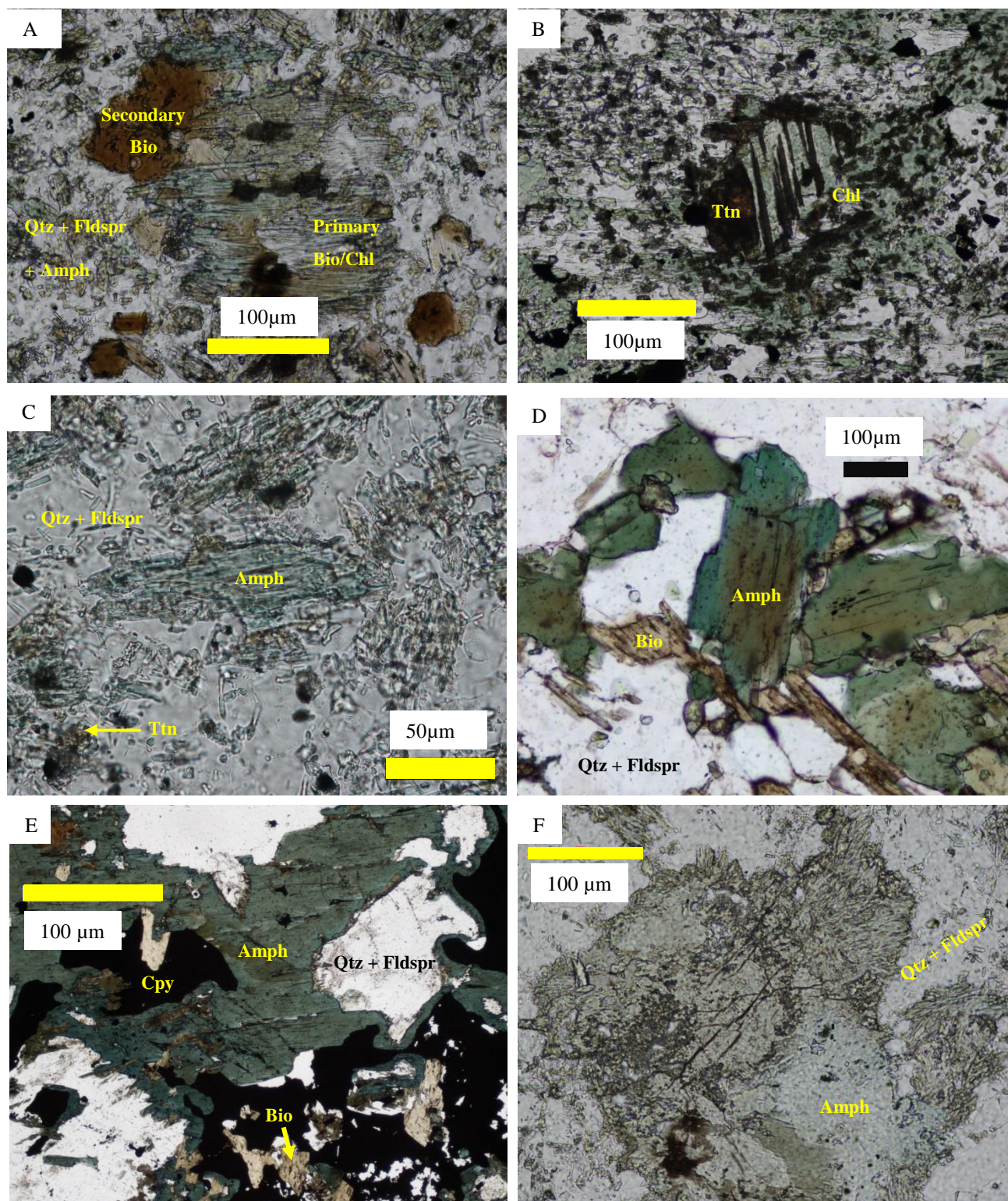


Figure 3.5: (A) PPL thin section image of chlorite pseudomorphs replacing biotite in breccia matrix distal to mineralization at Coleman mine. Secondary biotite is present as a deep-red-brown, variety that can be poikiloblastic. (B) PPL images of chlorite with titanite lamellae parallel to cleavage planes in alteration selvages adjacent to footwall sulfide veins at Coleman Mine. (C) PPL image of acicular, colourless actinolite distal to mineralized zones. (D) PPL image of zoned amphibole-hornblende proximal to mineralization at Creighton mine, and nickel-bearing, blue-green ferro-tschermakite enclosing remobilized sulfide grains (E). (F) PPL image from Coleman mine of the larger, anhedral amphibole clots observed in samples proximal to mineralization. See figure 3.3 for explanation of abbreviations.

(<200 m from mineral zones) is composed of quartz, plagioclase, K-feldspar, stilpnomelane, biotite, with rare epidote, allanite and very fine grained, acicular actinolite-tremolite. Biotite becomes more abundant and shifts from being light brown to dark brown to green in colour with proximity to the mineral zone at Creighton Deep, though its platy form and size remain relatively consistent. In contrast, stilpnomelane in the breccia matrix appears to be primarily associated with the presence of entrained Huronian gabbro or metabasalt clasts, in which this mineral is a common component. Amphibole is rare in Sudbury breccia distal to the Creighton Deep mineral zone, primarily being observed as very fine-grained, acicular grains (Fig. 3.4C). Within <200 meters of the mineralized zone a second, coarser-grained (>100 μm), prismatic and zoned amphibole, exhibiting a brown core and green rim is present (Fig. 3.4D). A third, pleochroic green-blue variety of amphibole is preserved as intergrowths with sulfide stringers within mineral zones (Fig. 3.4E). Titanite is common throughout the Creighton area and does not change in appearance or abundance with proximity to sulfide mineralization. Unlike at Coleman Mine, titanite is rarely found as a rim on euhedral magnetite grains, instead it is primarily present as late-stage, subtly zoned, anhedral clusters that overprint biotite and amphibole assemblages (Fig. 3.3F). Ilmenite is absent in the samples from the Creighton embayment and magnetite is only observed as very fine disseminated grains in samples <200 m from mineralization. No pyroxene or chlorite was observed in samples from Creighton Mine.

3.7 Results

Polished thin section observations demonstrate gradational variations with proximity to sulfide zones, in the content, form and potential origin of several mineral species in Sudbury breccia from the Creighton and Coleman Mines, some of which have been noted in previous research (e.g. McCormick et al., 2002a; McCormick et al., 2002; Hanley and Mungall, 2003; Hanley and Bray, 2009; White, 2012). This mineral chemistry study focused in particular on the key minerals observed in Sudbury breccia matrix, the micas, chlorite, amphiboles, titanite and oxides, and sought to compare and contrast the assemblages in the North and South Range with proximity to ore bearing Sudbury breccia. Major element wt. % oxide data obtained by electron microprobe was used to calculate stoichiometries and apfu (atoms per formula unit); trace element LA-ICP-MS data are referred to in the text as elemental ppm. Representative analyses of each mineral from the two mine localities are presented in tables 3-2 to 3-6.

Table 3-2: Representative Titanite and Biotite Analyses from Creighton Mine

Distance from ore zone (m)	Titanite					Biotite				
	0	100	160	320	400	0	100	160	320	400
n=	7	11	7	6	10	8	13	9	5	16
Bulk Comp. (wt%)										
SiO ₂	29.95	30.50	30.50	30.09	31.04	34.38	38.30	35.97	36.26	35.08
Al ₂ O ₃	2.23	1.30	2.12	2.89	3.53	15.48	14.25	15.39	16.04	16.29
FeO	0.59	0.52	0.71	0.69	0.93	27.16	21.26	21.74	21.01	25.50
MgO	0.00	0.01	0.01	0.00	0.07	4.55	8.86	9.12	9.13	6.58
MnO		0.04			0.05	0.41	0.37	0.31	0.33	0.32
CaO	28.05	28.62	28.11	28.01	28.71	0.04	3.60	0.05	0.02	0.08
TiO ₂	36.04	37.70	35.94	34.82	34.70	1.56	1.10	1.35	1.18	1.27
Na ₂ O	0.02	0.03	0.02	0.03	0.01	0.06	0.03	0.31	0.07	0.03
K ₂ O	0.02	0.03	0.02	0.02	0.07	9.42	6.23	9.62	9.79	9.68
Cl	0.00	0.00	0.00	0.00	0.00	0.23	0.18	0.19	0.25	0.28
F	0.75	0.09	0.41	0.82	0.93	0.34	0.29	0.47	0.72	0.75
O= F, Cl	-0.314	-0.001	-0.193	-0.348	-0.235	0.291	-0.126	-0.242	-0.359	-0.353
Total wt.%	97.33	98.76	97.66	97.03	99.80	93.92	94.34	94.53	94.45	95.49
apfu										
Si	0.99	1.01	1.01	1.00	1.01	2.76	2.80	2.80	2.79	2.75
Al	0.09	0.05	0.09	0.11	0.21	1.46	1.43	1.41	1.45	1.50
Fe	0.01	0.01	0.01	0.01	0.02	1.87	1.40	1.41	1.35	1.67
Mg	0.00	0.00	0.00	0.00	0.01	0.60	1.10	1.06	1.05	0.77
Mn	0.00	0.00	0.00	0.00	0.00	0.03	0.02	0.02	0.02	0.02
Ca	1.00	1.02	1.00	1.00	0.99	0.02	0.00	0.00	0.00	0.01
Ti	0.90	0.94	0.89	0.87	0.74	0.10	0.08	0.08	0.07	0.07
Na	0.00	0.00	0.99	0.00	0.00	0.01	0.01	0.02	0.01	0.00
K	0.00	0.00	0.00	0.00	0.00	0.91	0.97	0.96	0.96	0.97
Cl	0.00	0.00	0.00	0.00	0.00	0.03	0.02	0.03	0.03	0.03
F	0.08	0.00	0.05	0.09	0.14	0.07	0.07	0.12	0.17	0.12
Σ Cations	3.06	3.02	4.04	3.07	3.12	7.86	7.89	7.90	7.90	7.91
Trace Metal (ppm)										
Ni	6	6	1	6	7	268	296	147	168	270
Cu	15	9	9	4	34	15	2	2	1	16
Cr	43	384	120	97	200	45	285	91	174	226
V	169	354	267	360	319	131	116	189	156	164
Rb	6	6	4	19	9	811	706	724	1025	519
Y	3780	3105	1157	1471	1694	0	14	1	0	1
Ce	53	192	310	28	153	1	13	0	0	0
Nb	2635	3160	1160	1098	1747	18	9	10	8	5
Ta	178	168	70	86	143	0	0	0	0	0
Tl	0	0	0	0	0	9	5	5	7	4
U	1	21	20	14	13	0	1	0	0	0
Th	1	2	13	1	5	0	1	0	0	0

Table 3-3: Representative Titanite and Biotite Analyses from Coleman Mine

Distance from ore zone (m)	Titanite				Biotite			
	0 ¹	0 ²	20	427	0 ²	20	100	427
n=	7	9	11	4	9	5	5	4
Bulk Comp. (wt%)								
SiO ₂	30.73	31.47	30.46	30.00	37.19	37.41	37.43	35.69
Al ₂ O ₃	3.24	1.98	2.27	0.73	13.74	14.23	14.72	15.02
FeO	1.11	1.94	1.24	0.68	19.18	18.11	17.71	19.03
MgO	0.15	0.96	0.22	0.04	10.43	11.40	11.67	10.98
MnO	0.04				0.20	0.13	0.19	0.12
CaO	28.81	26.34	28.08	28.07	0.05	0.04	0.06	0.08
TiO ₂	34.69	33.53	34.88	38.33	3.09	1.57	1.55	1.22
Na ₂ O	0.02	0.10	0.06	0.04	0.06	0.10	0.07	0.19
K ₂ O	0.00	0.10	0.04	0.01	9.54	9.51	9.72	9.50
Cl	0.01	0.02	0.03	0.01	0.11	0.11	0.08	0.12
F	0.50	0.08	0.17	0.00	0.30	0.35	0.28	0.09
O= F, Cl	-0.212	-0.037	-0.080	-0.004	-0.150	-0.172	-0.138	-0.066
Total wt.%	99.09	96.48	97.38	97.90	93.75	92.79	93.35	91.97
apfu								
Si	1.07	1.02	1.02	1.00	2.87	2.90	2.88	2.82
Al	0.08	0.13	0.09	0.03	1.25	1.30	1.33	1.40
Fe	0.02	0.01	0.02	0.01	1.24	1.17	1.14	1.26
Mg	0.05	0.01	0.01	0.00	1.20	1.31	1.34	1.30
Mn	0.00	0.00	0.00	0.00	0.01	0.01	0.01	0.01
Ca	0.96	1.02	1.01	1.01	0.00	0.00	0.00	0.01
Ti	0.85	0.86	0.88	0.96	0.18	0.09	0.09	0.07
Na	0.01	0.00	0.00	0.00	0.01	0.01	0.01	0.03
K	0.00	0.43	0.00	0.00	0.94	0.94	0.95	0.96
Cl	0.00	0.00	0.00	0.00	0.01	0.01	0.00	0.02
F	0.01	0.00	0.02	0.00	0.07	0.09	0.07	0.02
∑ Cations	3.05	3.49	3.05	3.02	7.80	7.84	7.84	7.90
Trace Metal (ppm)								
Ni	1358	33	146		2770	216	467	45
Cu	12	40	995		85	10	9	3
Cr	198	554	8433		32	258	166	206
V	480	6535	3487		216	353	347	361
Rb		5	31		352	336	338	358
Y	155	14	27		0	2	1	4
Ce	3	4	49		1	6	1	16
Nb	458	2085	370		24	22	23	20
Ta	18	76	20		1	2	1	1
Tl	0	1	0		1	2	15	2
U	5	3	2		0	0	0	0
Th	1	2	5		0	0	0	0

Table 3-4: Representative Amphibole Analyses from Coleman and Creighton Mine

Distance from ore zone (m)	Amphibole (Coleman)				Amphibole (Creighton)		
	0 ²	20	100	427	0	100	160
n=	10	10	6	3	10	19	14
Bulk Comp. (wt%)							
SiO ₂	51.03	52.89	51.97	50.78	40.54	45.88	46.27
Al ₂ O ₃	3.67	2.47	3.06	3.98	10.79	8.11	7.34
FeO	15.16	11.40	14.01	13.79	26.36	19.27	19.40
MgO	13.24	15.95	13.74	14.12	3.71	9.00	9.07
MnO	0.39	0.29	0.36	0.22	0.66	0.48	0.46
CaO	11.51	11.91	12.31	10.96	10.75	11.82	11.74
TiO ₂	0.16	0.15	0.18	0.21	0.43	0.35	0.53
Na ₂ O	0.35	0.32	0.33	0.29	1.22	0.83	0.82
K ₂ O	0.22	0.21	0.15	1.15	1.40	0.88	0.87
Cl	0.04	0.04	0.05	0.04	0.17	0.09	0.15
F	-0.05	0.05	-0.09	0.00	0.15	0.07	0.11
O = F, Cl	0.011	-0.032	0.027	-0.010	-0.100	-0.047	-0.080
Total wt.%	95.73	95.65	96.09	95.53	96.07	96.74	96.67
apfu							
Si	7.03	7.66	7.65	7.72	6.41	6.96	7.44
Fe ²⁺	2.04	1.22	1.61	1.42	2.30	2.16	1.62
Fe ³⁺	0.40	0.30	0.10	0.16	1.05	0.29	0.25
Mg	2.11	3.30	2.95	3.23	1.09	2.03	2.83
Mn	0.06	0.04	0.05	0.03	0.08	0.06	0.05
Ca	1.88	1.87	1.94	1.92	1.65	1.92	1.90
Ti	0.04	0.02	0.02	0.01	0.06	0.04	0.03
Na	0.23	0.10	0.10	0.08	0.31	0.25	0.15
K	0.16	0.04	0.03	0.03	0.41	0.17	0.08
Cl	0.02	0.01	0.02	0.01	0.05	0.02	0.02
F	0.04	0.03	0.01	0.00	0.08	0.03	0.03
Al ^{IV}	0.35	0.13	0.19	0.15	0.40	0.42	0.22
Al ^{VI}	0.97	0.34	0.35	0.27	1.59	1.04	0.56
ΣCation	15.32	15.04	15.02	15.02	15.48	15.39	15.17
Trace Metal (ppm)							
Ni	249	10	201	115	50	74	55
Cu	7	1	0	0	3	1	72
Cr	978	68			12	170	98
V	693	165			53	94	169
Rb	3	1			67	2	8
Y	62	21			6	13	69
Ce	38	54			3	6	170
Nb	1	0			4	3	25
Ta	0	0			0	0	2
Tl	0	0			1	0	0
U	0	0			0	0	0
Th	2	1			0	0	1

Table 3-5: Representative Chlorite Analyses from Coleman Mine

Distance from ore zone (m)	Chlorite				
	0 ¹	0 ²	20	100	427
n=	10	8	1	4	3
Bulk Comp. (wt%)					
SiO ₂	25.50	28.66	29.00	25.82	26.99
Al ₂ O ₃	18.79	16.83	16.36	19.09	17.96
FeO	29.05	23.86	21.39	23.48	21.94
MgO	10.21	14.58	17.99	14.36	14.50
MnO	0.29	0.30	0.20	0.35	0.21
CaO	0.05	0.24	0.09	0.14	0.14
TiO ₂	0.04	0.24	0.03	0.11	0.23
Na ₂ O	0.06	0.10	0.12	0.19	0.27
K ₂ O	0.01	0.48	0.05	0.38	1.84
Cl	0.04	0.06	0.05	0.04	0.07
F	0.01	0.06	0.33	0.02	0.00
O= F, Cl	-0.012	-0.037	-0.149	-0.019	-0.016
Total wt.%	84.03	85.37	85.45	83.97	84.13
apfu					
Si	2.88	2.67	3.07	2.84	2.96
Fe ²⁺	3.86	2.24	1.90	2.16	2.01
Fe ³⁺	0.00	0.38	0.00	0.00	0.00
Mg	0.27	1.85	2.84	2.35	2.37
Mn	0.10	0.03	0.11	0.03	0.02
Ca	0.00	0.00	0.01	0.02	0.02
Ti	0.00	0.00	0.00	0.01	0.02
Na	0.02	0.00	0.03	0.04	0.06
K	0.19	0.00	0.01	0.05	0.26
Cl	0.07	0.00	0.01	0.01	0.01
F	0.01	0.00	0.11	0.01	0.00
Al ^{IV}	1.12	1.33	0.93	1.16	1.04
Al ^{VI}	1.45	1.18	1.12	1.31	1.27
∑Cation	9.99	9.70	10.13	9.98	10.03
Trace Metal (ppm)					
Ni	13436	7214	805	1731	255
Cu	100	1385	3709	11	10
Cr	184	18	871	1161	1362
V	246	37	1103	1518	867
Rb	14	63	22	64	56
Y	2	2	98	42	21
Ce	1	2	80	29	10
Nb	12	9	4	5	6
Ta	0	1	1	0	0
Tl	0	7	0	3	1
U	0	0	1	1	2
Th	0	0	10	13	13

Table 3-6: Average Ilmenite and Magnetite Analyses from Coleman Mine

Distance from mineralisation (m)	Ilmenite					Magnetite			
	0 ¹	0 ²	20	100	427	13	20	100	427
n=	6	5	5	5	5	3	3	4	4
Bulk Comp. (wt%)									
SiO ₂	0.94	0.05	0.11	0.33	0.06	0.08	0.15	0.28	0.14
Al ₂ O ₃	0.00	0.00	0.01	0.06	0.01	0.02	0.04	0.03	0.02
FeO	41.33	39.11	40.67	34.00	38.65	82.93	86.12	86.87	85.29
Fe ₂ O ₃	1.41	2.71	0.53	6.20	7.36	2.74	0.00	0.80	2.11
MgO	0.05	0.05	0.18	0.09	0.14	0.00	0.01	0.00	0.03
MnO	2.86	5.14	3.69	4.23	3.00	0.01	0.02	0.03	0.10
CaO	0.00	0.29	0.28	1.63	0.03	0.05	0.12	0.15	0.07
TiO ₂	50.17	52.30	51.81	50.39	47.71	0.07	0.08	0.08	1.72
Total wt. %	96.77	99.65	97.28	96.94	96.96	88.81	87.37	89.36	89.59
apfu									
Mn	0.05	0.06	0.08	0.09	0.07	0.01	0.00	0.00	0.01
Fe ²⁺	0.90	0.86	0.87	0.74	0.85	2.81004	2.92	2.90	2.86
Fe ³⁺	0.03	0.05	0.02	0.12	0.15	0.08	0.00	0.02	0.06
Ti	0.99	1.00	1.00	0.96	0.93	0.06	0.00	0.02	0.04
Cr	0.01	0.01	0.01	0.01	0.01	0.01	0.01	0.01	0.00
Al	0.01	0.01	0.01	0.04	0.00	0.02	0.02	0.01	0.02
V	0.01	0.00	0.00	0.00	0.01	0.02	0.02	0.03	0.02
Σ Cations	1.99	2.00	1.98	1.96	2.02	3.01	2.98	2.99	3.01
Trace Metals (ppm)*									
Ni	89	1065	79	17	36	97	68	233	168
Cu	91	38	60	25	98	237	188	13	100
Cr	117	299	535	341	272	2126	209	6100	3155
V	694	2112	1003	369	3078	2665	107	7938	7777

¹ Sample adjacent to pyrrhotite-pentlandite (type 1) vein

² Sample adjacent to bornite-millerite (type 2) vein

3.7.1 Major and trace element results for biotite

The stoichiometry of biotite was calculated assuming eleven equivalent oxygen atoms per formula unit and that all iron is present as ferrous iron (Fe^{2+}). Biotite was ubiquitous in the breccia matrix in both localities. It primarily appears in a light brown, sub-hedral, bladed form; with the Y axes of grains from Creighton aligned parallel to the breccia vein contacts. Generally, the Mg# [$(\text{Mg}^{2+} / (\text{Fe}^{2+} + \text{Mg}^{2+}))$ (wt. %)] of biotite shifts from the annite-phlogopite join towards the annitic end member near mineralization at both Creighton (from 0.32 to 0.07) and Coleman mine (from 0.45 to 0.07), the exception to this being the most distal samples from Creighton (>427 m), where the biotites also sit within the Fe-rich, annitic compositional field. At both localities the Al content is <1.6 apfu (<17 wt. %), ruling out a phlogopite-eastonite or annite-siderophyllite component (Al apfu >2.5). At both localities, the Ti content of the biotite increases proximal to mineralization, (from 0.04 to 0.10 apfu at Creighton and 0.07 to 0.21 apfu at Coleman), corresponding with the appearance of secondary, deep-red, poikiloblastic species at Coleman, and a darkening-brown coloration at Creighton. At Coleman, Cr, Ta, U and V are depleted in the metalliferous biotites compared with distal samples, whereas only Cr shows a strong depletion proximal to mineralization at Creighton mine. Nickel (II) and Cr^{3+} commonly substitute for Mg^{2+} in the M-site of biotite. Although there is no correlation between Ni and Cr vs. Mg/Fe in distal samples, in mineralized samples there is a magnitude increase in Ni^{2+} content (up to 0.59 wt% Ni at Coleman, and 0.21 wt% Ni at Creighton), matched by depletion in Cr^{3+} (Fig. 3.6C). This elevation in Ni content is only observed within ~5m of mineralization, beyond which it drops from >2,000 ppm to <300 ppm. Thallium is also enriched in the nickeliferous biotites at both mine sites, particularly Coleman (up to 340 ppm) and exhibits a similarly sharp decrease away from sulfide zones (>20 ppm within 10m). In distal samples, Tl^+ and Rb^+ have a positive relationship and a fairly consistent ratio (Tl/Rb >0.05 at Coleman, >0.01 at Creighton), replacing K^+ in the biotite lattice, whereas in mineralized zones at both mines there is a magnitude increase in Tl/Rb ratios (up to 1.06 at Coleman and 0.05 at Creighton) that mirrors increased Ni/Cr ratios (Fig. 3.6B).

3.7.2 Major and trace element results for chlorite

Chlorite was only observed in samples from Coleman mine, where its geochemistry largely reflects replacement of biotite (Fig. 3.6A). The stoichiometry and proportions of Fe^{2+} , Fe^{3+} and Al^{IV} , Al^{VI} in chlorite were calculated using WinCcac software developed by Yavuz

(et al., 2015), assuming fourteen equivalent oxygen atoms per formula unit. Magnesium and Iron have a substitution relationship in which Mg decreases from >2.00 to ≤ 0.31 *apfu* and Fe_{tot} increases from <2.12 to >3.56 *apfu* towards sulfide zones. The transition from clinchlore (Mg-rich) towards the chamosite (Fe-rich) end member mirrors the similar compositional shift of precursor biotite from phlogopite to annite. Uranium, Th, V and Zn decrease from distal samples towards mineralized zones (e.g., from $>1,000$ ppm to <500 ppm V), as does Si, which falls to <2.70 *apfu*, compared with up to 3.28 *apfu* in un-mineralized samples. Iron (III) is only present in samples adjacent to type 2 veins, where it is between 0.13 and 0.43 *apfu*. Al^{VI} and Al^{IV} results are generally scattered, though there is a discrete distinction in the latter between chlorites distal ore ($Al^{VI} < 1.2$ *apfu*) and proximal to ore zones ($Al^{VI} > 1.1$ *apfu*).

Within the thin alteration assemblage adjacent to type 1 and 2 mineralization at Coleman Mine, a two chlorite species were observed; one appears to be primary, with a radial growth pattern, and hosted within the sulfide veins, whereas the second is present as anhedral clots throughout the adjacent breccia matrix. Both of these chlorite species have elevated Ni values (up to 0.66 wt. % next to type 1 veins and 1.47 wt. % next to type 2 veins) and, unlike distal specimens, contain ferric iron (Fe^{3+}) (up to 0.25 *apfu*). Nickel is substituted into chlorite at the octahedral site (Fe^{2+} , Mg^{2+}) site, creating a distinct series from Fe-bearing chamosite to ‘nickeliferous’ chlorite (Fig. 3.5A). Although indistinguishable in appearance, the chlorites adjacent to type 1 veins are much more enriched in Cu (up to 3500 ppm)

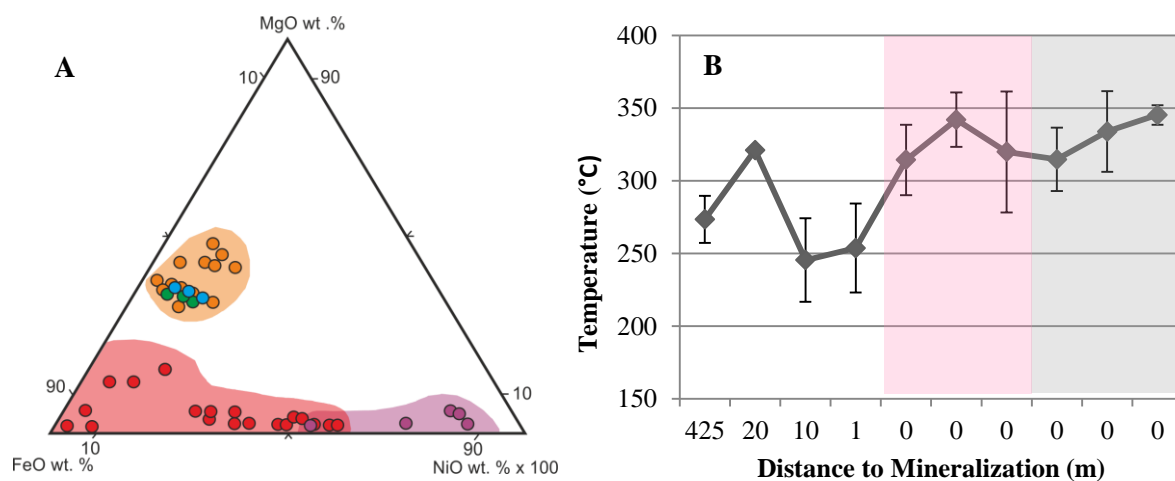


Figure 3.6: (A) Mg-Fe-Ni substitution series in chlorites from Coleman mine, displaying two distinct groups. Distal (orange, green) are chlorite pseudomorphs of biotite, whereas chlorites within mineralized zones (type 1 vein: red, type 2 vein: purple) (B) Octahedral vacancy chlorite geothermometer, demonstrating the difference in formation temperature in distal towards proximal chlorites. Chlorites adjacent to type 1 veins: red area, type 2 veins: blue area.

compared with chlorites at type 2 veins and in distal samples (1 – 200 ppm Cu) that likely represents the presence of discrete CuS inclusions. Chlorine and to a lesser extent fluorine are also elevated in chlorites adjacent to type 1 veins (up to 0.18 and 0.04 *apfu* respectively), whereas no enrichment in the halogens is observed in chlorites at type 2 veins.

3.7.3 Major and trace element results for amphibole

Based on the stoichiometry and nomenclature of Leake et al. (1997), amphibole formula was calculated on the basis of an idealized formula $[A_{0-1}B_2C_5T_8O_{22}(OH)_2]$, using the eCNK calculation developed by Schumacher (1991) to constrain the proportions of Fe^{2+} , Fe^{3+} and Al^{IV} , Al^{VI} . The calculation assumes 13 nominal cations, in which the cation T site is summed to 8.00 using Si, Al and Ti and the OH site filled with F, Cl and OH to sum 2.00.

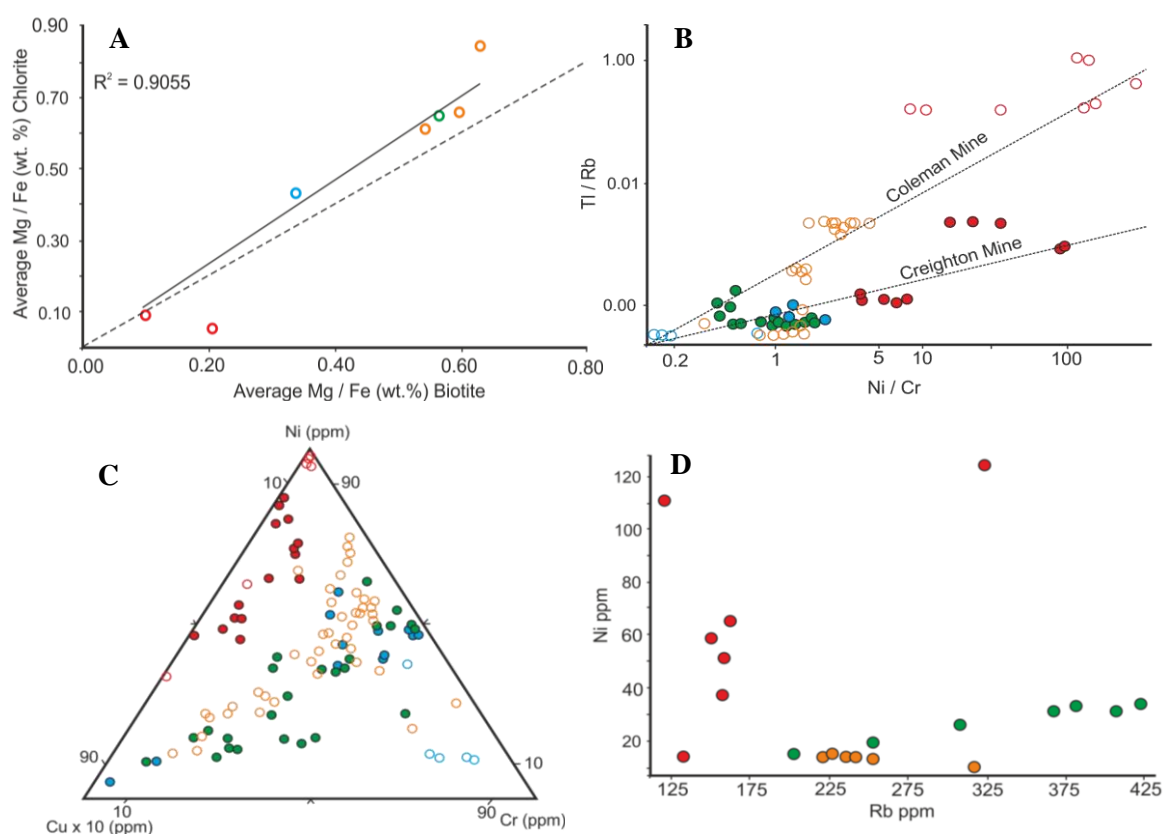


Figure 3.7: Biotite from Coleman (open circles) and Creighton (filled circles) with proximity to ore from distal to mineralized samples (blue-green-yellow-red). (A) Mg/Fe in chlorites and biotites, displaying the inherited geochemistry of replacement chlorites, compared with coexisting biotites. (B) Tl/Rb vs Ni/Cr shows a relative increase in Tl content in mineralized samples, though the signature is reduced at Creighton mine. (C) Ni-Cu-Cr ternary plot demonstrating increased Ni/Cr towards ore, whereas Cu results are more scattered. (D) Whole rock geochemical data from Creighton Mine, demonstrating the decreasing Rb values with proximity to mineralization that may reflect increasing Tl substitution into biotite over K, Rb and Ce.

All the amphiboles analyzed in this study contained ≥ 1.50 Ca *apfu*, which falls into the calcic classification scheme (Leake et al., 1997). The amphiboles from Coleman mine are primarily very fine-grained, bladed and euhedral, plotting within the actinolite field ($\text{Si } apfu > 7.50 + \text{Mg\#} > 0.5 < 0.9$). Their very fine grained form, particularly distal to mineralization, complicates laser ablation transects, resulting in only a few grains providing precise trace metal readings. Closer to mineralization, larger, anhedral clots of amphibole ($> 100 \mu\text{m}$) were also observed, in some cases exhibiting zonation in which the cores are compositionally closer to the tremolite endmember ($\text{Mg\#} > 0.9$), whereas the rims are actinolite. At Coleman, amphiboles < 5 m from mineralized zones exhibited depletions in Mg, Si and Ca, and slight enrichments in Fe^{3+} , Ni (up to 384 ppm), V, Cr and Al^{VI} ; however, results were more scattered and there are no obvious signatures to distinguish amphiboles in ore zones from proximal and distal samples. Instead, the enrichment noted above likely reflects amphibole inheriting elements from the pyroxene grain that it is observed replacing.

Zoned amphiboles are far more common in samples from Creighton Mine compared with samples from the 153 deposit at Coleman Mine, with brown actinolite cores and green ferro-hornblende rims ($\text{Si} < 7.50$ and > 6.50 *apfu*, $\text{Mg\#} < 0.5$) (Fig. 3.7A). In samples distal to mineralization, as at Coleman mine, the amphiboles tend to be very fine-grained, bladed with a sub- to euhedral form. Towards mineralized zones and the SIC, the grain size and abundance of the amphiboles increase, but in contrast to Coleman mine, they retain a bladed

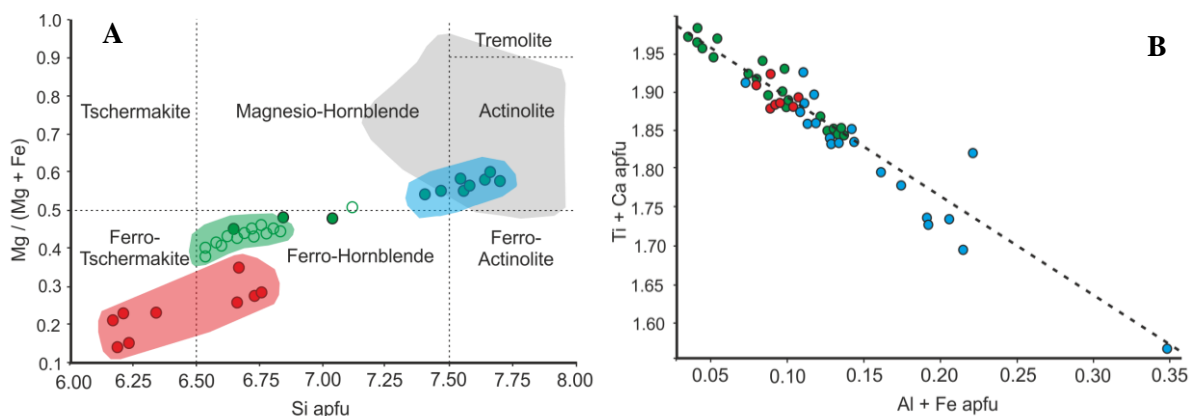


Figure 3.8: (A) Calcic amphibole classification scheme from Leake et al. (1997) demonstrating the difference between amphibole cores (blue) and rims (green), and the similarity between the latter and amphiboles in mineralized zones (red) at Creighton mine. The grey area represents amphibole from Coleman mine. (B) Titanite analyses from Creighton mine, exhibiting the increased Al+Fe content from distal samples, ~ 0.5 -1 km from the embayment (blue) to samples within the Creighton Deep zone (red).

form and anhedral clots are absent. Immediately adjacent to type 1 mineralization in Creighton Deep, the amphiboles wrap around sulfide grains and do not display any zonation, instead falling within either the ferro-hornblende or ferro-tschermakite ($\text{Si} < 6.50 \text{ apfu}$) composition fields ($\text{Al} + \text{Fe}^{3+} + 2\text{Ti} \geq 1.5 \text{ apfu}$) (Fig. 6a). These amphiboles also exhibit elevated Mn, Fe^{2+} , Fe^{3+} , Na, As, Y, Nb, Al^{VI} and Ni (up to 750 ppm Ni) and depleted Si, Mg, V, Cr and Ca relative to distal amphiboles (e.g. a decrease from 483 ppm Cr in distal amphiboles to >2 ppm).

3.7.4 Major and trace element results for ilmenite and magnetite

As titanite is spatially associated as alteration rims on ilmenite at Coleman mine, ilmenite grains were analyzed by WD-EM. Trace elements in ilmenite were not analyzed. Stoichiometry was calculated assuming $\sum \text{cations} = 2$ and that all iron was present as Fe^{2+} (Table 3-6). Ilmenite is present at both localities as fine-grained, disseminated, anhedral grains. Titanite alteration rims and magnetite lamellae were only observed on ilmenite grains from Coleman mine. Mg, V, Ca and Mn are substitute for Fe^{2+} , forming the series; ilmenite (Fe)-Geikilelite (Mg)-Pyrophanite (Mn). Ni^{2+} can also substitute for Fe and was recorded in ilmenite adjacent to type 2 veins (NiO up to 0.15wt. %). Ilmenites adjacent to type 1 veins are strongly enriched in Ni, Mn and Ti and are depleted in Fe, Ca, Mg compared with more distal samples. Comparison of the ilmenites beside each of the two vein types highlights a reversal in the Ni enrichment compared with the other minerals analysed in this study. As the oxides would be expected to have crystallised from the initial Sudbury breccia melt, rather than forming by later hydrothermal interaction (e.g. as is the case for the chlorites), the difference in the Ni content may reflect the initial conditions of the breccia matrix prior to alteration.

Magnetite at Coleman mine was observed as both very fine disseminated grains and as <5 μm exsolution lamellae within ilmenite grains, whereas as at Creighton mine the magnetite was less abundant and only observed as disseminations in samples distal to mineral zones. Stoichiometric values were calculated assuming three cations (AB_3O_4), with Fe^{2+} and Fe^{3+} calculated using the methodology of Droop (1987). Ni, Cr and V are elevated in grains distal to mineralization in contrast with Cu, which tends to show a reverse trend (e.g., towards mineralization Ni average decreases from 168 – 97ppm, Cu average increases from 100 – 237 ppm). Results for Ti and Fe exhibit a negative relationship, a reflection of the coupled substitution between the two elements (Nadoll et al., 2014). Comparison of the Ni/Cr ratio has been successfully applied in previous studies to differentiate magmatic versus hydrothermal magnetite (Dare et al., 2014a). In this study, all the magnetite analyses have a

Ni/Cr ratio <1 and Ti values <1 wt. %, indicative of formation from a felsic melt, rather than a hydrothermal origin. Although Ni/Cr ratios are considered diagnostic for comparing magmatic and hydrothermal magnetite, Ti would be expected to preferentially incorporate into ilmenite, thereby reducing the Ti content of coexisting magnetite and thus making it unsuitable for determining the composition of the initial melt (i.e., mafic versus felsic) (Nadoll, 2011).

3.7.5 Major and trace element results for titanite

Titanite data were recalculated to provide stoichiometric values, assuming five equivalent oxygen atoms per formula unit, and assuming all iron is present as Fe³⁺. The titanites from Coleman Mine are present as both an alteration rim surrounding grains of ilmenite and as lamellae within chlorites, whereas the South Range titanites are a combination of amalgamations of fine-grained, zoned and anhedral crystals, and less commonly, alteration rims on fine oxide grains. Titanites from Coleman mine were only found proximal to mineralization and tend to exhibit more scatter in their major element geochemistry compared with samples from Creighton mine, which display a gradual increase in Ti (from 0.73 to 0.91 *apfu*) relative to F (0.18 to 0.03 *apfu*) and Al (0.16 to 0.8 *apfu*) (Fig. 3.7B), towards footwall mineralization. Comparison of distal and proximal samples at Creighton mine also indicate a general increase in Nb (from an average of 1747 ppm to 2635 ppm) and Y (from an average of 1471 ppm to 3790 ppm) closer to mineralization, though there is significant scatter in samples peripheral to ore zones. In Coleman mine, the titanites have slightly higher average Mg and Fe contents (up to 0.27 and 0.09 *apfu* respectively) compared with Creighton, and F content is scattered. Si values were consistently around 1 *apfu* in both sample localities.

At Creighton, Ni values are below detection limit (< 3.5 ppm) for most titanites, and do not show any variation consistent with proximity to mineralization. Although Cu is reported between 3 to 47 ppm, it likewise shows no apparent relationship with distance to mineralization, whereas Cr decrease to below 100 ppm within 130m from mineralization. Titanites adjacent to type 2 veins at Coleman mine contain higher Ni abundances (up to 6300 ppm) and Cu values <80 ppm. In contrast, Cu values in titanite proximal to type 1 veins were up to 340 ppm, and Ni values were ≤33 ppm. Although all efforts were made to avoid ilmenite inclusions in the titanite, some of the trace metal values may have been affected by ablation of discrete oxide inclusions associated with the alteration.

3.7.6 *In-situ U-Pb dating of titanite*

Titanites in one sample of Sudbury breccia from each mine locality were analyzed for U-Pb isotope geochronology. The two sets of results were plotted on U-Pb Tera-Wasserburg Concordia diagrams with the sample age corresponding to the lower intercept value (Fig. 3.8A, B). Errors for the age intercept values were determined to a 95% confidence by the application of a Monte Carlo regression simulation using Isoplot 4.1 TM (Raychaudhuri 2008). Titanites from Coleman mine yielded an age Range of 1358 ± 78 Ma ($n=17$, MSWD= 1.7), with U values between 0.4 – 9.2 ppm and U/Th ratios between 0.9 – 3.67. Titanites from Creighton Deep provided an age Range of 1616 ± 33 Ma ($n= 25$, MSWD= 1.17), with 7.4 – 25.1 ppm U and U/Th ratios between 3.0 and 26.9.

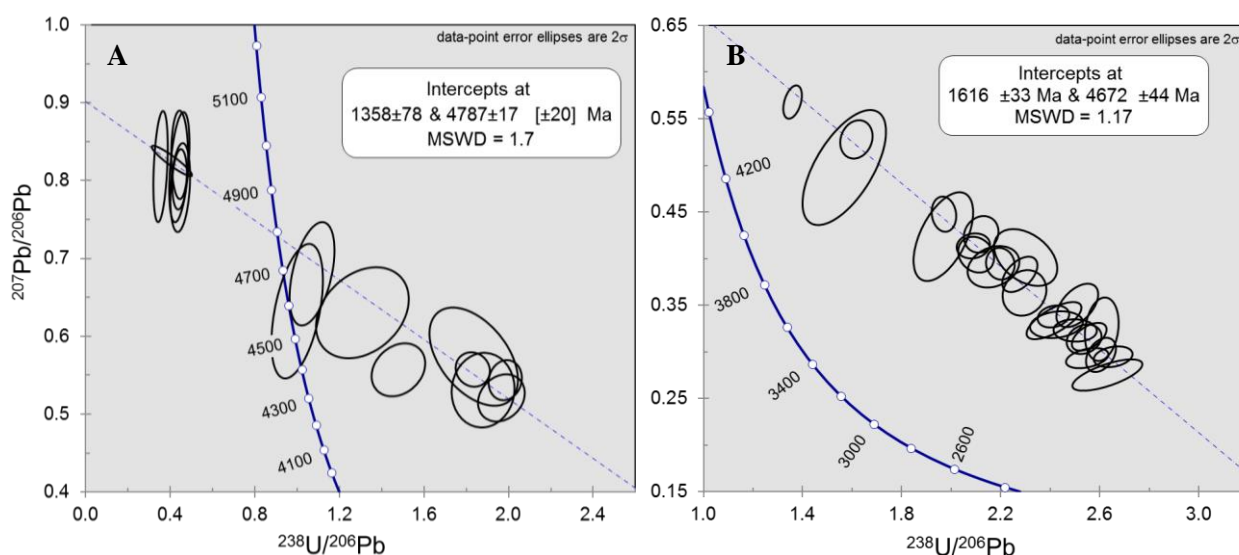


Figure 3.9: U-Pb Tera-Wasserburg Concordia diagrams for titanites from (A) Coleman mine ($n=17$) and (B) Creighton Deep ($n= 25$), with Monte Carlo adjusted age estimates and mean squared deviation values.

3.8 Discussion

3.8.1 *Mineralogy and Geochemical Variations at Creighton Mine*

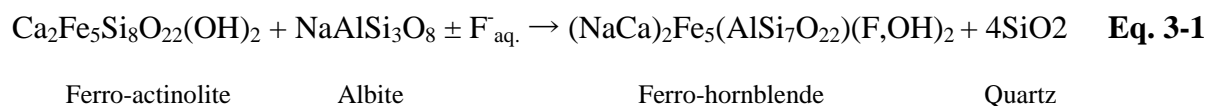
Several footwall-style deposits in the Creighton embayment and at other mines in the South Range appear to be closely associated with shear zones, into which the sulfides were remobilized (Dare et al., 2010; Gibson et al., 2011). These shear zones acted as important pathways for subsequent hydrothermal-metamorphic fluids that have interacted with the

sulfides to varying degrees (Bailey et al., 2006; Mukwakwami, 2012; Snelling et al., 2013). The same post-impact metamorphic activity also resulted in recrystallization and alteration of primary mineral assemblages throughout the South Range, re-equilibrating to greenschist-amphibolite facies (Fleet et al., 1987; Bennet et al., 1991). Despite the extensive post-impact metamorphism, recent whole rock geochemical studies have demonstrated that the geochemistry of Sudbury breccia in the Creighton area can still be reconstructed accurately using a mixture of locally derived lithologies (O'Callaghan et al., in press). The implication is that post-impact metamorphic and hydrothermal modification of the trace metal and geochemical signatures of the assemblages was limited and that potential vectoring tools may have been preserved that could offer clues to the proximity of footwall mineralization. However, the absence of any extensive geochemical or mineralogical halo around massive Ni-Cu contact-style mineralization, such as the Creighton deposit, also implies that any hydrothermal modification or remobilization of sulfides was spatially restricted (Lightfoot and Zotov 2005; Lightfoot 2007).

The earliest mineral phases identified in Sudbury breccia at Creighton mine comprise quartz, feldspars, biotite and rare Fe-oxides. Biotite is a ubiquitous constituent of Sudbury breccia throughout the South Range. As noted by White (2012), the compositional shift observed in biotites from the South Range appears to be largely controlled by the lithologies from which the Sudbury breccia matrix was derived. Increasing Mg# in Sudbury breccia-hosted biotite towards the Creighton Deep zone is controlled by the relative proportion of mafic Huronian metabasalts and gabbros (which host biotites with an Mg# ~0.36), relative to the felsic Creighton granite and granodiorites (in which biotites have an Mg# between 0.25 and 0.08). The reversal in Mg# and increased Ni content in biotites closest to sulfide veinlets may be indicative of an alternative origin, under conditions with greater availability of metals derived from the sulfides. The elevated Ni/Cr ratio and decreasing Mg# with proximity to mineralization reported here is very similar to studies by Warren et al. (2015) at the Worthington offset dike (~20 km South West of the Creighton embayment), which also identified two distinct species of biotite. One species is associated with ore mineralization (Ni + Cr > 1000 ppm and Mg/Fe ratio of 0.5 – 1.0) and another relating to post-ore regional metamorphism (<1000 ppm Ni + Cr and Mg/Fe ratio of 0.3 – 0.7). As previously observed, in both offset dike and footwall mineral systems, the Ni enrichment in biotite is intimately associated with the presence of sulfides, which is confirmed by the abrupt decrease in biotite-hosted Ni within a few meters of mineralization (Hanley and Bray, 2009; Nelles, 2012; Warren et al., 2015). Aside from Ni + Fe enrichment, biotites at Creighton mine also exhibit

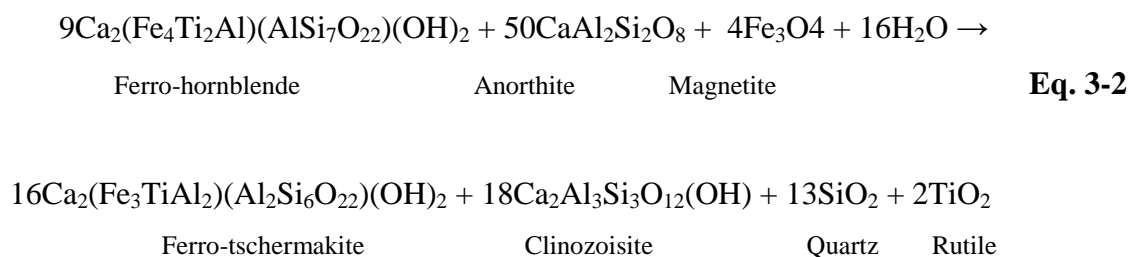
an elevated Tl content. Research on Tl substitution into micas is limited, but experiments by Riber (1966), Duchesne et al. (1983) and Ikramuddin et al. (1983) demonstrated that Tl^+ readily substitutes for K^+ and Rb^+ in biotites and that its distribution is controlled by hydrothermal solutions, being particularly enriched in lower temperature fluids, such as epithermal systems.

Amphiboles at Creighton mine display similar, albeit subdued, Ni/Cr and Tl trends that are restricted to mineralized zones. There is also a compositional shift away from the actinolite series and towards the more Fe-rich, ferro-tschermakite and ferro-hornblende series. Compositionally, this shift is very similar to the Na-K-Fe-Cl rich amphiboles observed by Hanley and Mungall (2003) and Magyarosi et al. (2002) adjacent to mineralization at the Fraser Mine in the North Range and Copper Cliff Mine in the South Range, which was attributed to retrograde alteration that post-dated magmatic fluids associated with the SIC. It is also consistent with observations made by Fleet et al. (1987) in the South Range, who linked the changes in amphibole species to progressive replacement of primary amphibole by secondary, metamorphic equivalents under increasing temperature and pressure conditions during the Penokean orogeny. In particular, the zoned ferro-actinolite→ferro-hornblende grains can be accredited to formation under progressively higher pressure conditions (Grapes and Graham, 1978). The greater halogen content in the ferro-hornblende rims implies that the reaction took place in the presence of halogen-bearing fluids, though the reaction itself is primarily a response to pressure rather than temperature or high fH_2O conditions (Grapes and Graham, 1978).



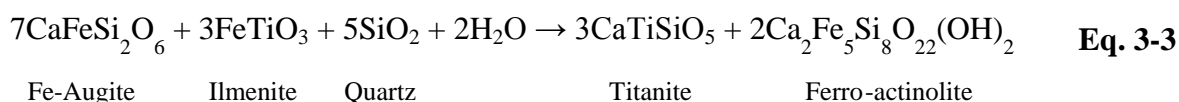
A third amphibole species, ferro-tschermakite, was only observed enclosing disseminated sulfides (Fig. 3.4E). The spatial transition between the two amphibole species reflects a continuum influenced by increasing pressures (and to a lesser extent temperatures), which may be associated with proximity to active shear zones in the footwall. Under increased pressures and temperatures, $Al^{IV,VI}$ is more readily incorporated into the amphibole lattice at the expense Si^{+4} and Ti^{+4} , resulting in the shift from hornblende series towards the

tschermakite end-member (Fleet et al., 1987; Bossiere, 1991). Excess Al could have been created by the hydration of feldspar, producing epidote, quartz and rutile as by-products:



In addition to rutile, Ti^{4+} (with Fe^{2+}) can be substituted for Fe^{3+} and Al^{3+} in allanite (Gieré and Sorensen, 2004), which is also present as a minor component in Sudbury breccia. Equation 2 also explains the absence of magnetite in samples from Creighton mine and may contribute to the occurrence of zones of oikiocrystic ‘flood’ quartz noted in several studies (Morrison et al., 1994; McCormick et al., 2002a; Hanley and Mungall, 2003).

The hydrosilicate phases at Creighton mine are over-printed by anhedral clusters of titanite. The U/Pb age dates for titanites from Creighton (1616 ± 38 Ma) correspond closely with $^{207}\text{Pb}/^{206}\text{Pb}$ values obtained by Bailey et al. (2004) for titanites at the Thayer-Lindsley mine (1658 ± 68 Ma), which are contemporaneous with the Mazatzalian orogeny (1.7 – 1.6 Ma) that reactivated several shear zones in the South Range (Van Schmus et al., 1993). Further evidence of a link between the titanites and shear zones is demonstrated by comparing Ca, which increases in titanite at high formational temperatures, against Al and Fe, which substitute for Ti in titanite at lower temperatures (Fig. 3.7B) (Harlov et al., 2006; Che et al., 2013). Increasing Ca+Ti/Al+Fe is indicative of a heat gradient towards Creighton Deep that, when combined with the age dates, are strong indicators for the presence of a Mazatzalian metamorphic-hydrothermal fluid that was focused along the active shear zones. The titanites may form from the breakdown of pyroxenes and Fe-oxide (Rene, 2011), which, may partially explain the absence of these minerals in samples from Creighton:



However, in addition to the observation of titanite grains overprinting the prismatic ferro-actinolite grains, the Mazatzalian age of the titanites would require the augite in equation 3-3 to have already survived greenschist-amphibolite facies metamorphism in the earlier

Penokean Orogeny. Chloritization of biotite can also produce titanite, but chlorite is similarly absent in samples from Creighton Deep (Sharp and Buseck, 1988; Shau et al., 1991). Alternatively, experiments by Tronnes et al. (1985) noted that high temperature, Ti-bearing phlogopites break down at ≤ 800 °C to form Ti-depleted phlogopite, rutile and either sanadine or vapor. As phlogopite that forms under higher temperatures can accommodate more Ca and Ti, Shau et al. (1991) suggest that decreasing temperatures could lead to an excess in these elements resulting in a breakdown of Ca-Ti-bearing magmatic phlogopite under decreasing temperatures to produce Ti-Ca-depleted metamorphic phlogopite with titanite and rutile overgrowths. In the absence of chlorite and augite, the partial replacement of phlogopite in the waning stages of the Mazatzalian orogeny is the most plausible origin for titanites.

3.8.2 Mineralogy and Geochemical Variations at Coleman Mine

The sharp-walled chalcopyrite-pyrrhotite (type 1) and bornite-millerite (type 2) veins within the Coleman-Levack embayment represent a more typical footwall-style mineralization compared with structurally remobilized types found at the Creighton mine. Although the North Range is considered to be further from the center of post-impact orogenic activity and represents a shallower depth of formation (Fleet et al., 1987), the mineral zones have been affected by several post-emplacement hydrothermal and tectonic events, including the reactivation of strike-slip faults (e.g., the Bob's Lake and Fecunis faults) and the intrusion of the 1.24 Ga Sudbury and 590 Ma Grenville diabase dike swarms.

As at Creighton, distal to mineral zones, Sudbury breccia matrix is primarily composed of quartz, feldspars and biotites, with minor amphibole and Fe-oxide. Compositionally, the biotites in this study are similar to those analyzed by Hanley and Mungall (2003) at Fraser Mine and fall within the magmatic biotite field, compared to those with a hydrothermal origin, which would have a lower Mg# and greater halogen content. The biotites exhibit increased chloritization towards the SIC and mineralized zones that has been attributed by Hanley and Mungall (2003) to retrograde metamorphism under cooling temperatures adjacent to the SIC. Application of a chlorite geothermometer based on vacancies in the octahedral site, developed by Kranidiotis and MacLean (1987) (Eq. 3-4), combined with a chlorite geothermometry calculator developed by Yavuz (et al., 2015), provides an estimated temperature of formation for the chlorites between 250 – 350°C (Fig. 3.5B):

$$TKML_{87-Al^{IV}} (^{\circ}C) = 106 \times \left(Al_{O_{28}^{IV}} + 0.7 \left[\frac{Fe}{Fe+Mg} \right] \right) + 18 \quad \text{Eq. 3-4}$$

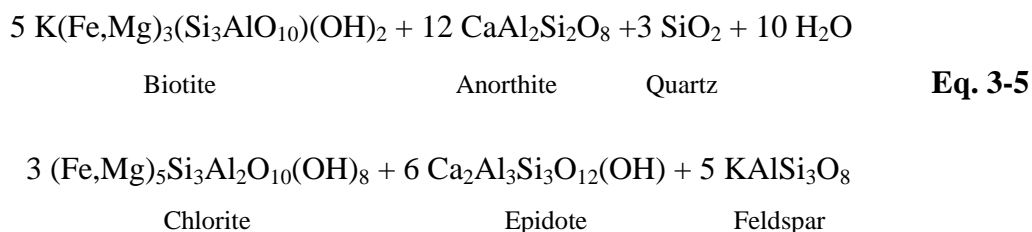
This is in agreement with 300 – 400°C estimate of Hanley and Mungall (2003) that is based on activity diagrams for an assemblage of chlorite + epidote + actinolite, but it is higher than the <170 °C fluid inclusion values obtained by Tuba et al. (2014) in similar chlorite-calcite alteration at the Amy Lake PGE zone in the East Range. Figure 3.6A compares the Mg# of the two phyllosilicates and demonstrates the control that the precursor biotite has on the replacement chlorite pseudomorphs, in contrast with the nickeliferous chlorites and Fe-Ti biotites that, as noted in previous studies, appear to have a different origin and are restricted to within a few meters of mineralization (McCormick et al., 2002a; Hanley and Mungall, 2003; White, 2012).

Recent research by Nelles (2012) suggests that as type 2 veins tend to be thin (<1 m wide) compared with type 1 veins, they are more susceptible to fluid-wall rock interaction. Nelles (2012) thus argues that the particularly high trace-metal content in the hydrosilicate assemblages adjacent to type 2 veins could be a product of greater interaction between residual sulfide melt and adjacent wall rock. This resulted in the expulsion of Fe and S, thereby driving the melt into the bornite and millerite solid-solution zone of the Fe-Cu-Ni-S system and possibly contributing to the development of LSHPM-style mineralization. Alternatively the type 2 veins may represent the end product of a sequence of sulfide fractionation during emplacement, which advanced from the pyrrhotite-pentlandite contact ores, through chalcopyrite-cubanite to bornite-millerite as the sulfide melt cooled (Ebel and Naldrett, 1996; Beswick, 2002; Péntek et al., 2013). This is supported by the spatial location of type 2 veins, which tend to be furthest into the footwall and at the termination of vein systems. The metalliferous chlorites could therefore represent the expulsion of late stage, metal-bearing volatile-rich fluids in these more fractionated sulfide veins (Molnar et al., 2001; Hanley et al., 2005; Hanley et al., 2011; Dare et al., 2014b), or a greater interaction with hydrothermal fluids in the footwall, further out from the SIC heat aureole.

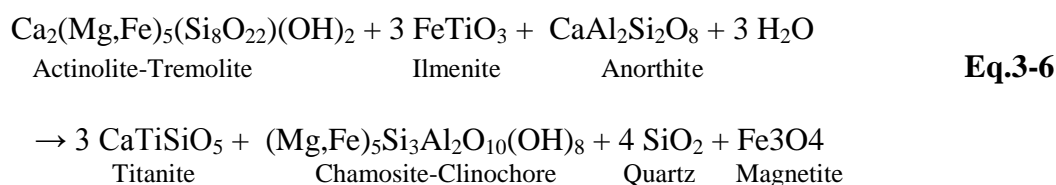
Molnar et al. (1999; 2001) identified an early, high temperature (up to 350°C), saline fluid with elevated KCl, NaCl, and Fe-chlorides that circulated within the footwall of the SIC and interacted with mineralization, potentially remobilizing some metals into the wall-rock. This hydrothermal system was driven by a combination of heat from the SIC and syn-impact greenschist-amphibolite facies metamorphism and is characterized by the presence of chlorite + actinolite + pyrosmalite + epidote rich assemblages, with quartz + biotite + carbonates.

This assemblage is largely consistent to that observed adjacent to mineralization in this study, but does not account for the presence of titanite-oxide grains or the notable absence of amphibole within the thin alteration selvage that borders the sharp-walled sulfide veins at the McCeedy 153 East ore body.

As noted previously, titanite is observed as both a lamellae within the chlorite clots and an alteration rim on ilmenite-magnetite grains. The magnetite lamellae observed on some grains of ilmenite is considered an incomplete product of post-mineralization, oxidation-exsolution processes and is not directly associated with mineralizing fluids (Gasparrini and Naldrett 1972; McCormick et al., 2002a). Both titanite species have an anhedral form and scattered geochemical signatures inherited from pre-existing Fe-oxides and hydrosilicates (Fig. 3.3E, 3.4B). Titanite lamellae are a common byproduct of chloritization of biotite (Fig. 3.4A,B) caused by the incompatibility of Ti and Al in the chlorite lattice (Ferry 1979; Veblen and Ferry 1983; Yui et al., 2001). The reaction also produces excess K, Fe, Mg, Al and Si that may contribute to the formation of epidote and K-feldspar (Janeczek, 1994; Hanley and Mungall, 2003):



The chloritization of amphibole can also produce titanite, as significant Ca^{2+} is released during the retrograde reaction. If ilmenite is present it may serve as a nucleus for the formation of titanite. Replacement of actinolite by chlorite in Sudbury breccia has previously been observed by Hanley and Mungall (2003) and McCormick and McDonald (1999), and may, as is the case in this study, also explain the relative absence of feldspar in the alteration selvages:



Equation 3-6 is similar to oxidation / rehydration reactions observed by Rene (2008) in hydrothermally altered amphibolites, though, in the case of Sudbury, with amphibole as the reactant rather than clinopyroxenes. In both studies, the magnetite produced was observed as individual grains within the titanite and / or ilmenite. The reactant assemblages in equations 5 and 6 are considered to be the product of combination of high temperature (>400°C) early magmatic-hydrothermal fluid that, over time, were diluted by saline brines in the footwall (Marshall et al., 1999; Molnar et al., 2001; Hanley et al., 2011). However, the chlorite + epidote alteration product assemblages in equations 3-5 and 3-6 have been attributed to a later, 150-250°C, NaCl-CaCl₂-H₂O fluid related to the remobilization of Canadian Shield brines (Molnar et al., 2001). Based on equation 3-6, chloritization took place concurrent with the formation of titanite. The implication is that the titanite U-Pb age dates of 1358 ± 78 Ma also constrain the formation of the thin, nickeliferous chlorite-bearing alteration selvages adjacent to the sulfide veins at the McCreedy 153 East zone. The 1358 ± 78 Ma age post-dates Penokean, Blezardian and Mazatzalian orogenic activity, but roughly corresponds with two hydrothermal-metamorphic events recorded in the North Range.

Around 1.24 Ga, several olivine diabase intrusions cut through the Coleman-Levack embayment, including a 38 m wide intrusion ~150 m from the sample sites in this study. These mafic intrusions were derived from partial melting of the lithosphere and may have remobilized 250 °C, Ca²⁺ rich Canadian Shield brines (Krogh et al., 1987; Rousell et al., 1997; Marshall et al., 1999; Molnar et al., 2001; Shellnut and MacRae, 2011; Tuba et al., 2014). In addition to the fluid inclusion temperatures that correspond with the chlorite geothermometer results of this study, these brines were preferentially transported along the same northeast-orientated structures that host the Cu-Ni-PGE footwall deposits at the McCreedy 153 East (Molnar et al., 2001). This would have enabled interaction between the brines and the sulfide veins to create the metalliferous hydrosilicates as well as producing the decreasing temperature gradient noted in chlorites away from the fluid and sulfide bearing structures. However, there is a notable discrepancy between the ages of the mafic intrusions and the titanites hosted in the selvages that pertains to an alternative hydrothermal-metamorphic event.

An alternative explanation of the titanite ages from Coleman mine can be evaluated. The new titanite age correlates well with results of ⁴⁰Ar/⁴⁹Ar age dating of K-feldspars in North Range Sudbury breccia (from the Dowling and Cartier townships). These studies yielded ⁴⁰Ar/⁴⁹Ar ages around 1340 ± 20 Ma (Thompson et al., 1998). The closest comparable ages in

the South Range are $^{40}\text{Ar}/^{49}\text{Ar}$ ages obtained from shear-zone hosted micas (1450 – 1480 Ma) (Bailey et al., 2004; Szentpeteri 2009). In both examples, the results have been attributed a tectono-thermal event associated with tonalitic and granodioritic magmatism in the Grenville province, which was synchronous with the Chieflakian orogeny (1470 – 1440 Ma) (Fueten and Redmond 1997; Thompson et al., 1998; Corfu and Easton 2000; Raharimahefa et al., 2014). The tectonic effects of the Chieflakian orogeny are primarily recorded in the South Range, where ductile deformation fabrics and brittle tightening of fold structures has been recorded (Fueten and Redmond 1997; Szentpeteri 2009). Although it has been proposed that the Chieflakian orogeny was responsible for the development of the South Range Shear Zone, this is complicated by the presence of earlier Mazatzalian titanites found in this study and by Bailey et al., (2004), which imply that the shear zones were already active prior to the Chieflakian event. Deutsch et al., (1989) report Rb/Sr ages of 1430 ± 15 Ma obtained from a concentrate of epidote-chlorite-actinolite collected from footwall breccia in the North Range, and Fullagar et al., (1971) reported similar 1430 ± 65 Ma Rb/Sr ages from glassy inclusions in the Onaping Formation. In both cases, the ages are considered to represent a sub-greenschist to greenschist facies thermal overprint that resulted in radiogenic Sr loss. Calculating the closure temperature of Rb/Sr is complicated by influences on isotopic and chemical exchange rates such as grain size, but is roughly considered to lie between 300 – 400°C for biotite, consistent with a sub-greenschist facies overprint (Jenkin et al., 2001). As titanite has a higher closure temperature for Pb diffusion of 550 – 700°C (amphibolite facies) (Scott and St-Onge, 1995; Schone and Bowring 2006), it is unlikely to have been affected by Pb loss during the Chieflakian and could instead represent primary titanite exsolution during chloritization of biotite and amphibole as a result of far field effects associated with the waning stages of the Chieflakian Orogeny. If the titanites are a product of the Chieflakian event, then there are implications for the co-existing nickeliferous chlorite alteration selvages adjacent to sulfide mineralization. Although Molnar et al. (2001) suggests that the 150 – 250°C Canadian shield brines were mobilized in response to the emplacement of the 1.24 Ga Sudbury diabase dikes, the far-field effects of the Chieflakian orogeny could provide an alternative heat-source that mobilized the brines and caused the localized modification of the sharp-walled sulfide veins. In the latter case, fluids may have been transported via the North-South trending Bob's Lake and Fecunis faults, or the SW-NE trending Pumphouse Creek Deformation Zone, which cuts through the Coleman-Levack embayment and is considered comparable to the South Range Shear Zone (Card 1994).

3.8.3 *Comparisons between Creighton and Coleman Mine*

Although some post-impact hydrothermal activity, such as the early, high temperature magmatic fluids, were regional (Marshall et al., 1999; Molnar et al., 2001), the variations between the mineral assemblages observed in Sudbury breccia at Creighton and Coleman Mine reflect the influence of more localized hydrothermal and metamorphic fluids. There are compositional variations between the tonalitic gneiss footwall lithologies at Coleman mine versus the mixture of granite and mafic metavolcanics at Creighton Mine, which may inhibit or encourage particular mineral assemblages to form.

At Creighton Mine, the spatial transition from ferro-actinolite → ferro-hornblende → ferro-tschermakite is indicative of increasing pressure conditions associated with shear zones that host remobilized footwall sulfide mineralization. Titanites at Creighton mine post-date the amphibole + biotite assemblage and do not appear to have modified the sulfides, though their geochemistry does indicate a temperature gradient towards shear zones, affirmed by their syn-orogenic Mazatzalian U-Pb ages. In contrast, chlorite is notably absent at Creighton Mine, which could be the result of prolonged higher temperatures and/or pressures in the South Range owing to the greater depth of the South Range prior to tectonic uplift and the closer proximity to the center of post-impact orogenic activity. This is also supported by the absence of mineral assemblages diagnostic of the SIC thermal aureole in the South Range, compared to the North Range, where the hornfels halo (e.g., pyroxene-hornblende, epidote-hornblende zones) has been preserved (Farrow and Watkinson, 1992; Prevec and Cawthorn, 2002; Hanley and Mungall, 2003). Amphiboles are relatively uncommon in the McCreedy 153 East deposit, despite being widely reported elsewhere in the North Range; this is possibly because of the more extensive chloritization observed in samples from this study (McCormick and McDonald, 1999; Hanley and Bray, 2009).

Titanite is ubiquitous at both Creighton and Coleman mine, however the estimated temperature of the fluids associated with the titanite formation (<350 °C) is too low for Zr to be used as a geothermometer, which is only effective in temperatures exceeding 600°C (Hayden et al., 2008). However, co-existing chlorite geothermometry is consistent with a low temperature (150 – 250 °C), metamorphic-hydrothermal fluid identified by several studies in the Coleman-Levack embayment (Molnar et al., 2001; Pentek et al., 2008; Tuba et al., 2014). Although some chlorites are clearly pseudomorphs of precursor biotite, the nickeliferous

species present adjacent to sulfide veins at Coleman Mine represent a more intense, albeit localized, alteration associated with brines remobilized along the same NW-SE structures as occupied by the sulfides. Based on the titanite age dates, the alteration appears to be a far-field effect of the 1.45 Ga Chieflakian orogeny. Fluids may have also been introduced along pre-existing structures such as the Pumphouse Creek Deformation Zone that transects the North Range, though the age of the structure is poorly constrained (Card 1994). A comparable Chieflakian chlorite-titanite assemblage was not observed at Creighton mine, but Szentpeteri's (2009) study on the nearby Worthington offset dike (~20 km's South West of Creighton) concluded that sulfides and precious metals were remobilized by a similar combination of saline shield brines and CO₂-rich metamorphic fluids, which were concentrated along contemporaneous Chieflakian deformation zones. Combined with the Mazatzalian titanite from Creighton, this serves to confirm that the South (and possibly North) Range shear zones acted as conduits for multiple metamorphic-hydrothermal fluids, some of which are associated with modification of pre-existing sulfide zones.

In addition to the Ni contents of chlorite and amphibole, variations in Tl/Rb content in biotite also appears to be a potential vectoring tool towards mineralized zones at both localities. Substitution of Tl and Rb for K in biotite can be associated with primary magmatic fluids or lower temperature, epithermal fluids. Warren et al. (2015) also noted that Ni/Cr can be used to discriminate between biotites associated with mineralizing fluids and post-ore metamorphic fluids. Combining Tl/Rb vs Ni/Cr in biotite demonstrates a positive relationship at both Coleman and Creighton mine, though the signature is diluted at the latter site, possibly due to the greater mobility of Tl at lower temperatures, combined with the more prolonged, post-impact metamorphic activity experienced in the South Range. Although Tl is usually below detection limits in whole rock geochemical results, it has been noted that Rb and Ce decrease significantly in bulk geochemical results from mineralized zones (e.g., from 203 to 59 ppm Rb) (Fig. 3.6D). As Tl, Rb and Ce are all primarily hosted in biotites; this relationship could reflect Tl enrichment in biotites resulting in expulsion of Rb and Ce. Thus, Tl/Rb vs Ni/Cr may serve as a useful whole-rock or mineral-chemistry vectoring tool associated with magmatic-hydrothermal fluids that interacted with mineralized zones in the North and South Range, and complements the recent Ni-Cr-Cu biotite vectoring tool identified by Warren et al. (2015) at the Worthington offset dike. It is, however, important to note that at both localities the trace metal values within the hydrosilicate assemblages falls exponentially with distance from the sulfide occurrences indicating that, although

hydrothermal modification of the sulfides has taken place, the anomalous trace metal halo surrounding the ore zones may be spatially limited (possibly to within tens of meters). This may explain why there is an absence of a large, detectable sulfide or trace metal halo surrounding the massive contact-style deposits, as noted by Lightfoot (2007).

3.9 Conclusion

By analyzing and comparing the mineral chemistry and assemblage of Sudbury breccia from Coleman and Creighton Mine, this study has identified elemental and mineralogical variations towards mineral zones in the North and South Ranges that relate to the localized remobilization of footwall style sulfides. Although regional hydrothermal events, such as magmatic fluids associated with the cooling impact melt sheet, have been identified in the footwall environment by previous studies, this investigation has demonstrated that there are geochemical signatures and mineral assemblages that are spatially associated with post-impact brittle and ductile structures at both Creighton Deep and the McCreedy 153 East deposits:

- At Creighton Deep, the amphibole assemblage exhibits evidence of trace metal remobilization concurrent with increasing P-T geochemical signatures, both of which are associated with proximity to shear zones that host the Creighton Deep footwall deposit. The assemblage is overprinted by a later, Mazatzalian event that is also spatially associated with the shear zones and resulted in the breakdown of Ti-phlogopite to form titanite, though there is no evidence of interaction between this later fluid and the existing sulfides.
- The Sudbury breccia mineral assemblage in the McCreedy 153 East deposit has been affected by a lower grade, chloritization event that is roughly contemporaneous with the waning stages of the Chieflakian orogeny. Instead of the Sudbury diabase intrusions, this study suggests that the thermal gradient was associated with the Chieflakian orogeny and mobilized Ca-rich shield brines and metamorphic fluids that moved along the same structures as the footwall sulfide mineralization. This resulted in the localized redistribution of trace metals as a thin, metaliferous alteration selvage. It is possible, but yet to be determined whether the Pumphouse Creek Deformation Zone acted as an alternative heat source for the brine remobilization. Although not observed in this study, similar Chieflakian-aged modification of sulfides has been noted in the South Range. The ratios of Tl/Rb vs Ni/Cr in biotite show a positive relationship towards mineralized zones at both Creighton and Coleman Mine that relates to an interaction between the

sulfide zones and either a high temperature SIC-derived magmatic fluid or lower temperature, hydrothermal-metamorphic fluid. This corresponds with decreased Ce and Rb vs Ni/Cr in bulk geochemical results, and thus may serve as a whole rock and mineral chemistry vectoring tool towards prospective zones of Sudbury breccia. Although more work is required to constrain the extent of the elevated Tl/Rb ratio in biotite at Creighton mine, it appears to be elevated at least 20m from sulfide veins in the McCreedy 153 East deposit.

3.10 References

- Ames, D.E., Davidson, A., and Wodicka, N., 2008, Geology of the Giant Sudbury Polymetallic Mining Camp, Ontario, Canada: *Economic Geology*, v. 103, p. 1057–1077.
- Ames, D., and Farrow, C., 2007, Metallogeny of the Sudbury mining camp, Ontario., in Goodfellow, W.D. ed., *Mineral Deposits of Canada: A Synthesis of Major Deposit-Types, District Metallogeny, the Evolution of Geological Provinces, and Exploration Methods*, Geological Association of Canada, Mineral Deposits Division, Special Publication, p. 329–350.
- Anders, D., Osinski, G.R., Grieve, R.A.F., and Brillinger, D.T.M., 2015, The Basal Onaping Intrusion in the North Range: Roof rocks of the Sudbury Igneous Complex: *Meteoritics & Planetary Science*, v. 50, no. 9, p. 1577–1594.
- Bailey, J., Lafrance, B., McDonald, A.M., Fedorowich, J.S., Kamo, S., and Archibald, D.A., 2004, Mazatzal–Labradorian-age (1.7–1.6 Ga) ductile deformation of the South Range Sudbury impact structure at the Thayer Lindsley mine, Ontario: *Canadian Journal of Earth Sciences*, v. 41, no. 12, p. 1491–1505.
- Bailey, J., McDonald, A.M., Lafrance, B., and Fedorowich, J.S., 2006, Variations in Ni content in sheared magmatic sulfide ore at the Thayer Lindsley Mine, Sudbury, Ontario: *Canadian Mineralogist*, v. 44, no. 5, p. 1063–1077.
- Beswick, A., 2002, An Analysis of Compositional Variations and Spatial Relationships within Fe-Ni-Cu Sulfide Deposits on the North Range of the Sudbury Igneous Complex: *Economic Geology*, v. 97, p. 1487–1508.

- Card, K.D., 1994. Geology of the Levack gneiss complex, the northern footwall of the Sudbury structure, Ontario. *Current Research 1994-C*; Geological Survey of Canada, p. 269- 278.
- Caritat, P.D.E., Hutcheon, I.A.N., and Walshe, J.L., 1993, Chlorite Geothermometry: A Review: *Clays and Clay Minerals*, v. 41, no. 2, p. 219–239.
- Che, X.D., Linnen, R.L., Wang, R.C., Groat, L. a., and Brand, a. a., 2013, Distribution of Trace and Rare Earth Elements in Titanite From Tungsten and Molybdenum Deposits in Yukon and British Columbia, Canada: *The Canadian Mineralogist*, v. 51, no. 3, p. 415–438.
- Dare, S. a. S., Barnes, S.-J., Prichard, H.M., and Fisher, P.C., 2014, Mineralogy and Geochemistry of Cu-Rich Ores from the McCreedy East Ni-Cu-PGE Deposit (Sudbury, Canada): Implications for the Behavior of Platinum Group and Chalcophile Elements at the End of Crystallization of a Sulfide Liquid: *Economic Geology*, v. 109, p. 343–366.
- Dare, S.A.S., Barnes, S.-J., Prichard, H.M., and Fisher, P.C., 2010, The Timing and Formation of Platinum-Group Minerals from the Creighton Ni-Cu-Platinum-Group Element Sulfide Deposit , Sudbury , Canada : Early Crystallization of PGE-Rich Sulfarsenides: *Economic Geology*, v. 105, p. 1071–1096.
- Davis, D.W., 2008, Sub-million-year age resolution of Precambrian igneous events by thermal extraction–thermal ionization mass spectrometer Pb dating of zircon: Application to crystallization of the Sudbury impact melt sheet: *Geology*, v. 36, no. 5, p. 383–386.
- Deutsch, A., Lakomy, R., Buhl, D., 1989, Strontium- and neodymium-isotopic characteristics of a heterolithic breccia in the basement of the Sudbury impact structure, Canada: *Earth and Planetary Science Letters*, v. 93, pp. 359-370.
- Dietz R.S., 1964, Sudbury Structure as an Astrobleme: *The Journal of geology*, v. 72, no. 4, p. 412–434.

- Dressler, B., 1984, The Effects of the Sudbury Event and the Intrusion of the Sudbury Igneous Complex on the Footwall Rocks of the Sudbury Structure, in Pye, E.G., Naldrett, A.J., and Giblin, P.E. eds., *Geology and Ore Deposits of the Sudbury Structure*, Ontario Geological Survey, p. 99–131.
- Duchesne, J.C., Rouhart, A., Schoumacher, C., Dillen, H., Gologie, L. De, Geochimie, P., Liege, U. De, and Tilman, S., 1983, Thallium , Nickel , Cobalt and Other Trace Elements in Iron Sulfides from Belgian Lead-Zinc Vein Deposits: *Mineralium Deposita*, v. 18, p. 303–313.
- Ebel, D.S., and Naldrett, A. J., 1996, Fractional crystallization of sulfide ore liquids at high temperature: *Economic Geology*, v. 91, p. 607–621.
- Enami, M., Suzuki, K., Liou, J.G., and Bird, D.K., 1993, Al-Fe³⁺ and F-OH substitutions in titanite and constraints on their P-T dependence: *European Journal of Mineralogy*, v. 5, p. 219–231.
- Fairbairn, H., Faure, G., Pinson Jr, W., and Hurley, P., 1968, Rb-Sr whole-rock age of the Sudbury lopolith and basin sediments: *Canadian Journal of Earth Sciences*, v. 5, no. 3, p. 707–714.
- Farrow, C.E.G., Everest, J.O., King, D.M., and Jolette, C., 2005, Sudbury Cu-(Ni)-PGE systems: Refining the classification using McCreehy West mine and Podolsky project case studies, in Mungall, J.E. ed., *Exploration for Deposits of Platinum-Group Elements*, Mineralogical Association of Canada, p. 163–180.
- Farrow, C.E.G., and Watkinson, D.H., 1992, Alteration and the Role of Fluids in Ni , Cu and Platinum-Group Element Deposition, Sudbury Igneous Complex Contact, Onaping-Levack area, Ontario: *Mineralogy and Petrology*, v. 46, p. 67–83.
- Ferry, J.M., 1979, Reaction mechanism, physical conditions and mass transfer during hydrothermal alteration of mica and feldspar in granitic rocks from south-central Maine, USA: *Contributions to Mineralogy and Petrology*, v.68, p. 125 – 139.

- Fleet, M.E., Barnett, R.L., and Morris, W.A., 1987, Prograde Metamorphism of the Sudbury Igneous Complex: *Canadian Mineralogist*, v. 25, p. 499–514.
- Fuerten, F., and Redmond, D.J., 1997, Documentation of a 1450 Ma contractional orogeny preserved between the 1850 Ma Sudbury impact structure and the 1 Ga Grenville orogenic front, Ontario: *Bulletin of the Geological Society of America*, v. 109, no. 3, p. 268–279.
- Fullagar, P.D., Bottino, M.L., French, B.M., 1971, Rb-Sr study of shock metamorphosed inclusions from the Onaping Formation, Sudbury, Ontario: *Canadian Journal of Earth Sciences*, v. 8, p. 435-443.
- Gibson, A.M., Lightfoot, P.C., and Evans, T.C., 2010, Contrasting Styles of Low Sulfide High Precious Metal Mineralisation in the 148 and 109 FW Zones : North and South Ranges of the Sudbury Igneous Complex , Ontario , Canada, in 11th International Platinum Symposium, Sudbury, Canada, 4 p.
- Grieve, R.A.F., Ames, D.E., Morgan, J. V., and Artemieva, N., 2010, The evolution of the Onaping Formation at the Sudbury impact structure: *Meteoritics & Planetary Science*, v. 45, no. 5, p. 759–782.
- Hanley, J.J., and Bray, C.J., 2009, The Trace Metal Content of Amphibole as a Proximity Indicator for Cu-Ni-PGE Mineralisation in the Footwall of the Sudbury Igneous Complex, Ontario, Canada: *Economic Geology*, v. 104, p. 113–125.
- Hanley, J.J., and Mungall, J.E., 2003, Chlorine Enrichment and Hydrous Alteration of the Sudbury breccia Hosting Footwall Cu-Ni-PGE Mineralization at the Fraser Mine, Sudbury, Ontario, Canada.: *The Canadian Mineralogist*, v. 41, p. 857–881.
- Hanley, J.J., Mungall, J.E., Bray, C.J., and Gorton, M.P., 2004, The Origin of Bulk and Water Soluble Cl and Br Enrichments in Ore Hosting Sudbury breccia in the Fraser Copper Zone, Strathcona Embayment, Sudbury, Ontario, Canada: *The Canadian Mineralogist*, v. 42, p. 1777–1798.

- Hanley, J.J., Mungall, J.E., Pettke, T., Spooner, E.T.C., and Bray, C.J., 2005, Ore metal redistribution by hydrocarbon–brine and hydrocarbon–halide melt phases, North Range footwall of the Sudbury Igneous Complex, Ontario, Canada: *Mineralium Deposita*, v. 40, no. 3, p. 237–256.
- Harlov, D., Tropper, P., Seifert, W., Nijland, T., and Förster, H.-J., 2006, Formation of Al-rich titanite ($\text{CaTiSiO}_4\text{O}-\text{CaAlSiO}_4\text{OH}$) reaction rims on ilmenite in metamorphic rocks as a function of $f\text{H}_2\text{O}$ and $f\text{O}_2$: *Lithos*, v. 88, p. 72–84.
- Hayden, L.A., Watson, E.B., and Wark, D.A., 2008, A thermobarometer for sphene (titanite): *Contributions to Mineralogy and Petrology*, v. 155, no. 4, p. 529–540.
- Heaman, L.M. 1989. U-Pb dating of mafic dyke swarms: what are the options?; abstract in *International Association of Volcanology and Chemistry of the Earth's Interior, Continental Magmatism, New Mexico Bureau of Mines and Mineral Resources, Bulletin 131*, p.125.
- Ikramuddin, M., Asmeron, Y.A., Nordstrom, P.M., Kinart, K.P., Martin, W.M., Digby, S.J.M., Elder, D.D., Nijak, W.F., and Afemari, A.A., 1983, Thallium: A potential guide to mineral deposits: *Journal of Geochemical Exploration*, v. 19, p. 465–490.
- Keays, R.R., and Crockett, A.J., 1970, A study of precious metals in the Nickel Irruptive ores; *Economic Geology*, v. 65, p. 438-450.
- Keays, R.R., and Lightfoot, P.C., 2004, Formation of Ni-Cu-PGE sulphide mineralization in the Sudbury Impact Melt Sheet: *Mineralogy and Petrology*, v.82, pp. 217-258.
- Krogh, T.E., Corfu, F., Davis, D.W., Dunning, G.R., Heaman, L.M., Kamo, S.L., Machado, N., Greenough, J.D. and Nakamura, E. 1987. Precise U-Pb isotope ages of diabase dikes and mafic to ultramafic rocks using trace amounts of baddeleyite and zircon; in *Mafic Dike Swarms*, Geological Association of Canada, Special Paper 34, p.147-152.
- Krogh, T.E., Davis, D.W. and Corfu, F. 1984. Precise U-Pb zircon and baddeleyite ages for the Sudbury area; in *The Geology and Ore Deposits of the Sudbury Structure*, Ontario Geological Survey, Special Volume 1, p.431-446.

- Krogh, T.E., Kamo, S.L. and Bohor, B.F. 1996. Shocked metamorphosed zircons with correlated U-Pb discordance and melt rocks with concordant protolith ages indicate an impact origin for the Sudbury Structure; in *Earth Processes: Reading the Isotope Code*, American Geophysical Union, Monograph 95, p.343-352.
- Lafrance, B., and Kamber, B.S., 2010, Geochemical and microstructural evidence for in situ formation of pseudotachylitic Sudbury breccia by shock-induced compression and cataclasis: *Precambrian Research*, v. 180, p. 237–250.
- Leake, B.E., Woolley, A.R., Arps, C.E.S., Birch, W.D., Gilbert, C.M., Grice, J.D., Hawthorne, F.C., Kato, A., Kisch, H.J., Krivovichev, V.G., Linthout, K., Laird, J., Mandarino, J. a., Maresch, W. V., et al., 1997, Nomenclature of Amphiboles: Report of the Subcommittee of the International Commission on New Minerals and Mineral Names: *The Canadian Mineralogist*, v. 35, p. 219–246.
- Leshner, C.M., Golightly, J.P., Gregory, S.K., Huminicki, M.A., and Pattison, E.F., 2009, Genesis of Ni-Cu-PGE Mineralization Associated with the 1.85 Ga Sudbury Impact Event, in *Geological Association of Canada*, Toronto, Canada, p. 2.
- Li, J.-W., Deng, X.-D., Zhou, M.-F., Liu, Y.-S., Zhao, X.-F., and Guo, J.-L., 2010, Laser ablation ICP-MS titanite U–Th–Pb dating of hydrothermal ore deposits: A case study of the Tonglushan Cu–Fe–Au skarn deposit, SE Hubei Province, China: *Chemical Geology*, v. 270, p. 56–67.
- Li, C., and Naldrett, A.J., 1993, High Chlorine Alteration Minerals and Calcium-rich Brines in Fluid Inclusions from the Strathcona Deep Copper Zone, Sudbury, Ontario.: *Economic Geology*, v. 88, p. 1780–1796.
- Lieger, D., Riller, U., and Gibson, R.L., 2009, Generation of fragment-rich pseudotachylite bodies during central uplift formation in the Vredefort impact structure, South Africa: *Earth and Planetary Science Letters*, v. 279, p. 53–64.
- Lightfoot, P.C., 2016, *Nickel Sulfide Ores and Impact Melts: Origin of the Sudbury Igneous Complex*: 1st edition, Elsevier, 620 p.

- Lightfoot, P.C. and Zotov, I., 2005, Geology and geochemistry of the Sudbury Igneous Complex, Ontario, Canada: Origin of nickel sulfide mineralization associated with an impact-generated melt sheet: *Geology of Ore Deposits*, v.47, pp. 349 – 381.
- Lightfoot, P.C., Keays, R.R., Morrison, G.G., Bite, A., and Farrell, K.P., 1997, Geologic and Geochemical Relationships between the Contact Sublayer, Inclusions, and the Main Mass of the Sudbury Igneous Complex: A Case Study of the Whistle Mine Embayment: *Economic Geology*, v. 33, pp. 647-673
- Lightfoot, P.C., 2015, Structural Controls on Nickel Sulfide Mineralization at Sudbury, Thompson and Voisey's Bay: Prospectors and Developers Association of Canada, Toronto, Canada.
- McCormick, K.A., Fedorowich, J.S., McDonald, A.M., and James, R.S., 2002, A Textural , Mineralogical , and Statistical Study of the Footwall Breccia within the Strathcona Embayment of the Sudbury Structure: *Economic Geology*, v. 97, p. 125–143.
- McCormick, K.A., and McDonald, A.M., 1999, Chlorine-bearing amphiboles from the Fraser mine, Sudbury, Ontario, Canada: description and crystal chemistry: *The Canadian Mineralogist*, v. 37, p. 1385–1403.
- Meldrum, A., Abdel-Rahman, A.-F.M., Martin, R.F., and Wodicka, N., 1997, The nature , age and petrogenesis of the Cartier Batholith , northern flank of the Sudbury Structure, Ontario, Canada: *Precambrian Research*, v. 82, p. 265–285.
- Molnar, F., Watkinson, D.H., and Everest, J.O., 1999, Fluid-inclusion characteristics of hydrothermal Cu-Ni-PGE veins in granitic and metavolcanic rocks at the contact of the Little Stobie deposit, Sudbury, Canada: *Chemical Geology*, v. 154, p. 279–301.
- Molnar, F., Watkinson, D.H., and Jones, P.C., 2001, Multiple Hydrothermal Processes in Footwall Units of the North Range, Sudbury Igneous Complex, Canada, and Implications for the Genesis of Vein-Type Cu-Ni-PGE Deposits: *Economic Geology*, v. 96, p. 1645–1670.

- Morrison G.G., 1984, Morphological features of the Sudbury structure in relation to an impact origin: Ontario Geological Survey Special Volume 1, p. 513-522.
- Morrison G.G., Jago B.C., White T.L., 1994, Footwall mineralization of the Sudbury Igneous Complex, in Lightfoot P.C. and Naldrett A.J., eds., Proceedings of the Sudbury-Noril'sk Symposium. Ontario Geological Survey, Special Volume 5, p. 57-64.
- Mukwakwami, J., Leshner, C.M., and Lafrance, B., 2014, Geochemistry of Deformed and Hydrothermally Mobilized Magmatic Ni-Cu-PGE Ores at the Garson Mine, Sudbury: *Economic Geology*, v. 109, p. 367–386.
- Naldrett, A.J., Asif, M., Schandl, E., Searcy, T., Morrison, G.G., Binney, W.P., and Moore, C., 1999, Platinum-Group Elements in the Sudbury Ores: Significance with Respect to the Origin of Different Ore Zones and to the Exploration for Footwall Orebodies: *Economic Geology*, v. 94, p. 185–210.
- Nelles, E.W., 2012, Genesis of Cu-PGE-rich Footwall-Type Mineralization in the Morrison Deposit, Sudbury: Laurentian University, Sudbury, Canada, 96 p.
- Parmenter, A.C., Lee, C.B., and Coniglio, M., 2002, “Sudbury breccia” at Whitefish Falls, Ontario: evidence for an impact origin: *Canadian Journal of Earth Sciences*, v. 39, no. 6, p. 971–982.
- Pentek, A., 2009, Partial melting and melt segregation within the contact aureole of the Sudbury Igneous Complex (Ontario, Canada) and their significance in hydrothermal Cu-Ni-PGE mineralization of the footwall: Eotvos Lorand University, Budapest, Hungary, 10 p.
- Pentek, A., Molnár, F., Tuba, G., Watkinson, D.H., and Jones, P.C., 2013, The significance of partial melting processes in hydrothermal low sulfide Cu-Ni-PGE mineralization within the footwall of the Sudbury Igneous Complex, Ontario, Canada: *Economic Geology*, v. 108, p. 59–78.
- Pentek, A., Molnar, F., Watkinson, D.H., and Jones, P.C., 2008, Footwall-type Cu-Ni-PGE Mineralization in the Broken Hammer Area, Wisner Township, North Range, Sudbury Structure: *Economic Geology*, v. 103, p. 1005–1028.

- Petrus, J. a., Ames, D.E., and Kamber, B.S., 2015, On the track of the elusive Sudbury impact: geochemical evidence for a chondrite or comet bolide: *Terra Nova*, v. 27, no. 1, p. 9–20.
- Pettke T., Oberli F., Audetat A., Guillong M., Simon A., Hanley J. J., Klemm L.M., 2012, Recent developments in element concentration and isotope ratio analysis of individual fluid inclusions by laser ablation single and multiple collector ICP-MS: *Ore Geology Reviews*, v. 44, p. 10–28
- Prevec, S.A., and Cawthorn, R.G., 2002, Thermal evolution and interaction between impact melt sheet and footwall: A genetic model for the contact sublayer of the Sudbury Igneous Complex, Canada: *Journal of Geophysical Research*, v. 107, no. B8, p. 1–14.
- Prevec, S., Lightfoot, P., and Keays, R., 2000, Evolution of the sublayer of the Sudbury Igneous Complex: geochemical, Sm–Nd isotopic and petrologic evidence: *Lithos*, v. 51, p. 271–292.
- Raharimahefa, T., Lafrance, B., and Tinkham, D.K., 2014, New structural , metamorphic , and U – Pb geochronological constraints on the Blezardian Orogeny and Yavapai Orogeny in the Southern Province, Sudbury, Canada: *Canadian Journal of Earth Sciences*, , no. 51, p. 750–774.
- Raychaurhuri S., 2008, Introduction to Monte Carlo Simulation: [Ext. Abs] Proceedings of the 2008 Winter Simulation Conference, Miami, Florida, [eds.] Mason S.J., Hill R.R., Monch L., Rose O., Jefferson T., Fowler J.W., p 91 - 100
- Reimold, W.U., Wannek, D., Hoffmann, M., Hansen, B.T., Hauser, N., Schulz, T., Siegert, S., Thirlwall, M., Zaag, P.T., and Mohr-Westheide, T., 2015, Vredefort Pseudotachylitic Breccia and Granophyre (Impact Melt Rocks): Clues to their Genesis from New Field, Chemical and Isotopic Investigations, in *Bridging the Gap III*, Freiburg, Germany, 2 p.
- Riller, U., 2009, Felsic Plutons, in *A Field Guide to the Geology of Sudbury Ontario*, Ontario Geological Survey Open File Report 6243, p11-13
- Riller, U., Lieger, D., Gibson, R.L., Grieve, R.A.F., and Stoffer, D., 2010, Origin of large-volume pseudotachylite in terrestrial impact structures: *Geology*, v. 38, no. 7, p. 619–622.

- Rousell, D.H., and Brown, G.H., 2009, A Field Guide to the Geology of Sudbury, Ontario (D. H. Rousell & G. H. Brown, Eds.): Ontario Geological Survey, Open File Report 6243, 223p.
- Rousell, D.H., Fedorowich, J.S., and Dressler, B.O., 2003, Sudbury breccia (Canada): a product of the 1850 Ma Sudbury Event and host to footwall Cu–Ni–PGE deposits: *Earth-Science Reviews*, v. 60, p. 147–174.
- Rousell, D.H., Gibson, H.L., and Jonasson, I.R., 1997, The Tectonic, Magmatic and Mineralisation History of the Sudbury Structure: *Exploration and Mining Geology*, v. 6, no. 1, p. 1–22.
- Schoene, B., Bowring, S.A., 2007, Determining accurate temperature-time paths from U-Pb thermochronology: An example from the Kaapvaal craton, southern Africa: *Geochimica et Cosmochimica Acta*, v. 71, p. 165-185.
- Schuiling, R.D., and Feenstra, A., 1980, Geochemical Behaviour of Vanadium in Iron-Titanium Oxides: *Chemical Geology*, v. 30, p. 143–150.
- Schumacher, J.C., 1991, Empirical Ferric Iron Corrections: Necessity, Assumptions, and Effects on Selected Geothermobarometers: *Mineralogical Magazine*, v. 55, no. 378, p. 3–18.
- Scott, D., St-Onge, M.R., 1995, Constraints on Pb closure in titanite based on rocks from the Ungava orogeny, Canada: Implications for U-Pb geochronology and P-T-t path determinations: *Geology*, v. 23, pp.1123-1126.
- Shellnutt, J.G., and MacRae, N.D., 2011, Petrogenesis of the Mesoproterozoic (1.23 Ga) Sudbury dike swarm and its questionable relationship to plate separation: *International Journal of Earth Sciences*, p. 3–23.
- Snelling, P.E., Godin, L., and McKinnon, S.D., 2013, The role of geologic structure and stress in triggering remote seismicity in Creighton Mine, Sudbury, Canada: *International Journal of Rock Mechanics and Mining Sciences*, v. 58, p. 166–179.

- Stout, A.E., Leshner, C.M., Gregory, S.K., Deslauriers, M., Lafrance, B., McDonald, J., Davis, C., and Gauld, C., 2010, Genesis of the McCreedy East Ni-Cu-PGE Contact-Footwall Ore System, Sudbury, Ontario, in 11th International Platinum Symposium, p. 4.
- Suarez, S., Nieto, F., and Velasco, F., 2009, Copper inclusions in chlorite from the Aguablanca Ni-Cu-PGE sulfide deposit (SW Spain): *Revista de la Sociedad Espanola de Mineralogia*, v. 11, p. 173–174.
- Thompson, L.M., and Spray, J.G., 1996, Pseudotachylyte petrogenesis: constraints from the Sudbury impact structure: *Contributions to Mineralogy and Petrology*, v. 125, no. 4, p. 359–374.
- Thompson, L.M., Spray, J.G., and Kelley, S.P., 1998, Laser probe argon-40/argon-39 dating of pseudotachylyte from the Sudbury Structure: Evidence for postimpact thermal overprinting in the North Range: *Meteoritics & Planetary Science*, v. 33, p. 1259–1269.
- Tuba, G., Molnár, F., Ames, D.E., Péntek, A., Watkinson, D.H., and Jones, P.C., 2014, Multi-stage hydrothermal processes involved in “low-sulfide” Cu(–Ni)–PGE mineralization in the footwall of the Sudbury Igneous Complex (Canada): Amy Lake PGE zone, East Range: *Mineralium Deposita*, v. 49, p. 7–47.
- Van Schmus, W. R., and Bickford, M. E., 1993, Transcontinental Proterozoic Provinces: Location and Extent, in Reed, J. C., Jr., Bickford, M. E., Houston, R. S., Link, P. K., Rankin, D. W., Sims, P. K., and Van Schmus, W. R., eds., *Precambrian: Conterminous U.S.: Geological Society of America Geology of North America*, v. C-2, p. 172–176
- Veblen, D.R. and Ferry, J.M., 1983, A TEM study of the biotite-chlorite reaction and comparison with petrologic observation: *American Mineralogist*, v. 68, p. 1160 – 1168.
- Warren, M.R., Hanley, J.J., Ames, D.E., and Jackson, S.E., 2015, The Ni–Cr–Cu content of biotite as pathfinder elements for magmatic sulfide exploration associated with mafic units of the Sudbury Igneous Complex, Ontario, Canada: *Journal of Geochemical Exploration*, v. 153, p. 11–29.

- White, C.J., 2012, Low-Sulfide PGE-Cu-Ni Mineralization From Five Prospects Within The Footwall Of The Sudbury Igneous by Low-Sulfide PGE-Cu-Ni Mineralization from Five Prospects with the Footwall of the Sudbury Igneous Complex , Ontario , Canada: University of Toronto, 337 p.
- Wilkinson, J.J., Chang, Z., Cooke, D.R., Baker, M.J., Wilkinson, C.C., Inglis, S., Chen, H., and Bruce Gemmell, J., 2015, The chlorite proximator: A new tool for detecting porphyry ore deposits: *Journal of Geochemical Exploration*, v. 152, p. 10–26.
- Williamson, B.J., Herrington, R.J., and Morris, A., 2016, Porphyry copper enrichment linked to excess aluminium in plagioclase: *Nature Geoscience*, v. 9, p. 237-241.
- Witter, J.B., and Kuehner, S.M., 2004, A simple empirical method for high-quality electron microprobe analysis of fluorine at trace levels in Fe-bearing minerals and glasses: *American Mineralogist*, v. 89, p. 57–63.
- Xu, L., Bi, X., Hu, R., Tang, Y., Wang, X., and Xu, Y., 2015, LA-ICP-MS mineral chemistry of titanite and the geological implications for exploration of porphyry Cu deposits in the Jinshajiang – Red River alkaline igneous belt, SW China: *Mineralogy and Petrology*, v. 109, p. 181–200.
- Yavuz, F., Karakaya, N., Yildirim, D.K., Karakaya, M.Ç., and Kumral, M., 2015, A Windows program for chlorite calculation and classification of chlorite: *Computers and Geosciences*, v. 81, p. 101–113
- Yui, T., Shen, P., Liu, H., 2001, Titanite inclusions in altered biotite from granitoids of Taiwan: Microstructures and origins: *Journal of Asian Earth Sciences*, v. 19, p. 165 – 175.

Chapter 4

4 Conclusion:

The goal of this study was to determine the contribution of footwall and impact melt material in the Sudbury breccia, thereby elucidating its formational processes (i.e., impact melt derived or in-situ melting). Understanding the genetic processes for the breccia also assists in determining a background value for trace metals, highlighting regions with anomalous metal contents that may be prospective for sharp-walled or LSHPM footwall systems. Mineral chemistry analysis at Creighton and Coleman mines takes a step in from the regional whole rock geochemical study, in order to determine how the subsequent hydrothermal and metamorphic activity in the region may have affected the trace element and metal signature of Sudbury breccia. Below are the key observations and conclusions derived from this study and how they fit into previous research on impactite breccias at both Sudbury and other impact structures:

1. The statistical mixing model results from across the Sudbury basin, although not definitive guides to the relative contributions of footwall lithologies, provide convincing evidence that Sudbury breccia can be reconstructed without the requirement of an impact melt component. In some cases, a minority of samples appear to require a negligible contribution of quartz diorite (<6%), however the inconsistency at individual sample locations and the low values of melt required seem incompatible with the regional drainage of a relatively homogenous melt into the footwall of the SIC. The results imply that there is a degree of localized mixing between different units within the footwall (e.g., diabase and granite), which is corroborated by the observation of clasts that appear to have been transported over 10s of meters at several localities and the presence of Sudbury breccia at lithological boundaries (Mungall and Hanley, 2004; Pentek pers. comms. 2016), which would have acted as planes of weakness along which the breccia could preferentially form. Mixing and transportation of material may have also been facilitated by the development of low-pressure, tensile regions adjacent to zones of breccia development, into which the melt could be drawn. Tensile features, such as en-echelon fractures and jig-saw fit veins have been observed hosting breccia matrix in both this study and by Lieger et al. (2011) at the Vredefort structure. Although proposed as a transport mechanism for drawing impact melt into the crater footwall, such features

could also be attributed to mobilizing locally derived melts. Thus, rather than purely in-situ, the melt should be classified as being parautochthonous, that is ‘having a character intermediate between that of autochthonous rock (which is native to its location) and allochthonous rock (which has been transported into the location)’.

2. Flow banding, used by Dressler and Johns (1997) and Rousell et al. (2003) to diagnose cataclastic varieties of Sudbury breccia, was observed in samples from both the South Range and North Range. However, clast analysis results from several localities and evidence of devitrified melt and high temperature partial melting of quartz + feldspar, indicate that the breccia matrix reached very high temperatures that facilitated thermomechanical erosion. Rather than evidence of cataclasis, the flow banding may represent incomplete assimilation and mixing of material at the interface between the high-temperature, mobile melt and the local footwall unit, similar to the theory proposed by Lieger et al. (2011), albeit with the melt derived locally rather than from the overlying impact melt sheet.
3. Field work in both the North and South Range failed to identify any evidence of significant displacement in units adjacent to zones of Sudbury breccia, which is incompatible with theories on frictional melting along major fault systems during crater collapse (Thompson and Spray, 1996; Mungall and Hanley, 2004). By ruling out an impact melt component, combined with the lack of evidence for a frictional melting or cataclasis process leads the author towards two concepts:
 - A. Sudbury breccia formed via shock-heating – pressure-release melting during either the passage of the low pressure zone behind the initial excavation shock wave and/or subsequent rebound of the crater floor during the formation of the central uplift and/or peak ring structure (Ivanov and Melosh 2003). The development of tensile features such as the en-echelon fractures observed in this study support a pressure-release event and may have also acted as a low pressure zone that encouraged transportation and mixing of the melt.
 - B. Alternatively, acoustic fluidization caused by impact-induced ground seismic vibrations and motions can induce pressure fluctuations that result in a similar pressure release melting to concept A. Melting and viscous behaviour in the rock would occur during low pressure events in between periods of higher

ambient lithostatic pressure (Melosh 1979; Melosh and Ivanov 2003; Kenkmann et al., 2013).

Acoustic fluidization or shock-heating/pressure release has been demonstrated to develop thin pseudotachylite veins in experimental conditions and has been associated with thin veins of pseudotachylite occasionally observed outline shattercone features, but has not previously been applied in the context of the larger zones of pseudotachylitic breccia found at Sudbury. Both of these processes could have facilitated the creation of a high temperature in-situ melt that would have preferentially assimilated minerals/rocks with lower thermal conductivities, such as mafic units (Spray 2010). This may explain the requirement for a minor or significant mafic component in the mixing model at several localities, despite its absence as a clast component in the breccia matrix. In both cases, zones of weakness, such as pre-existing faults and lithological contacts can act as a focus for the melting and development of breccia zones (Kenkmann et al., 2013).

4. The economic implication of a parautochthonous, shock-heating, pressure-release origin for the breccia matrix is that its trace metal content must either have been derived from footwall lithologies or remobilized from ore zones by hydrothermal fluids (i.e., no magmatic sulfides were transported into the footwall in an impact melt, as at the offset dikes). Whole rock geochemical principal component analysis at Creighton and Coleman Mine demonstrate that Ni and Cr content in the breccia correlates with increased MgO, MnO and FeO, which are typically associated with mafic lithologies. On the other hand, Cu does not show any particularly strong correlation in distal samples, whereas in samples proximal to footwall ore zones the metal shows a weak correlation with CaO and Al₂O₃, which could be attributed to discrete sulfide inclusions in epidote and mica veins and alteration associated with late metal remobilization, as noted by Molnar et al. (2001) in the Coleman-Levack embayment.
5. Although the South Range experienced higher grade post-impact metamorphic events compared with the North Range, that the whole-rock Sudbury breccia signature can be reconstructed accurately with local units suggests that mineral chemistry vectors may have been preserved despite the subsequent alteration and dilution. At Creighton mine, variations in the amphibole and titanite geochemistry and trace metal content are consistent with increasing P-T conditions towards shear zones into which the sulfide ores have been remobilized by post-impact tectonic activity. Decreasing Rb with proximity to

ore in whole rock geochemical data appears to be in response to increased Tl in biotites (at the expense of K and Rb), which is concurrent with elevated Ni content and consistent with hydrothermal remobilization of metals by either magmatic or epithermal fluids.

6. In the McCreeedy 153 East footwall deposit at Coleman mine, the amphibole and biotite variations reported in elsewhere from the North Range (McCormick et al., 2002; Hanley and Mungall 2003; Hanley and Bray 2009) appear to have been partially to wholly overprinted by localized, nickeliferous chloritization. Similar nickel-rich chlorites proximal to footwall deposits have also been identified by White (2012) in the Wisner and Levack area. Using U-Pb dating of contemporaneous titanites, this study has constrained some of the Ni-chlorites to the 1.45 Ga. Chieflakian orogeny. The chloritization is particularly intense adjacent to sharp-walled sulfide veins, which occupy the same structures along which the later, Ca-rich shield brines and metamorphic fluids were transported, mobilized by the far-field thermal event associated with the orogeny. Although unproven at this time, the Pumphouse Creek Deformation Zone that transects the North Range may have served as the heat engine and pathway for Chieflakian metamorphic fluids. Similar modification of sulfides by Chieflakian-aged fluids and structures has been noted at the Worthington offset dike in the South Range (Szentpeteri 2009). Thus the relatively thin, intense alteration selvages adjacent to sharp-walled veins in the McCreeedy 153 deposit and elsewhere may represent fluids associated with the Chieflakian orogeny, rather than the later, 1.24 Ga intrusion of the Sudbury diabase or earlier fluids expelled from the cooling sulfide veins and impact melt sheet, as proposed in previous studies (Li and Naldrett 1993; Molnar et al., 2001).

4.1 Recommendations for future work

This study has provided strong evidence that Sudbury breccia is a parautochthonous melt derived from local lithologies in the footwall of the Sudbury structure, possibly during shock-heating, pressure-release melting. Hydrothermal modification of breccia-hosted sulfides in both the North and South Range took place during post-impact orogenic activity. The next steps recommended below are designed to further test and refine the above study and conclusions.

- Refinement of the statistical mixing model would be best served by introducing more end-member components beyond the current four input parameters. If possible, the introduction of element weighting would be beneficial, as the model results would thus be more sensitive to restrictions on detection limits from the different whole rock analytical methods used (e.g. Lithium-metaborate versus four acid digestion ICP-MS).
- A more detailed and regular, step-out sampling strategy at Creighton and Coleman mine would assist in validating the biotite vectoring tool identified in chapter two and confirm its spatial distribution away from mineralized zones. It would also serve to better constrain the extent of the anomalous nickel-content in chlorites surrounding ore zones at the McCreedy 153 East deposit.
- At this time, there is no constraint on the age of the Pumphouse Creek Deformation Zone in the North Range. In the South Range there is a spatial association between shear zones and remobilized sulfide ores, including LSHPM-styles. In the North Range, there is evidence of a Chielflakian-aged event that has modified the sulfide zones. Age dating of titanites hosted in the Pumphouse Creek Deformation Zone may assist in constraining the origin of the heat and metamorphic fluids associated with the formation of the nickeliferous hydrosilicates present in the McCreedy 153 East ore zone.

4.2 References

- Dressler, B.O., and Johns, G.W., 1997, Large meteorite impacts and planetary evolution: *Geoscience Canada*, v. 24, no. 4, p. 203–204.
- Hanley, J.J., and Bray, C.J., 2009, The Trace Metal Content of Amphibole as a Proximity Indicator for Cu-Ni-PGE Mineralisation in the Footwall of the Sudbury Igneous Complex, Ontario, Canada: *Economic Geology*, v. 104, p. 113–125.
- Hanley, J.J., and Mungall, J.E., 2003, Chlorine Enrichment and Hydrous Alteration of the Sudbury breccia Hosting Footwall Cu-Ni-PGE Mineralization at the Fraser Mine, Sudbury, Ontario, Canada.: *The Canadian Mineralogist*, v. 41, p. 857–881.

- Kenkmann, T., Collins, G.S., and Wünnemann, K., 2013, The Modification Stage of Crater Formation, in *Impact Cratering: Processes and Products*, p. 60–75.
- Li, C., and Naldrett, A.J., 1993, High Chlorine Alteration Minerals and Calcium-rich Brines in Fluid Inclusions from the Strathcona Deep Copper Zone, Sudbury, Ontario: *Economic Geology*, v. 88, p. 1780–1796.
- Lieger, D., Riller, U., and Gibson, R.L., 2011, Petrographic and geochemical evidence for an allochthonous, possibly impact melt, origin of pseudotachylite from the Vredefort Dome, South Africa: *Geochimica et Cosmochimica Acta*, v. 75, no. 16, p. 4490–4514.
- Marshall, D., Watkinson, D., Farrow, C., Molnár, F., and Fouillac, A.-M., 1999, Multiple fluid generations in the Sudbury igneous complex: fluid inclusion, Ar, O, H, Rb and Sr evidence: *Chemical Geology*, v. 154, p. 1–19.
- McCormick, K.A., and McDonald, A.M., 1999, Chlorine-bearing amphiboles from the Fraser mine, Sudbury, Ontario, Canada: description and crystal chemistry: *The Canadian Mineralogist*, v. 37, p. 1385–1403.
- Melosh, H., 1979, Acoustic fluidization: A new geologic process?: *Journal of Geophysical Research*, v. 84, pp. 7513 – 7520.
- Melosh, H., Ivanov, B., 1999, Impact Crater Collapse: *Annual Review of Earth and Planetary Sciences*, v. 27, pp. 385 – 415.
- Molnar, F., Watkinson, D.H., and Jones, P.C., 2001, Multiple Hydrothermal Processes in Footwall Units of the North Range, Sudbury Igneous Complex, Canada, and Implications for the Genesis of Vein-Type Cu-Ni-PGE Deposits: *Economic Geology*, v. 96, p. 1645–1670.
- Mungall, J.E., and Hanley, J.J., 2004, Origins of Outliers of the Huronian Supergroup within the Sudbury Structure: *The Journal of Geology*, v. 112, no. 1, p. 59–70.
- Reimold, W.U., Gibson, R.L., 2005, “Pseudotachylites” in Large Impact Structures: in *Impact Tectonics* (eds., Koeberl, C., Henkel, H.). Springer, pp. 1-53.

- Rousell, D.H., Fedorowich, J.S., and Dressler, B.O., 2003, Sudbury breccia (Canada): a product of the 1850 Ma Sudbury Event and host to footwall Cu–Ni–PGE deposits: *Earth-Science Reviews*, v. 60, p. 147–174.
- Thompson, L.M., and Spray, J.G., 1996, Pseudotachylyte petrogenesis: constraints from the Sudbury impact structure: *Contributions to Mineralogy and Petrology*, v. 125, no. 4, p. 359–374.
- Spray, J.G., 2010, Frictional Melting Processes in Planetary Materials: From Hypervelocity Impact to Earthquakes: *Annual Review of Earth and Planetary Sciences*, v. 38, no. 1, p. 221–254.
- White, C.J., 2012, Low-Sulfide PGE-Cu-Ni Mineralization From Five Prospects Within The Footwall Of The Sudbury Igneous by Low-Sulfide PGE-Cu-Ni Mineralization from Five Prospects with the Footwall of the Sudbury Igneous Complex, Ontario, Canada: Unpublished Ph.D.thesis, University of Toronto, Canada. 337 p.

5 *Curriculum Vitae*

Name: Jonathan W. O'Callaghan

Higher Education: 2009-2012
 Camborne School of Mines
 University of Exeter, Falmouth, United Kingdom
 B.Sc. Applied Geology, 1st with honors

2014-2016
 University of Western Ontario, London, Canada
 M.Sc. Geology, Candidate

Grants and Awards: 2015
 SRK Graduate Scholarship
 Gordan G. Suffel Scholarship for Graduate Studies in Applied
 Economic Geology
 Society of Economic Geology Canada Foundation Fellowship

2010
 Rio Tinto Undergraduate Scholarship
 Camborne School of Mines Scholarship

Work Experience: 2014-2016
 Graduate Research/Teaching Assistant
University of Western Ontario, London, Canada

2015
 Exploration Geological Assistant
Vale, Sudbury, Canada

2012-2014
 Exploration Geologist
Lonmin, Belfast, United Kingdom

2011
 Research Geologist
Tigris Resources, London, United Kingdom

Publications:

O'Callaghan, J.W., Osinski, G.R., Lightfoot, P.C., Linnen R.L., Weirich, J.R., 2016, Reconstructing the geochemical signature of Sudbury breccia, Ontario, Canada: Implications for its formation and trace metal content: *Economic Geology*, v. 111-7, in press.

O'Callaghan, J.W., Linnen, R.L., Lightfoot P.C., Osinski, G.R., 2016, Contrasting mineralogical and geochemical characteristics of Sudbury breccia adjacent to footwall Cu-Ni-PGE sulfide in the Crighton and Coleman deposits: *Canadian Mineralogist*, in review.